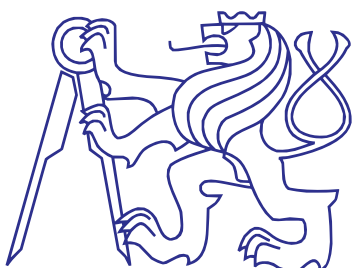


Snow extremes and structural reliability

(updated version, 24th September 2016)



Árpád Rózsás

Supervisors:

Nauzika Kovács, Ph.D.
Department of Structural Engineering
Budapest University of Technology and Economics

Miroslav Sýkora, Ph.D.
Department of Structural Reliability
Klokner Institute, Czech Technical University in Prague

This dissertation is submitted for the degree of
Doctor of Philosophy in Civil Engineering

June 2016

Declaration

I hereby declare that except where specific reference is made to the work of others, the contents of this dissertation are original and have not been submitted in whole or in part for consideration for any other degree or qualification in this, or any other university. This dissertation is my own work and contains nothing which is the outcome of work done in collaboration with others, except as specified in the text and Acknowledgments.

Árpád Rózsás
June 2016

Acknowledgements

I am grateful to my supervisors Nauzika Kovács and Miroslav Sýkora for their guidance and continuous support during the completion of this work. I owe my gratitude to László Dunai for allowing me to pursue the whim of my interest over the course of my studies. This work would have never been completed without his support and his trust in me. I am indebted to László Gergely Vigh for the valuable discussions and for jointly completed research. I highly appreciate his personal and professional help, which he is always eager to provide even amid his numerous activities.

I am thankful to all members of the Department of Structural Engineering for the friendly and supportive environment, for sharing their knowledge, and for nurturing my engineering insight. Special thanks go to Kitti Gidófalvy, Piroska Mikulásné Fegyó, and Mansour Kachichian for the personal conversations.

I am grateful to the members of Klokner Institute, particularly to those of the Department of Structural Reliability, where I spent a wonderful 10-month research stay. I am especially grateful to Miroslav Sýkora for making my stay in Prague an unforgettable experience, for the invigorating professional conversations, and for his friendship.

Special thanks to commander-in-chief Mogyi for her professional help and for her companionship in our journey ☺.

I am obliged to the countless people of past and present who shaped my world view and whose work and ideas are indispensable and inseparable part of my thinking. I wish I were able to add a grain of sand to the mountain of their amassed knowledge.

This work was partly supported by the Ph.D. Scholarship of the Hungarian State and by the International Visegrad Fund Intra-Visegrad Scholarship (contract no. 51401089), both are highly appreciated.

The numerical analyses are mainly completed using Matlab (Matlab, 2015), FERUM (Der Kiureghian et al., 2006), and R (R Core Team, 2015). The work and commitment of the developers of these applications are highly appreciated. In the spirit of reproducible and open research all of the related scripts, processed data, and results are available from the author and partially from the repositories of the following GitHub account:
<https://github.com/rozisasarpi>.

Abstract

This study is motivated by the sharp contrast between physical and probabilistic models of civil engineering. The current practice focuses on physical models while probabilistic ones are relatively underdeveloped. This unbalance can even hinder advances in physical models. Moreover, this rarely acknowledged asymmetry creates the illusion that our deterministic models accurately capture all or at least the main aspects of reality. Thus, this thesis aspires to subtly adjust this imbalance by focusing on probabilistic models.

The main contribution is that it explores often neglected or oversimplified aspects of probabilistic analysis in civil engineering. These distinct but related issues are: (*i*) selection of an appropriate distribution type; (*ii*) effect of statistical uncertainty; (*iii*) measurement uncertainty; (*iv*) long-term trends; and (*v*) dependence structure. These are demonstrated through analyzing extreme ground snow loads, although they are inevitably present for most random variables. Snow action, which has recently led to numerous structural failures in Central Europe, is treated as a vehicle of illustration to give a sharp focus to the study.

Methods developed in mathematical statistics, probability theory, information theory, and structural reliability are applied to tackle these issues. Fully statistical analysis of snow extremes is undertaken in conjunction with structural reliability analysis. The popular civil engineering approaches are compared with more advanced techniques that are able to capture the neglected effects in the former approaches. Snow water equivalent data of the Carpathian Region from more than 600 meteorological stations are analyzed, thus the results are representative for lowlands, for highlands, and for mountains as well. Furthermore, extensive parametric analyses are performed to extend the investigations to random variables other than ground snow intensity.

Based on the analysis of the above-listed issues the following main conclusions are drawn:

- (*i*) It is demonstrated that mountains and highlands are better represented by Weibull, while lowlands by Fréchet distribution. In comparison, the currently standardized Gumbel model recommended in Eurocode often appreciably underestimates the snow maxima of lowlands and thus leads to overestimation of structural reliability.
- (*ii*) It is shown that current practice, which neglects statistical uncertainties (parameter estimation and model selection uncertainties), can yield to even multiple orders of magnitude underestimation of failure probability. Bayesian posterior predictive

distribution and Bayesian model averaging is proposed to account for parameter estimation and model selection uncertainties, respectively.

- (iii) Statistical and interval based approaches are used to explore the effect of prevalently neglected measurement uncertainty on structural reliability. It is demonstrated that such simplification can lead to an order of magnitude underestimation of failure probability. If sufficient data are available to infer the probabilistic model of measurement uncertainty, then the statistical approach is recommended. Otherwise, the interval approach is advocated.
- (iv) Using non-stationary extreme value analysis, statistically significant decreasing trend is found in annual ground snow extremes for most of the Carpathian Region. For some locations the effect of the trend on structural reliability is practically significant. This change is favorable from safety point of view as it increases reliability. Hence, revision of current regulations due to long-term trends is not needed from safety reasons, though it might be desirable from economic considerations. However, record lengths are insufficient to draw strong conclusions and to include trends in predicting extreme values with return periods of hundreds of years.
- (v) Study of the widely used Gauss (normal, or Gaussian) copula assumption of time-continuous stochastic processes is performed. It reveals that Gauss copula can four times underestimate or even ten times overestimate time-variant failure probabilities obtained by other adopted copulas (t , Gumbel, rotated Gumbel, and rotated Clayton). Model averaging is proposed as a viable approach to rigorously account for copula function uncertainty.

Based on these findings, practical recommendations are made for normal and safety critical structures. The effects and proposed approaches are illustrated through real life examples. Reliability of the more than 130 years old wrought iron structure of Eiffel-hall and a steel hall of Paks Nuclear Power Plant is analyzed.

The tackled challenges are general and relevant for most random variables such as wind, traffic, and earthquake actions. Therefore, the findings can be applied for these as well and they can help to draft more consistent standards and to build safer structures.

Contents

Nomenclature	xii
1 Introduction	1
1.1 Motivation	1
1.2 Problem statement	1
1.3 Adopted approach	3
1.4 Structure of the thesis	3
1.4.1 Application examples	4
1.5 Position of the thesis in probabilistic engineering	4
1.6 Scope and limits	5
2 Overview of uncertainty modeling and structural reliability	7
2.1 Uncertainty modeling	7
2.2 Structural reliability	8
3 Effect of statistical uncertainties	11
3.1 Problem statement and the state of the art	11
3.2 Solution strategy	12
3.2.1 Data under study	13
3.3 Effect on representative fractiles	14
3.3.1 Return value–return period plots	16
3.3.2 Comparing representative fractiles	18
3.3.3 Model averaging	21
3.4 Effect on structural reliability	22
3.4.1 Conceptual framework	22
3.4.2 Mechanical and probabilistic model	23
3.4.3 Statistical analysis	24
3.4.4 Reliability analysis	26
3.5 Application example: Eiffel-hall of Budapest	27
3.6 Discussion	28
3.7 Summary and conclusions	30

4 Effect of measurement uncertainty	31
4.1 Problem statement and the state of the art	31
4.2 Solution strategy	32
4.2.1 Adopted approaches	32
4.2.2 Uncertainty representation and propagation	34
4.3 Example: reliability of a generic structure	37
4.3.1 Model description	37
4.3.2 Interval and reliability analysis	37
4.3.3 Statistical and reliability analysis	42
4.4 Application example: Turbine hall of Paks Nuclear Power Plant	46
4.5 Discussion	49
4.6 Summary and conclusions	50
5 Long-term trends in annual ground snow maxima	53
5.1 Problem statement and the state of the art	53
5.2 Solution strategy	54
5.3 Stationary model	56
5.4 Long-term trends, non-stationary models	56
5.5 Impact on structural reliability	59
5.5.1 Application example: Turbine hall of Paks Nucelar Power Plant . .	60
5.6 Discussion	61
5.7 Summary and conclusions	62
6 Effect of dependence structure	64
6.1 Problem statement and the state of the art	64
6.2 Stochastic processes	66
6.2.1 Autocorrelation function	66
6.2.2 Copula based dependence structure	67
6.3 PHI2 method	68
6.4 Example 1: simple time-variant problem	71
6.5 Example 2: corroding beam	73
6.6 Example 3: generic structure subject to snow load	76
6.7 Application example: Eiffel-hall of Budapest	80
6.8 Discussion	81
6.9 Summary and conclusions	81
7 Summary and conclusions	83
7.1 Purpose and significance of the study	83
7.2 Recapitulation of main conclusions	84
7.2.1 Distribution of annual ground snow maxima	84
7.2.2 Effect of statistical uncertainties	85

7.2.3	Effect of measurement uncertainty	87
7.2.4	Long-term trends in annual ground snow maxima	88
7.2.5	Effect of dependence structure	90
7.3	Concluding remarks	91
	Bibliography	93
	Appendix A Snow characteristics for the Carpathian Region	104
A.1	Interactive snow map	104
A.2	Posterior distribution of GEV parameters	105
	Appendix B Description of application examples	108
B.1	Nuclear power plant in Paks, turbine hall	108
B.1.1	Overview	108
B.1.2	Fragility curves	108
B.1.3	Snow action	110
B.2	Locomotive workshop in Budapest, Eiffel-hall	110
B.2.1	Overview	110
B.2.2	Selected truss member and failure mode	111
B.2.3	Snow action	111
	Appendix C Statistical tools, models and plots	113
C.1	Statistical tools	113
C.1.1	Point estimates	113
C.1.2	Interval estimates	115
C.1.3	Prediction	116
C.1.4	Goodness-of-fit measures	117
C.1.5	Model averaging	119
C.2	Distribution functions	120
C.3	Probability plots	121
	Appendix D Summary of contributions in Hungarian	124

Nomenclature

Roman Symbols

AIC	Akaike information criterion
$AICc$	sample size corrected Akaike information criterion
b	Bayesian weight
BIC	Bayesian information criterion
$C(\cdot)$	copula function
CV	coefficient of variation
$F(\cdot)$	cumulative probability distribution function
$f(\cdot)$	probability density function
$g(\cdot)$	performance function
$L(\cdot)/L$	likelihood function/value
$L_p(\cdot)$	pairwise likelihood function
M	model
n	number of observations
P	probability of an event
P_f	probability of failure
$p(\cdot)/p$	probability distribution/probability
RP	return period
RV	return value
t	time or any strictly monotonically increasing parameter
$t(\cdot)/t_2(\cdot)$	univariate/bivariate Student (or t) cumulative distribution function
w	Akaike weight

X/\mathbf{X} random variable(s)

x/\mathbf{x} realization(s) of a random variable or independent variable

Greek Symbols

α	FORM sensitivity factor
β	reliability index
χ	load ratio
ϵ_r	interval radius for measurement uncertainty
ν^+	out-crossing rate
$\Phi(\cdot)/\Phi_2(\cdot)$	univariate/bivariate standard Normal cumulative probability distribution function
ρ	Pearson's rho (correlation coefficient)
τ	Kendall's tau (correlation coefficient)/dummy variable
τ_F	correlation length
$\theta/\boldsymbol{\theta}$	inferred parameter(s)
ξ	shape parameter of GEV

Subscripts

i, j loop counter

Other Symbols

$*$	convolution operator
$\dot{\sim}$	asymptotically distributed as
\sim	distributed as
$E(\cdot)$	mean value, expectation operator
$\underline{\text{par}}, \overline{\text{par}}$	lower and upper interval bounds of a parameter (par)
$\text{Var}(\cdot)$	variance operator

Acronyms / Abbreviations			
AIC	Akaike information criterion	LN2	two-parameter Lognormal distribution
AICc	sample size corrected Akaike information criterion	LN3	three-parameter Lognormal distribution
BIC	Bayesian information criterion	LR	likelihood ratio
BMA	Bayesian model averaging	mad	median absolute deviation
BP	Bayesian posterior	MA	model averaging
BPM	Bayesian posterior mean	MC	Monte Carlo
BPP	Bayesian posterior predictive	MCMC	Markov chain Monte Carlo
CI	confidence interval	ML	maximum likelihood
DI	direct integration	MM	method of moments
eqi	equal tail credible interval	N	Normal distribution
FMA	frequentist model averaging	rot	rotated
FORM	first order reliability method	SORM	second order reliability method
GEV	Generalized extreme value distribution	std	standard deviation
GMM	Generalized method of moments	SWE	snow water equivalent
hdi	highest density credible interval	ZAMG	Central Institution for Meteorology and Geodynamics

Chapter 1

Introduction

This introductory chapter provides the motivation of the thesis, enumerates the examined questions, and outlines the adopted approach to answer them. Additionally, the organization, position, and scope of the thesis are presented.

1.1 Motivation

Probabilistic models in engineering are generally underappreciated and underdeveloped compared with physical ones. However, this unbalanced attention is not justified by their lower importance, since the same relative improvement in probabilistic models might yield to greater savings than that in physical models. In other words, advances in physical models are typically outweighed by the uncertainties in the probabilistic ones (McRobie, 2004). This study aspires to subtly adjust this imbalance by focusing on probabilistic models through investigating the effect of conventional engineering simplifications in structural reliability. Due to the vast range and diversity of probabilistic analysis, a sharp focus is needed for efficacy, thus this study is restricted to probabilistic models of extreme¹ ground snow loads. Despite the restricted subject, many of the considered issues are the same for other basic variables, especially climatic actions; hence, it is hoped that the findings presented here will be utilized for those as well.

1.2 Problem statement

Snow is an important climatic action, which governs the reliability of many structures, particularly of lightweight roofs. These should operate without major structural maintenance for typically 50 years, and their real working life often spans over 100 years. Therefore, it is of utmost importance that the expected actions are adequately anticipated during the design process.

¹Hereinafter extremes refers to structural engineering extremes, values that govern the design of load bearing structures. Their return period can vary from 50 to 10000 years.

The topic selection is partially motivated by the relatively large number of structural damages and collapses experienced around the world due to snow loads (Geis et al., 2011); e.g. recently in 2005/06 Central Europe, 2010/11 North-Eastern USA. One of the diverse causes of collapses appears to be the inadequate safety level provided by standards (Holický and Sýkora, 2009; Meløysund, 2010). Further motivations for the study are the perceived inconsistencies in the current European standard regarding exceptional ground snow load, and statistical treatment of snow measurements. The problems seem to be urgent particularly for lowland areas with continental climate where exceptional snowfalls are more likely than in mountains (Sanpaolesi et al., 1998). Thus, the topic has a great importance for Hungary and for neighboring countries. The relevance of the topic is also highlighted by a foreseen revision of design procedures within Eurocode.

The main issues examined in this study – with brief description and related questions – are summarized below (for detailed references see the relevant chapters):

1. There is a lack of agreement among reliability experts on the appropriate distribution function for ground snow maxima. Critical examination of current probabilistic snow models and application of statistically established methods are needed. *Which distribution function is the “best” to model ground snow extremes? What constitutes an appropriate model?*
2. Statistical uncertainties – arising from scarcity of observations – are typically neglected; however, they seem to be important as observation periods are only a small fraction of governing return periods, thus extrapolation to unobserved ranges is inevitable. *How large is the effect of statistical uncertainties on structural reliability? Is their neglect reasonable? How should these uncertainties be taken into account?*
3. Measurements are inevitably contaminated with measurement uncertainty, which is especially important for snow where measuring techniques are often burdened with large uncertainty. *How measurement uncertainty should be taken into account and propagated to structural reliability? Is the current practice, which neglects it, acceptable from reliability point of view? Is its effect on failure probability practically significant?*
4. Current civil engineering provisions are based on the assumption of stationarity; however, recent observations and climate models challenge this. *Is the stationary assumption tenable for snow extremes? What are the practical implications of time-trends for structural reliability?*
5. Correlation structure of stochastic processes is almost solely described by Gauss copula; however, this assumption is not corroborated by empirical evidence. *How large is the effect of copula assumption on time-variant structural reliability? Is the current practice conservative for snow loads? How can the copula function uncertainty be treated?*

1.3 Adopted approach

To explore the questions listed in Section 1.2, methods of structural reliability, mathematical statistics, and conventional civil engineering are applied. The general rationale of the investigations is the same:

1. Identification of potential gaps in current body of knowledge and/or non-conservative assumptions in practice.
2. Examination of the underlying concepts to support hypothesis formulation, then selection or development of tools for quantitative analysis of the identified questions.
3. Qualitative and quantitative comparison of popular civil engineering approaches with more advanced statistical techniques that are able to capture in the former neglected effects.
4. Parametric analysis using minimal² reliability problems that represent generic structures. Consideration of an extended parameter range to cover random variables other than ground snow intensity too.
5. Illustration of the effects and proposed approaches with real-life examples.
6. Discussion of the question and results from a broader, decision making perspective.
7. Formulation of practical recommendations and simplified rules.

1.4 Structure of the thesis

The thesis' organization is presented in Figure 1.1. After the introduction, an overview of the applied methods and terminology is presented (Chapter 2). Then each subsequent chapters (3-6) deal with one or two research questions. These are similarly structured and accompanied with application examples that are intended to highlight the practical importance of the questions and feasibility of proposed approaches. These question-chapters are loosely connected and these connections are indicated by dashed lines in Figure 1.1. Finally, the study concludes with the summary of the contributions (Chapter 7). The appendices gather supplementary materials and technical details in an extent to allow reproducibility. Further supporting materials are available from the following GitHub account: <https://github.com/rozsasarpi>.

²Minimal is used in the sense of minimal working example of programming. As simple as possible to capture the essential features of examined issue, but not simpler.

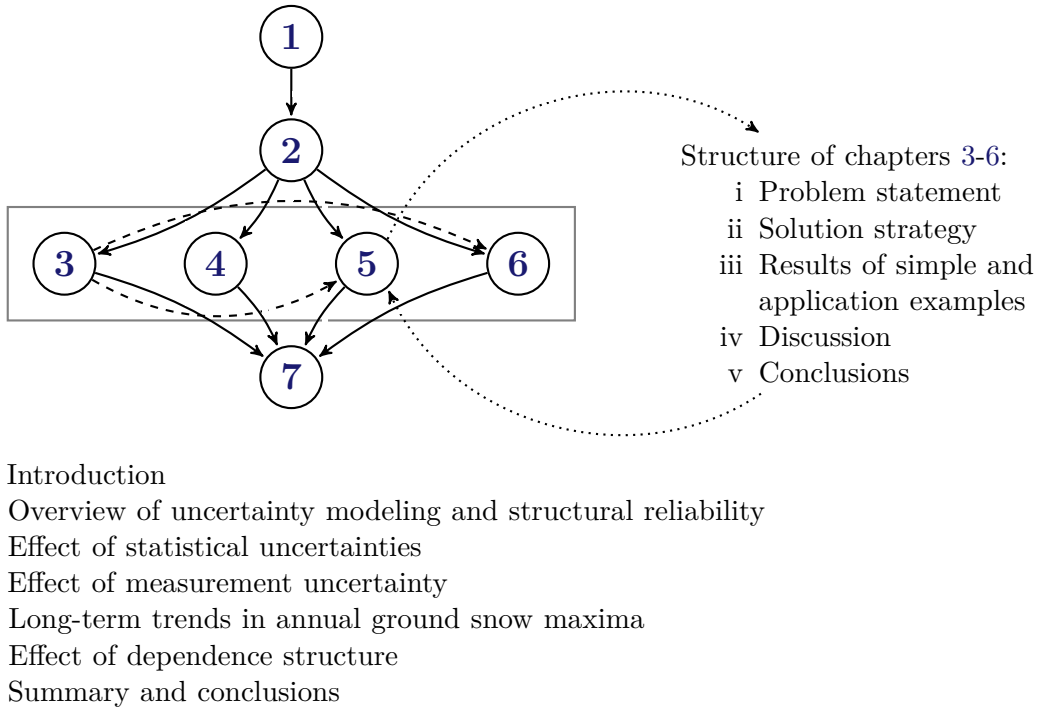


Figure 1.1 Overview of the organization of the thesis.

1.4.1 Application examples

To emphasize the practical importance and consequences of the examined issues, each one is demonstrated through real-life examples:

- *Turbine hall* of the Hungarian nuclear power plant in Paks. It is an example of probabilistic assessment of safety critical structures. The governing load of the steel hall is snow. Detailed description of the structure is given in Annex B.1.
- *Eiffel-hall* in Budapest. It is a more than 130 years old $95\text{m} \times 235\text{m} \approx 22000\text{m}^2$ floor area locomotive workshop constructed between 1883 and 1885. The planned change of its function requires the analysis of the structure that serves as an example for probabilistic analysis of existing structures. The governing load of the slender wrought iron hall is snow. Detailed description of the structure is given in Annex B.2.

1.5 Position of the thesis in probabilistic engineering

According to Nowak and Collins (2000) the origins of probabilistic engineering analysis and construction regulations can be traced back to centuries, even millennia. Although early attempts were not systematic, they recognized the inherent probabilistic nature of engineering design and tried to account for uncertainties in resistances and loads as well. Among the first modern advocates and pioneers of probabilistic design were Kazinczy (1921), Mayer (1926), and Freudenthal (1947), whose outstanding works have

shaped the field. Later other important contributions were made by Ang, Cornell, Der Kiureghian, Ditlevsen, Elishakoff, Ellingwood, Frangopol, Galambos, Grigoriu, Lind, Melchers, Rackwitz, Turkstra, and Wen. The results are organized into books, e.g. [Ang and Tang \(2006\)](#); [Cornell \(1967\)](#); [Ditlevsen and Madsen \(2007\)](#); [Elishakoff \(2004\)](#); [Melchers \(2002\)](#); [Nowak and Collins \(2000\)](#); [Thoft-Cristensen and Baker \(1982\)](#). The field is still actively researched with overarching scope and applications in almost all engineering fields.

Hungarian researchers also played an important role in the advancement of probabilistic engineering, most notably [Kazinczy \(1921\)](#). Motivated by scarce resources following World War II, Hungary was the first country to adopt semi-probabilistic design philosophy using partial factors for a countrywide code in 1950 ([Menyhárd et al., 1951](#)). Many Hungarian or Hungary related research engineers contributed and still contribute to the field ([Honfi, 2013](#); [Koris, 2009](#); [Lógó et al., 2011](#); [Mistéth, 2001](#); [Rad, 2011](#); [Szalai and Kovács, 2011](#)) along with statisticians and probabilists ([Galambos, 1978](#); [Habib and Szántai, 2000](#); [Prékopa, 1995](#); [Rényi, 1970](#); [Szántai and Kovács, 2012](#)).

1.6 Scope and limits

The main questions examined in this study are general and relevant for all basic variables affecting structural reliability, yet the focus is on ground snow extremes. These are analyzed from an engineering point of view, i.e. concentrating on issues with engineering significance, such as structural reliability and design regulations. Less attention is devoted to other questions that might be the interest of statisticians or meteorologists. Solely the time-variant component of ground snow load is analyzed thoroughly, although the time-invariant component: ground to roof conversion factor might be of similar importance. Moreover, the data-driven analyses are restricted to the climatic conditions of the Carpathian Region. The analyses are conducted with other climatic actions in mind, the parametric studies are extended to the range of actions other than snow. Thus the scope of the thesis is extreme ground snow loads but its limits extend to all random variables and stochastic processes considered in probabilistic engineering analysis.

All models in this study are fully statistical, this means that no physical arguments and principles are incorporated. This is a prevalent approach not only in engineering but in other fields as well. To our³ knowledge, first principle based meteorological models are not yet able to reliably predict extreme snow events. Especially if those are the product of a local atmospheric phenomenon⁴. The presented analyses are based on mathematical

³First person plural is used in this study to refer to the candidate's knowledge, work, decision, opinion, etc. The only exception is the formulation of theses in Chapter 7, where first personal singular is used for the same purpose in line with the requirements of the Vásárhelyi Pál Doctoral School.

⁴In this respect important advances are expected in the future. First principle based extreme event prediction might soon be available by extending the incorporated physical models and increasing the spatial and temporal resolutions of general circulation models. These advances can open up new possibilities to give substantially improved answers to the questions considered here.

statistics, e.g. the extreme value theory, which provides a strong theoretical support for the models under consideration.

The two main focuses of probabilistic engineering are (*i*) calculation of probability of rare events such as structural failure (structural reliability); and (*ii*) propagation of uncertainty through physical models. Both are concerned with uncertainty representation and with efficient solution of the posed problems. In this thesis only structural reliability problems are considered.

One can categorize uncertainties into the following groups:

- physical uncertainty (inherent, irreducible uncertainty in the adopted model space, “model universe”);
- statistical uncertainty (parameter estimation and probabilistic model selection uncertainties);
- measurement uncertainty;
- model uncertainty (physical model selection uncertainty);
- human error.

Based on its nature, uncertainty can be aleatory or epistemic. In this framework aleatory uncertainty refers to the uncertainty that cannot be reduced, inherent in the selected model space. While epistemic refers to uncertainty that is reducible, for example by obtaining and incorporating more data. This classification is not absolute and it is always conditioned on the selected model space. This thesis deals only with physical, statistical, and measurement uncertainties; and it focuses on epistemic uncertainties.

Since agreement is lacking on the nature, interpretation, and representation of uncertainty, it is not surprising that multitude of concepts are available and applied. These include probability theory, imprecise probability theory, fuzzy set theory, possibility theory, evidence theory, etc. (Ayyub and Klir, 2006; Corotis, 2015). In this study we mostly rely on probability theory, but interval analysis, which belongs to imprecise probability theory, is also used to represent a level ignorance that probability distributions cannot. Even within probability theory there is a lack of consensus on interpretation of probability (Hájek, 2012). We subscribe to the notion that “probability does not exist”⁵ (de Finetti, 1974) and probability is conditioned on the observer and on the selected model space.

The scrutinized questions cover only a small but important fraction of open questions even in engineering modeling of extreme snow loads and structural reliability. Still not only the treated questions are more general but the provided answers and solutions too. Hence, it is surmised that the findings can also be applied to issues out of the scope of this thesis.

⁵Maybe with the exception of the realm of quantum mechanics, which does not concern us herein.

Chapter 2

Overview of uncertainty modeling and structural reliability

This chapter presents a brief overview of uncertainty modeling and structural reliability. It focuses on topics discussed in this dissertation from an engineering point of view. The main aim is to present the concepts, terms, notations, and methods used in further chapters. Emphasis is put on subjects that are typically insufficiently treated, overly simplified, or neglected in current civil engineering practice.

2.1 Uncertainty modeling

Statistical and interval based approaches are used to model and to propagate uncertainties. The former is used for most of the calculations, while interval analysis is only applied to represent measurement uncertainty and to compare with statistical approaches. Thus, interval analysis is introduced in the relevant chapter (Chapter 4). Since the mathematical machinery often appreciably differs from chapter to chapter, the particular, chapter-specific methods are introduced there. Here only the common, in multiple chapters utilized concepts are exposed.

The statistical analyses are completed using two main paradigms: frequentist and Bayesian statistics. The former views probability as a long-run frequency and bases inference on comparing the relative likelihood of datasets given a parameter value. Probability in the latter reflects the analyst's current state of knowledge using all available information ("degree of belief"¹) and bases inference on the relative evidence of the parameter values given a dataset (Cornell and Benjamin, 1970; Spiegelhalter and Rice, 2009). The latter is also regarded as the extension of classical logic (Jaynes, 2003). It is out of the scope of this study to compare the frequentist and Bayesian paradigms in detail and to expose

¹It is often termed subjective probability; however, subjective here is not used in its everyday meaning. Instead it reflects the analyst's inevitable modeling assumptions and decisions, which are not solely based on the information conveyed by the data but on his or her expert judgment. Still the rationality and consistency are maintained: two analysts with the same experience and information would come up with the same inference.

Table 2.1 A brief comparison of frequentist and Bayesian statistics.

Category	Frequentist	Bayesian
Probability, P :	long-run frequency	degree of belief
Parameters:	fixed but unknown	random variables
Focuses on:	variability of data	uncertainty of knowledge
Mathematical machinery:	sampling distribution, repeated hypothetical experiments	Bayes' theorem, fixed data
Answers/calculates:	$P(\text{data} \text{hypothesis})$	$P(\text{hypothesis} \text{data})$
Source of information:	data (observations)	data (observations) + prior belief

the deep philosophical differences, see Barnett (1999); Jaynes (2003). A brief comparison is presented in Table 2.1, from which the most relevant for us are detailed in later sections. For a more comprehensive, practically oriented comparison see Jaynes (1976); Wagenmakers et al. (2008). In later chapters mostly the Bayesian statistics is advocated and used due to that (i) it represents all parameters with probability distribution thus enables the propagation and integration their uncertainty in further analysis, e.g. decision making; (ii) allows to combine information from different sources; (iii) and can efficiently handle complex problems with messy data.

The statistical techniques applied to estimate parameters, to construct uncertainty intervals, to account for distribution type uncertainty, to evaluate goodness-of-fit, and to predict future observations are detailed in Annex C.1. The descriptions are given in an extent to enable reproducibility. The statistical techniques and notation used in further chapters are summarized in Table 2.2.

2.2 Structural reliability

Structural reliability is concerned with the probabilistic analysis of engineering structures; most often this means the calculation of the failure probability of a structure with uncertain properties and subjected to uncertain actions. This problem is formulated using the limit state concept, which states that the boundary between safe and failure domain is sharp: characterized by a sudden change in performance. Accordingly, the related function is termed as performance function, $g(\mathbf{X})$. The limit state, $g(\mathbf{X}) = 0$, separates the disjoint safe and failure regions (Fig. 2.1). The failure probability can be calculated as the integral of the joint density function of the random variables over the failure domain²:

$$P_f = P(g(\mathbf{X}) < 0) = \int_{g(\mathbf{X}) < 0} p(\mathbf{x}) \cdot d\mathbf{x} \quad (2.1)$$

²This simple formulation is given for clarity, a more general formulation would include time, more general probabilistic models, and systems as well.

where $p(\cdot)$ represents a probability density function that is identified by its argument. For example $p(x)$ and $p(y)$ are in general completely different functions. This notation allows greater clarity and conciseness than in reliability engineering typically used notation, $p(x) \equiv f_X(x)$.

The two main challenges in structural reliability are the inference of probabilistic models in the face of information scarcity, and the calculation of the typically high-dimensional integral (Eq.2.1). The value of the integral is usually approximated by numerical techniques tailored for the particular features of structural reliability problems. These aim to reduce the required number of performance state function evaluations to minimal.

In this thesis, unless otherwise stated, the first order reliability method (FORM) (Hasofer and Lind, 1974) is used for approximating the integral. It is sufficiently accurate for most structural engineering problems (CEN, 2002), though the presented calculations are often verified by more accurate methods, such as second order reliability method (SORM), Monte Carlo simulation (MC), and importance sampling Monte Carlo simulation (isMC).

The improved Hasofer-Lind-Rackwitz-Fiessler algorithm (Rackwitz and Fiessler, 1979; Zhang and Der Kiureghian, 1995) is used to solve the constrained optimization problem in FORM. For correlated random variables – unless otherwise stated – the Nataf transformation (Liu and Der Kiureghian, 1986) with Cholesky decomposition is used to obtain independent, normally distributed random variables. The asymptotic formula of Breitung (1984) is used as a correction term in SORM. For isMC multivariate normal distribution used.

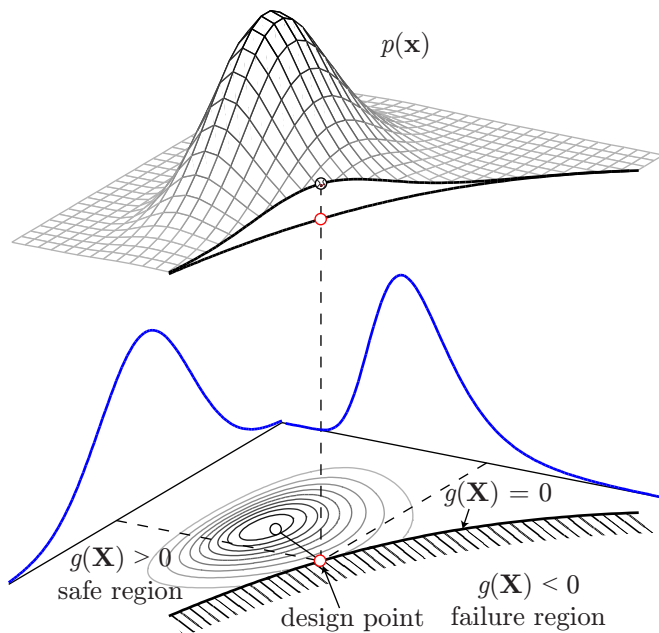


Figure 2.1 Illustration of limit state function, failure and safe regions, and design point.

Table 2.2 Summary of applied statistical methods and notations, for details see Annex C.1.

Name *	Point estimate	Uncertainty interval	Model averaging
Method of moments	MM	–	–
Generalized method of moments†	GMM	delta	delta method‡
Maximum likelihood†	ML	delta profile bootstrap	FMA (Eq.C.13-C.14)
Bayesian posterior mean	BPM	hdi eqi	highest density interval equal tail interval
Bayesian posterior predictive	BPP, (Eq.C.7)	–	–

* Examples for notation:

ML-delta: maximum likelihood estimate with uncertainty interval constructed using delta method;

BMA-BPM-hdi: Bayesian model averaged posterior mean estimate with highest density uncertainty interval.

† Frequentist paradigm.

‡ Similar to classic delta method but based on a special weighting matrix, see Section C.1.2.

– Not applicable/not available.

Chapter 3

Effect of statistical uncertainties

This chapter studies the effect of commonly neglected statistical uncertainties on representative fractiles and on structural reliability. The failure probability of a generic structural member, subjected to snow load is analyzed using frequentist and Bayesian techniques to quantify parameter estimation and model selection uncertainties in ground snow load. Various variable to dead load ratios are considered to cover a wide range of real structures. The analysis reveals that statistical uncertainties may have a substantial effect on reliability. By accounting for parameter estimation uncertainty, the failure probability can increase by more than an order of magnitude. Bayesian posterior predictive distribution is recommended to incorporate parameter estimation uncertainty in reliability studies.

3.1 Problem statement and the state of the art

One of the main concerns in structural reliability is the calculation of very small probabilities, such as events expected to occur once in 10000 years. A major difficulty in this is that actions, which structures should withstand, are inferred from 50-100 years of observations. This information might be supplemented by phenomenological or theoretical models but these are seldom available or far too complex to be used in engineering design.

Hence, probabilistic models of actions are affected by substantial uncertainty, which might dominate the reliability (Coles and Pericchi, 2003). These uncertainties, which are related to the identification of the probabilistic model on the basis of limited data, are referred hereinafter as statistical uncertainties. Only modeling of a random variable is considered, hence the statistical model uncertainty means the uncertainty in the selection of probabilistic model (distribution function), and the statistical parameter estimation uncertainty refers to the uncertainty in the identification of unknown parameters (e.g. location, scale, shape) of a particular distribution. These two are not entirely separable but it is convenient to use both terms. Statistical uncertainties stem from the scarcity of available information and inevitably present for every probabilistic models. For simplicity they are referred to as parameter estimation and model selection uncertainties.

In reliability studies and standardization statistical uncertainties are routinely neglected (Coles et al., 2003; Sanpaolesi et al., 1998; Sisson et al., 2006). However, this violates a basic requirement of probability calculation, namely that all information should be incorporated and all uncertainties accounted for (Der Kiureghian, 1989). The aim of this section is to explore the effect of this omission on selected fractiles and on structural reliability. Moreover, it critically compares some statistical approaches to incorporate statistical uncertainties into probabilistic models.

3.2 Solution strategy

The meteorological actions on structures are almost solely described by statistical distributions since the underlying natural phenomena are too complex to be represented by physical models. This approach is adopted here and the ground snow load intensity is modeled by a single random variable.

In line with the current engineering practice the block method (Coles, 2001) is applied. The block length is one year, covering a whole winter season. The annual ground snow maxima are treated as a sample for each location. The potentially more effective multiple block maxima or smaller block lengths are discarded, since the accumulative nature of snow loads makes it difficult to identify peaks and to justify their independence. For the same reason the peak over threshold approach (Reiss and Thomas, 2007) was also not used. To account for dependence between maxima from the same winter season a stochastic process based approach is presented in Chapter 6.

For other actions the dependence of maxima is typically lower, thus multiple block maxima and peak-over threshold approaches are advised to be considered. These methods often extends the sample size by orders of magnitude, thus might substantially reduce statistical uncertainties. For wind speed maxima it is demonstrated that these approaches can lead to 70% reduction in confidence interval for 1000-year fractiles compared with the annual block maxima approach (Rózsás and Sýkora, 2016a).

Since the main goal of this chapter is to demonstrate the effect of neglecting statistical uncertainties we believe that it is sufficient to use the one year block approach. This creates common ground for comparison, though in future works approaches that use more information should be considered.

Observations from the Carpathian Region are used to infer the distribution parameters (Section 3.2.1). The statistical and structural reliability machinery presented in Section 2 is utilized to explore the effect of statistical uncertainties on representative fractiles and on structural reliability, and to identify the appropriate distribution type for ground snow maxima.

3.2.1 Data under study

The meteorological data are obtained from the CarpatClim database, which is the outcome of a cooperation between nine countries of the Carpathian Region (Szalai et al., 2013). The research is completed under the leadership of the Hungarian Meteorological Service that coordinated the joint effort of the meteorological institutions of Austria, Croatia, Czech Republic, Poland, Romania, Serbia, Slovakia and Ukraine.

The database provides snow water equivalents (SWE) in about 10 km spatial and daily temporal resolution that corresponds to the period from 1961 to 2010. The daily maxima are recorded in the database. The climatological grid covers the region between latitudes 44°N and 50°N, and longitudes 17°E and 27°E (Figure 3.1-3.2a). The data are gathered from 288 climate stations and 355 precipitation stations with relatively homogeneous spatial distribution. These are homogenized and spatially interpolated using meteorological and statistical models, missing data are also filled in using these models. The post-processed data are available in the database.



Figure 3.1 Illustration of the studied region (black frame) with involved countries and meteorological stations.

Information about the available snow water equivalent data is taken verbatim from the supplementary document of the CarpatClim project (Szalai et al., 2013):

“The water equivalent of a snow cover is the vertical depth of the water that would be obtained by melting the snow cover (WMO, 2008).”

“a snow cover model employed operationally at ZAMG [Central Institution for Meteorology and Geodynamics, Austria], was applied to generate a 0.1° latitude/longitude

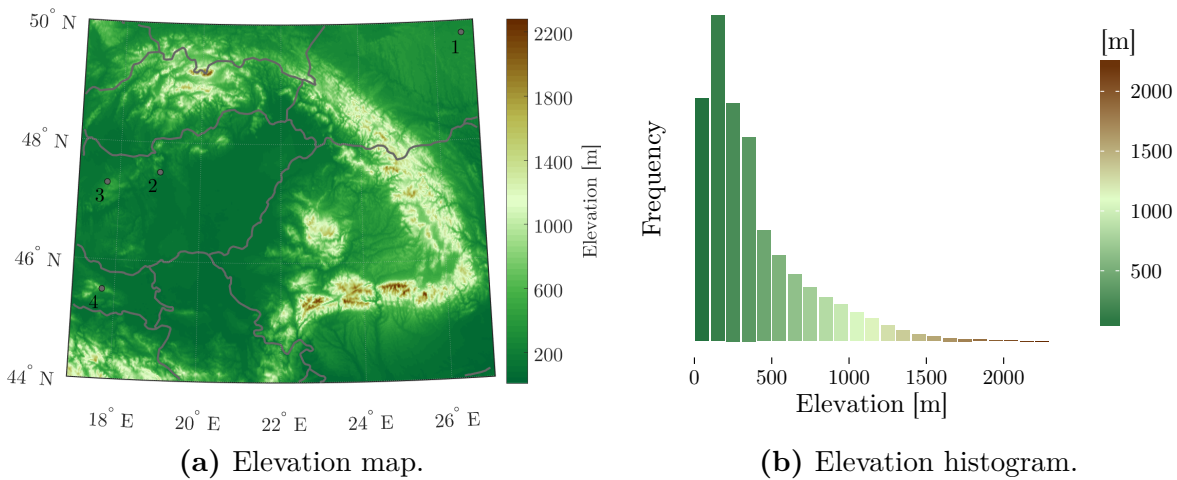


Figure 3.2 Illustration of the studied Carpathian region with elevation data with selected locations' ID (Table 3.1).

grid of daily mean snow cover and corresponding estimated water equivalent and snow depth simulations. The applied model is based on pre-finished CARPATCLIM grids of mean air temperature [$^{\circ}\text{C}$], precipitation sum [mm] and relative air humidity [%]. They are processed by the snow cover model regarding three main parts *accumulation of snow cover, ablation of snow cover and transformation of SWE to snow depth* [emphasis in the original].”

Further details about the applied procedures can be found in the cited document.

Uncertainty due to measurement error and due to the approximate nature of meteorological models are neglected. Unless otherwise noted this approach is taken in all chapters, Chapter 4 deals with this issue in details.

3.3 Effect on representative fractiles

Parameter estimation and model selection uncertainty quantifications are conducted for multiple locations of the Carpathian Region. The results of three representative locations are presented in more details: Location 1, 2 and 3 are identified as likely belonging to Weibull, Fréchet and Gumbel families, respectively (Table 3.1). To examine the annual ground snow load of other locations an online, interactive snow map is developed by the candidate (Annex A.1). Among others, it can be used to explore the effect of statistical uncertainties and to obtain characteristic ground snow loads.

Two-parameter Lognormal (LN2), three-parameter Lognormal (LN3), Gumbel and Generalized extreme value (GEV) distributions are selected for the comparative analysis (see Annex C.2). The LN2 model is typically adopted in the USA (ASCE, 2010) based on the research of Ellingwood and Redfield (1984), while the Czech Republic derived its snow map using LN3 distribution (Křivý and Stržíž, 2010). The Gumbel model is wide-spread in Europe (JCSS, 2001; Sanpaolesi et al., 1998). The GEV distribution comprises the

Table 3.1 Characteristics of selected locations to illustrate the effect of statistical uncertainties on representative fractiles.

Location ID*	Description	Representative of	Elevation [m]	Coordinates
1 (300)	Ukraine, highland	Weibull	299	49.8°N 26.7°E
2 (2735)	Hungary, lowland	Fréchet	241	47.3°N 17.7°E
3 (4553)	Croatia, highland	Gumbel	753	45.5°N 17.7°E
4 (2546)	Hungary, lowland	Fréchet [†]	226	47.5°N 19.0°E

* The first number is used as an identifier here, while the second – in brackets – is related to the database.

† Ambiguous, close to Gumbel.

Gumbel as a special type and it is supported by the extreme value theory (Coles, 2001). The standard parametrization of GEV distribution is used with shape (ξ), scale (σ) and location (μ) parameters, see Appendix C.2, Eq. C.20. The GEV distribution family comprises three special types: Weibull ($\xi < 0$), Gumbel ($\xi = 0$) and Fréchet ($\xi > 0$), see Figure 3.3. The first has an asymptotic upper bound while the latter two are unbounded.

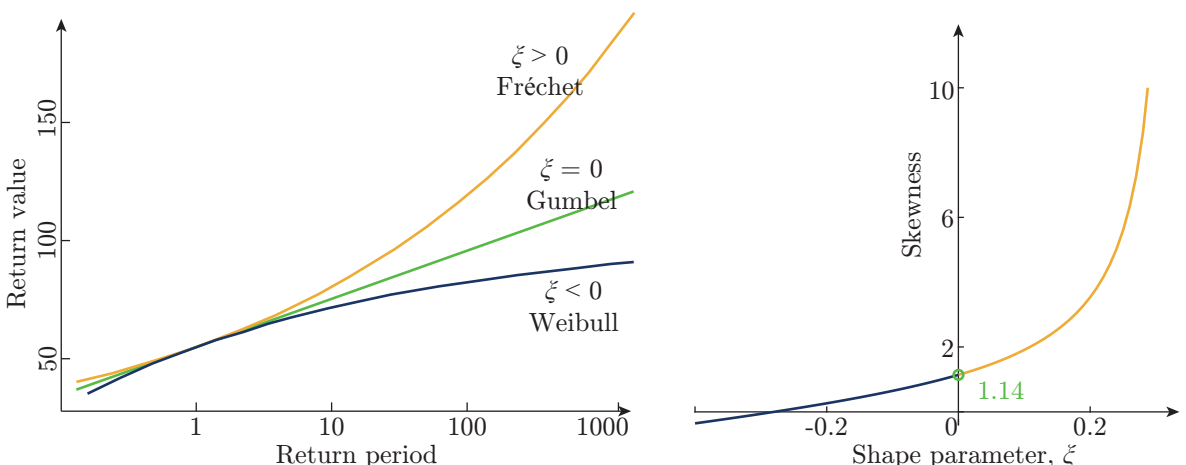


Figure 3.3 Illustration of GEV distribution family in Gumbel space (left), and the related skewness (right).

Generalized method of moments (GMM), maximum likelihood (ML), and Bayesian (B) approaches are applied to infer the parameters of the selected distributions. Uncertainty intervals are constructed using delta method, profile likelihood, and bootstrapping in the frequentist paradigm, and highest density and equal tail posterior distribution intervals in the Bayesian one¹. An important advantage of the Bayesian approach is that it treats unknown parameters as random variables, hence the incorporation of parameter estimation uncertainty into the model is straightforward. This is done by using the posterior predictive distribution (Eq.C.7).

¹These methods and terms are introduced in Chapter 2 and in Annex C.1.

3.3.1 Return value–return period plots

Maximum likelihood method is used to infer the distribution parameters and the results are plotted in Gumbel space (Annex C.3). Figure 3.4 compares the distribution functions fitted to the observations for Location 1. The edges of the colored ranges are the 90% confidence intervals obtained by delta method². From the plots it is clear that the model type substantially influences the extent of the uncertainty interval. The GEV plot shows that the observations likely belong to the Weibull family and have an upper bound. The other three distributions cannot capture such feature, since they have no upper bound by definition. The difference among the models becomes significant with increasing return period. Similar return value–return period plots are presented in Figure 3.5 and 3.6 for Locations 2 and 3, respectively.

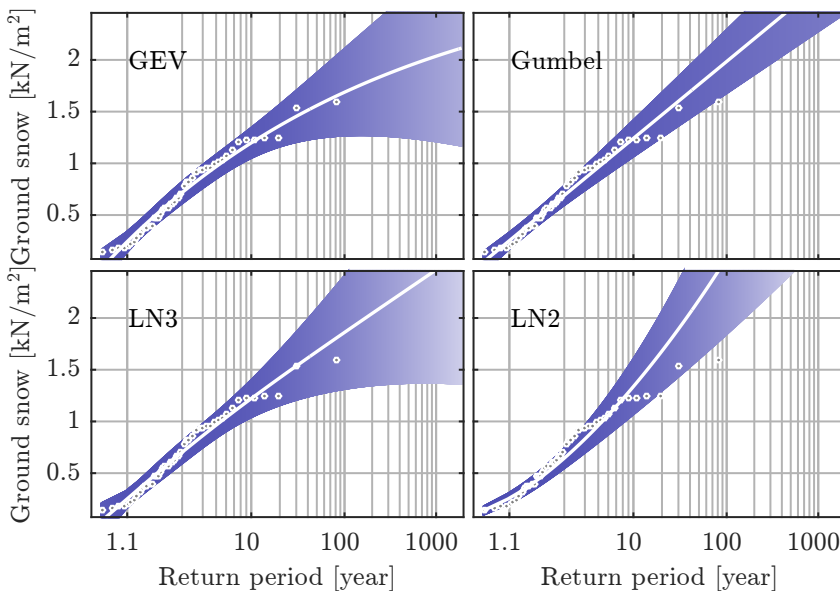


Figure 3.4 Location 1 (Weibull-like), ML fitted distributions with 90% confidence bands (delta method) in Gumbel space.

All return value–return period plots – with the exception of the Gumbel distribution – show that the confidence interval is rapidly widening as the number of observations reduces and with extrapolation to unobserved region. This is especially salient for the Fréchet-like location (Figure 3.5). Figure 3.6 indicates that even if the point estimates are similar, such as for GEV, Gumbel, and LN3, the confidence intervals can be substantially different in the extrapolated region. This information is completely lost if point estimates are considered only. Irrespectively of the location, the Gumbel distribution has significantly narrower confidence interval than the other models. This could be explained by its two parameters, which span smaller space.

²The coloring is “ink-preserving”: the same “amount of ink” is used for every vertical section, hence creating a linear transition from the narrowest (dark blue) to the widest interval (white). In a particular 2×2 figure, equal ranges have the same color on each subplot, thus the models are directly comparable based on coloring as well.

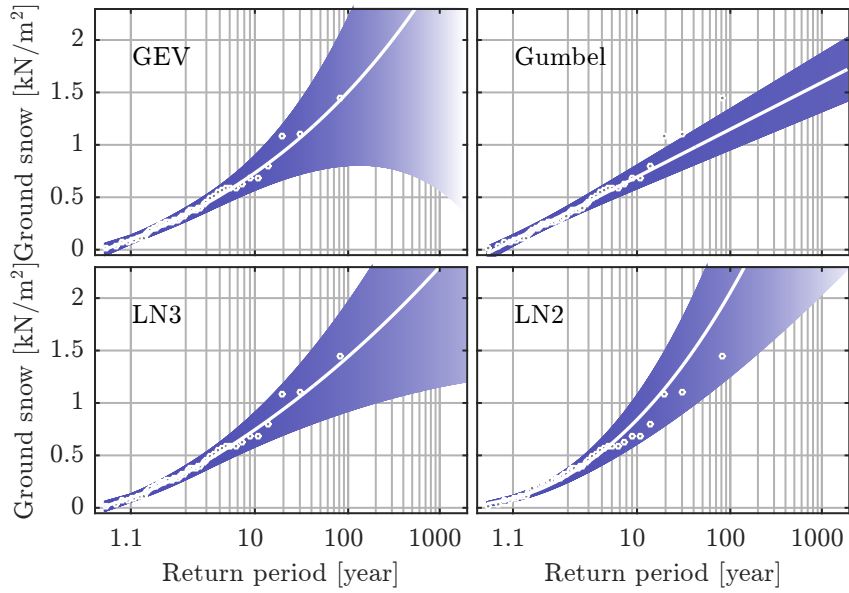


Figure 3.5 Location 2 (Fréchet-like), ML fitted distributions with 90% confidence bands (delta method) in Gumbel space.

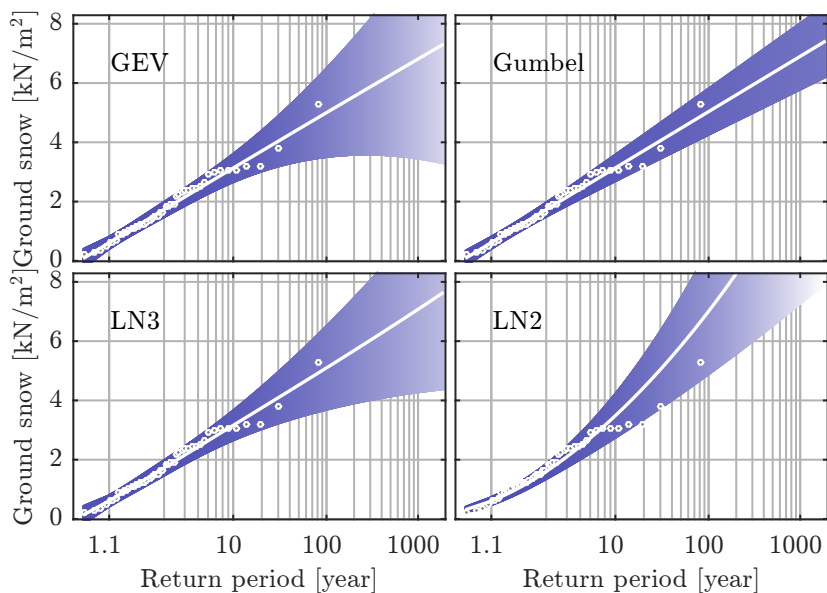


Figure 3.6 Location 3 (Gumbel-like), ML fitted distributions with 90% confidence bands (delta method) in Gumbel space.

By visual inspection the LN3 and GEV distributions seem to provide the best fit; however, in most cases their efficiency can hardly be proven by statistical and information theoretical methods, e.g. using Bayes weights (Eq.C.11) or AICc (Eq.C.9). On the other hand, the narrow confidence interval of the Gumbel model is unjustified and can be critical in the case of Fréchet-like observations. For Weibull and Gumbel-like samples the LN2 model seems to considerably overestimate the fractiles when compared with the other models.

3.3.2 Comparing representative fractiles

To further illustrate the extent and effect of statistical uncertainties, four representative fractiles are inferred using the same four distributions and various methods presented in Chapter 2. Return periods of 50, 100, 300 and 1000 years are selected. When these are interpreted as design point coordinates for the target reliability index of 3.8, then they correspond to sensitivity factors of 0.54, 0.61, 0.71 and 0.81, respectively. Thus, they are approximately representing structures with increasing susceptibility to snow loads; the former two may describe reinforced concrete and the latter two steel structures.

Point estimates with 90% level uncertainty intervals for Location 1 and 2 are presented in Figures 3.7 and 3.8. The bootstrapping point estimate represents the mean as the mode cannot be estimated directly from the sample. Based on 10 bootstrappings the standard error is less than 1% for LN2, LN3, and Gumbel distributions. It is about 7% for large return periods of GEV distribution, which implies that GEV fractiles are more sensitive to sampling variability.

For Location 1 the models show considerable difference even for the 50-year return period, for which the uncertainty intervals are relatively narrow. Compared with the Gumbel ML point estimate, the largest difference is observed for the Bayesian posterior predictive estimate of LN2 that is 1.4 times larger. The same ratios for 100, 300 and 1000-year return values are 1.5, 1.7 and 1.9, respectively. The uncertainty and the difference among point estimates for all the distributions become more significant with an increasing return period. The ML and Bayesian methods yield similar point estimates and comparable uncertainty intervals, the largest difference is observed for LN2. The GMM method gives smaller point estimates and narrower intervals than the other methods for Location 1, e.g. for LN3 it is 0.7-0.9 times smaller than the Bayesian posterior mean.

The results of comparative analyses for Location 2 are summarized in Figure 3.8. This location shows similar trends as of Location 1, but here the difference between Gumbel and the other models increases, particularly in respect of uncertainty intervals. The 1000-year return values based on the LN2, LN3, and GEV models – using the ML point estimates – are 2.4, 1.4, 1.6 times larger than that of the Gumbel distribution.

Besides the uncertainty intervals, the effect of parameter estimation uncertainty is quantified by the ratio of the corresponding posterior predictive and posterior mean fractiles (Table 3.2). The numbers indicate that particularly for GEV and LN3 distributions the

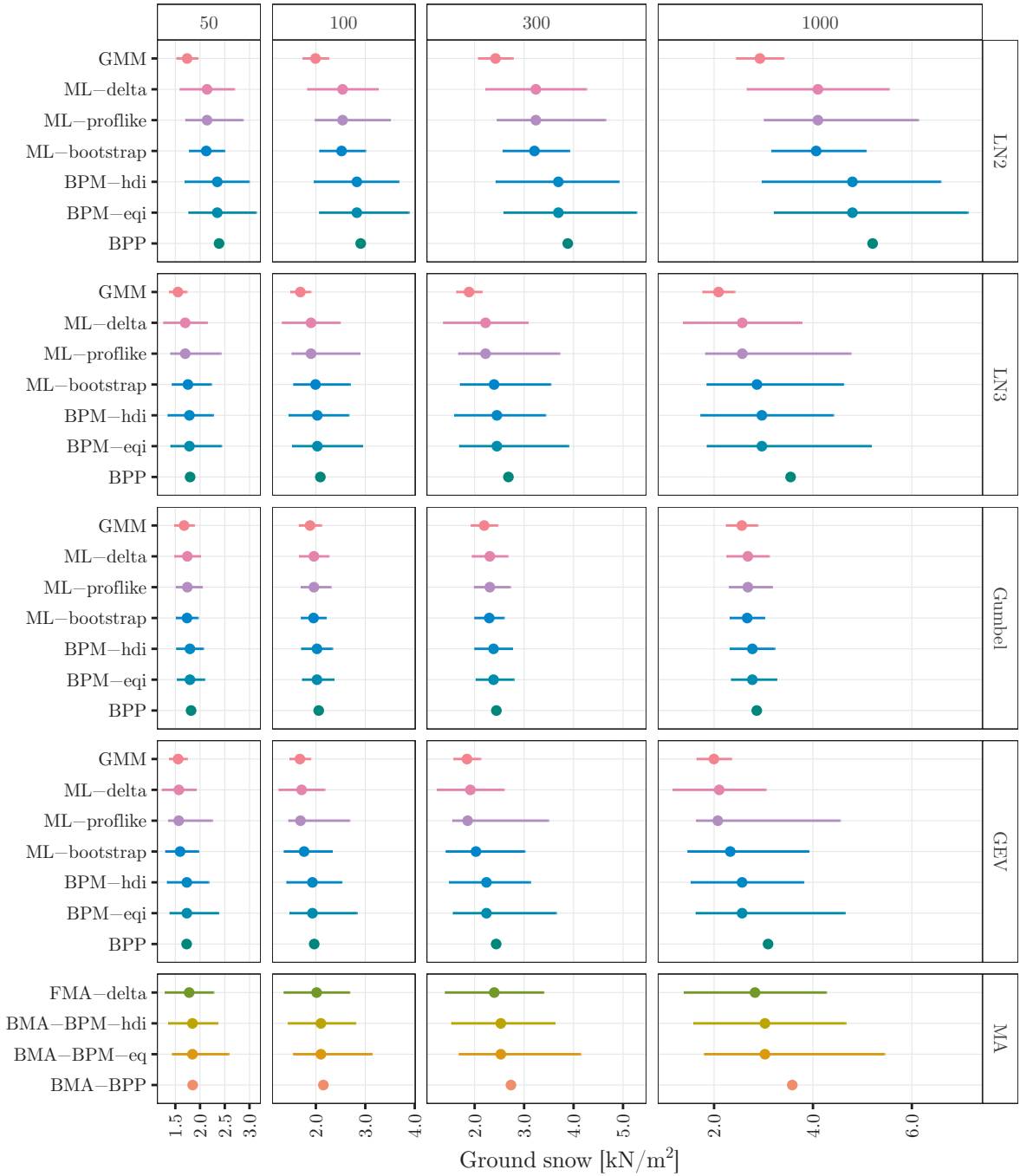


Figure 3.7 Location 1 (Weibull-like), summary of point estimates and 90% level uncertainty intervals for the considered models, methods and return periods (notations are explained in Table 2.2).

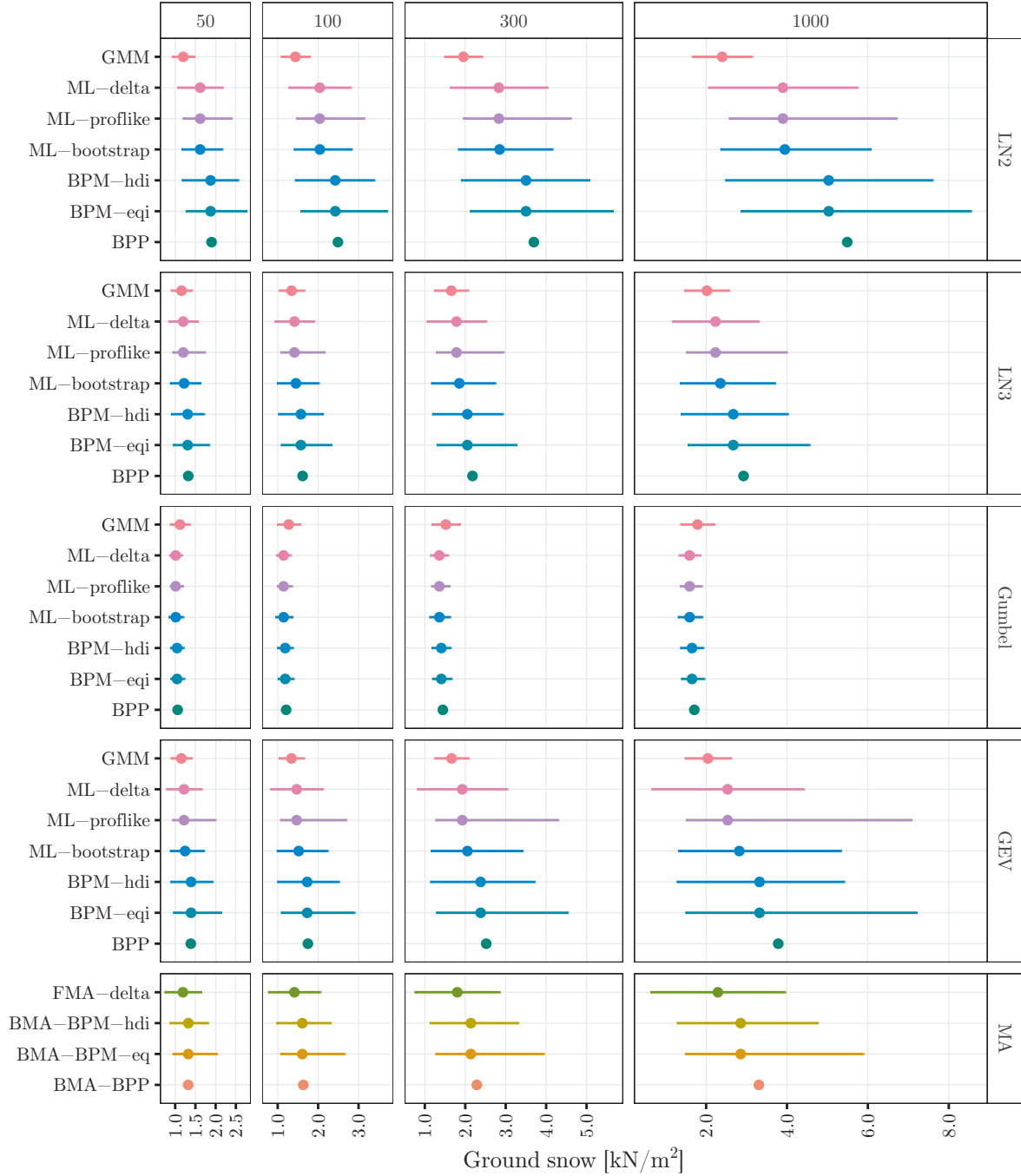


Figure 3.8 Location 2 (Fréchet-like), summary of point estimates and 90% level uncertainty intervals for the considered models, methods and return periods (notations are explained in Table 2.2).

effect of this uncertainty becomes significant with increasing return periods. For these the neglect of parameter estimation uncertainty leads to 20% underestimation of the return value.

Table 3.2 Location 1 (Weibull-like), ratio of the posterior predictive and posterior mean fractiles.

Return period [year]	50	100	300	1000
LN2	1.02	1.03	1.05	1.09
LN3	1.01	1.03	1.10	1.20
Gumbel	1.01	1.02	1.02	1.03
GEV	1.00	1.02	1.09	1.20
BMA	1.00	1.02	1.08	1.18

Return period estimates are compared for models with and without parameter estimation uncertainty in Table 3.3. For LN3 and GEV posterior predictive distributions, the return periods are half of those of the posterior mean distributions. The sampling variability has considerable effect on these values, hence they should be treated as indicative.

Table 3.3 Location 1 (Weibull-like), return periods, derived from posterior predictive distributions corresponding to 1000-year fractiles based on matching posterior mean distributions.

Distribution	LN2	LN3	Gumbel	GEV
Return period	704	436	779	413

The results (Table 3.2 and Figure 3.7-3.8) show that the distribution type has larger effect on the representative fractiles than the parameter estimation uncertainty. For example for Location 2 the ratios of the 1000-year fractile of the posterior predictive and posterior mean models are 1.09, 1.09, 1.03, 1.14 and 1.16 for LN2, LN3, Gumbel, GEV and MA models respectively. These illustrate the effect of parameter estimation uncertainty.

The model selection uncertainty can be assessed by comparing the posterior mean fractiles for different models. Normalizing the 1000-year fractile of posterior mean models with that of the Gumbel the ratios are 3.05, 1.62, 1.00, 2.01 and 1.73 for LN2, LN3, Gumbel, GEV and MA (model averaged) models respectively. For other locations the trend is similar but less pronounced.

3.3.3 Model averaging

Figures 3.7 and 3.8 show that the frequentist (FMA) and Bayesian (BMA) model averaged point and interval estimates yield comparable results, although the frequentist fractiles and intervals tend to be smaller. A more detailed exposition of model averaging of the Bayesian posterior marginals of the fractiles is illustrated in Figure 3.9. For larger return periods the difference among the models is increasing, thus the model averaged distribution might become multimodal. For Location 1, the Akaike weights are 0.19, 0.20, 0.43 and

0.18 for LN2, LN3, Gumbel, and GEV distributions, respectively. The Bayesian weights given in the same order are 0.13, 0.29, 0.30 and 0.28.

Model averaging certainly provides a better fit than any of the individual models, but since it typically requires considerable additional computational efforts, it is recommended mainly for critical structures and extreme hazards such as nuclear facilities and discharges, rather than common applications.

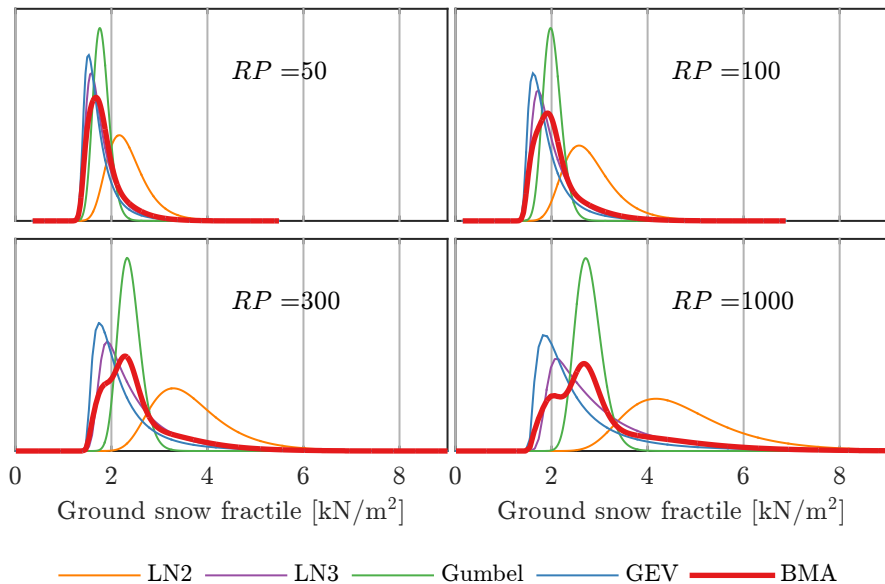


Figure 3.9 Location 1 (Weibull-like), posterior distributions of selected fractiles per different distribution types and Bayesian model averaging.

3.4 Effect on structural reliability

From a practical viewpoint the reliability index is often a more interesting parameter than representative fractiles. Thus the aim of this section is to investigate the effect of statistical uncertainties on structural reliability and to provide practical recommendations regarding their treatment. For this purpose, the reliability level of a generic structural member subjected to snow load is investigated. The effect of parameter estimation and model selection uncertainty in ground snow maxima is considered using frequentist and Bayesian techniques. In contrast with the typically used fixed model and “best” point estimates, model averaging and uncertainty intervals are used respectively.

3.4.1 Conceptual framework

To study the effect of statistical uncertainties, two sets of mechanical-probabilistic models with different representation of the ground snow load are compared. These two model sets are referred hereinafter as *analyzed* and *reference models*, and they differ solely in the ground snow distribution. For example, to illustrate the effect of parameter estimation

uncertainty, the *reference model* contains the posterior mean distribution while the *analyzed model* uses the posterior predictive distribution of ground snow. The *reference model* is used to find a mean value of the resistance to reach the target reliability level, which is selected as 3.8 for a considered 50-year reference period. The *analyzed model* has the same mean resistance and thus results based on this model show the effect of different ground snow representation. Throughout this section, different *analyzed-reference model* pairs are considered to illustrate various effects.

The ground snow data of Budapest are used for the analyses (Location 4 in Table 3.1). This location represents lowland areas in the Carpathian Region. Annual maxima from 49 winter seasons are extracted to infer the distributions.

3.4.2 Mechanical and probabilistic model

The mechanical model and loads of the analyzed structural member are presented in Figure 3.10. The flexural failure of a mid-span cross-section is selected as a representative ultimate limit state:

$$g(\mathbf{X}) = K_R \cdot R - K_E \cdot (\mu \cdot s_{g,50} + g_p) \cdot a \cdot \frac{L^2}{8}. \quad (3.1)$$

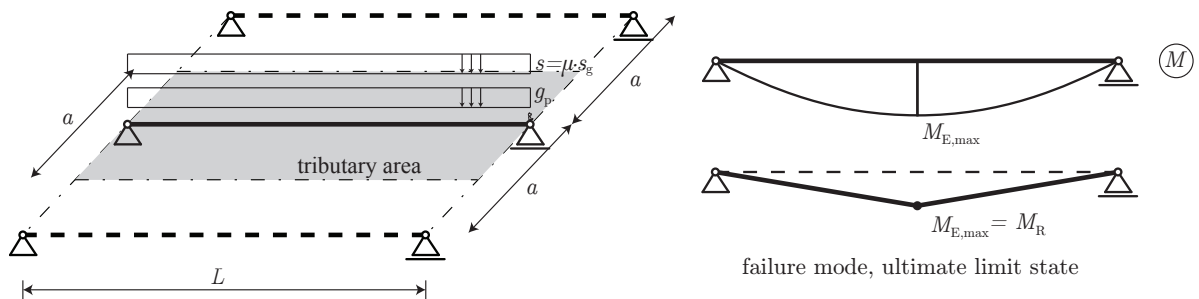


Figure 3.10 Illustration of the analyzed structural member and its failure mode.

The variables with their probabilistic model are given in Table 3.4. For the annual ground snow load ($s_{g,1}$) the sample mean and coefficient of variation (CV) are provided since these are also dependent on the fitted distribution type and technique applied to infer parameters of a distribution. The skewness of the analyzed sample is 1.6, indicating Fréchet-type distribution family (Figure 3.3). The commonly used Gumbel, Generalized extreme value, two-parameter Lognormal, and three-parameter Lognormal distributions are applied to represent the annual ground snow maxima. The connection between the 1-year and 50-year maxima distributions is established by assuming that the annual maxima are mutually independent.

Table 3.4 Probabilistic models of simple beam example.

Variable name	Distribution	Mean	CV	Reference
Resistance model uncertainty, K_R [-]	LN2	1.00	0.10	JCSS (2000b)
Resistance, R [kNm]	LN2	*	0.15	JCSS (2000b)
Load model uncertainty, K_E [-]	LN2	1.00	0.10	JCSS (2001)
Shape factor, μ [-]	LN2	0.80	0.17	Ellingwood and O'Rourke (1985)
Ground snow load, $s_{g,1}$ [kN/m ²]	†	0.4‡	0.7‡	Szalai et al. (2013)
Permanent load, g_p [kN/m ²]	N	§	0.10	JCSS (2001)
Beam span, L [m]	–	10	–	–
Bay distance, a [m]	–	3	–	–

* Based on FORM analysis to reach $\beta_{\text{target}} = 3.8$ with a fixed coefficient of variation.

† Gumbel, GEV, LN2, LN3, see Appendix C.2.

‡ Using unbiased moment estimates of the sample.

§ Varied to get different load ratios (χ).

– Not applicable/not available.

Different load ratios are achieved by varying the mean value of the permanent load while keeping its coefficient of variation fixed. The load ratio is defined as:

$$\chi = \frac{\mu_m \cdot s_{g,k}}{\mu_m \cdot s_{g,k} + g_m} \quad (3.2)$$

where the m and k subscripts refer to mean and characteristic values respectively.

3.4.3 Statistical analysis

Frequentist and Bayesian statistical techniques are applied to fit models to the snow maxima and to quantify statistical uncertainties. For the current analysis their most important difference is that the Bayesian approach treats parameters as random variables, thus makes it possible to integrate their estimation uncertainties into the failure probability.

Maximum likelihood and posterior mean are used as point estimates per frequentist and Bayesian approaches respectively. Accordingly, the distributions specified by these point estimates are referred to as maximum likelihood and posterior mean distributions (Table 2.2).

For the Bayesian calculations vague priors are applied for both to the parameters and to the models as well, and numerical integration is used to calculate the posterior and posterior predictive distributions. Practically infinite ranges are selected for the integrations and uniform priors are adopted on these intervals.

Results of distribution fitting

The statistical uncertainties of ground snow models are illustrated on return value-return period plots with confidence bands (Figure 3.11). The solid white lines and blue regions

show the ML point estimates and 90% confidence bands respectively; the latter illustrates the parameter estimation uncertainty. The dashed white line and green region correspond to the FMA point estimate and 90% confidence bands respectively. The extent of model selection uncertainty can be judged by comparing the blue regions to the green ones. For example, for the Gumbel distribution the blue region is considerably wider than the green, this implies that the Gumbel confidence interval is too narrow. This is also supported by the evidence that maxima of the sample are outside of the 90% confidence band (Figure 3.11). This can be observed also for other locations from the CarpatClim database with skewness exceeding 1.2.

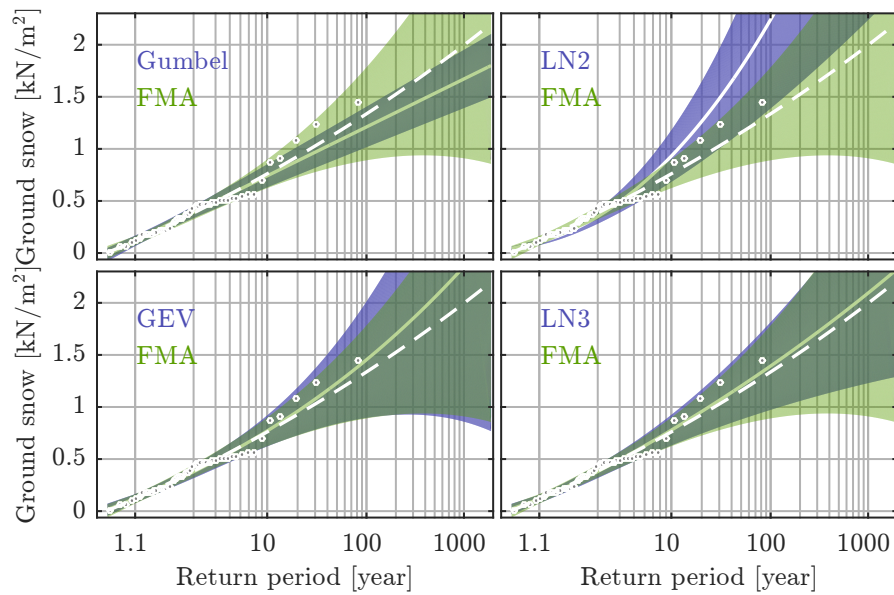


Figure 3.11 Annual maxima return value–return period plots with 90% confidence bands for the selected (blue + solid white) and FMA (green + dashed white) distributions in Gumbel space.

The Bayesian analysis yields to similar results as the frequentist, although the averaging weights are slightly favoring the three-parameter models over the two-parameter ones (Table 3.5). Both methods indicate that there is a strong evidence against the LN2 model for this location.

Table 3.5 Summary of model averaging weights.

Model	Akaike weight, w	Bayesian weight, b
GEV	0.29	0.37
Gumbel	0.43	0.25
LN3	0.28	0.38
LN2	0.004	0.002

Table 3.6 shows the characteristic values (0.98 fractile) for the considered models and statistical approaches. With the exception of LN2, which is not supported by the data, the models yield to comparable values. Due to parameter estimation uncertainty the

largest increase is observed for LN3, it is about 8%. The Gumbel model underestimates the model averaged characteristic value by about 10%. The results for this location are in good agreement with the 1.25 kN/m^2 characteristic value specified in the Hungarian National Annex of EN 1991-1-3.

Table 3.6 Summary of ground snow load characteristic values for Budapest [kN/m^2].

Distribution	Maximum likelihood (ML)	Bayesian posterior mean (BPM)	Bayesian posterior predictive (BPM)
GEV	1.23	1.34	1.38
Gumbel	1.07	1.11	1.12
LN3	1.20	1.18	1.28
LN2	1.78	1.90	1.98
FMA	1.16	—	—
BMA	—	1.21	1.27

– Not applicable.

3.4.4 Reliability analysis

Reliability of the selected structural member is analyzed using the first order reliability method (FORM) considering the various probabilistic representation of the ground snow maxima. Initially a commonly applied Gumbel distribution is investigated. The *reference model* is the Gumbel maximum likelihood distribution, while the analyzed models are the four selected maximum likelihood and the frequentist model averaged distributions. The reliability indices with approximate 90% confidence bands are presented in Figure 3.12. These bands express solely the statistical uncertainties in the ground snow distributions.

This analysis represents the following scenario: Gumbel ML distribution is adopted for snow maxima and a structural member is designed to achieve the target reliability. The failure probability is then calculated assuming that the snow maxima follows other distributions. Figure 3.12 shows the followings:

- The distribution type has substantial effect on the reliability, e.g. for large load ratios the GEV model yields to about 50 times larger failure probability than the Gumbel.
- All models yield to smaller reliability index than the *reference* Gumbel.
- Compared to the FMA model, the failure probability and uncertainty intervals are largely underestimated by the Gumbel model.

As the LN2 model is clearly far from the FMA, and not supported by the data (Table 3.5), it is discarded from the following analyses. The same analysis with BPM models yields to similar results as those of the maximum likelihood based. Since the Bayes

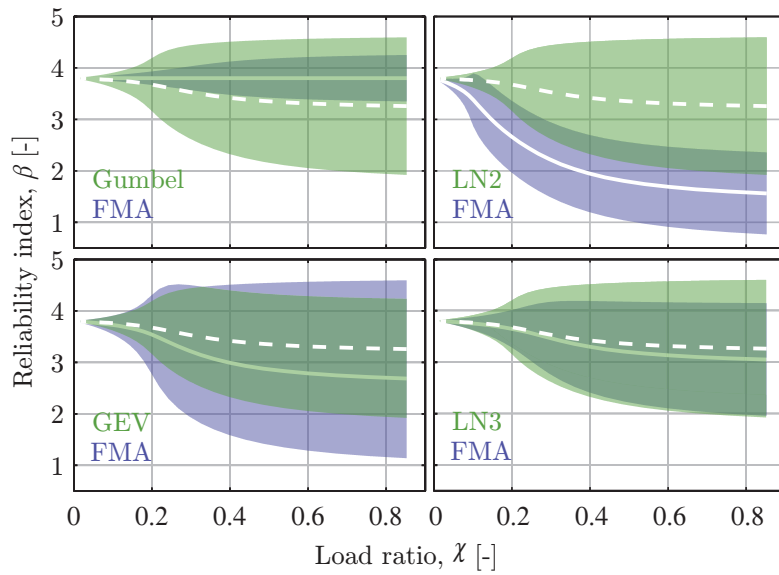


Figure 3.12 Load ratio—reliability index plots with 90% confidence bands for the selected (green + solid white) and FMA (blue + dashed white) ground snow distributions, using Gumbel ML as *reference model*.

weights favor the GEV and LN3 models, the underestimation of Gumbel model is even larger than in the case of FMA.

Figure 3.13 shows the effect of statistical uncertainties, here the *reference model* is the BPM for each selected model, hence the solid green line is horizontal, indicating the 3.8 value. The *analyzed models* are the BPP and BMA models. The main observations from Figure 3.13 are as follows:

- The effect of parameter estimation uncertainty within the Gumbel model is small; however, the model uncertainty has substantial effect, significantly exceeding an order of magnitude in failure probability.
- For GEV and LN3 the consideration of parameter estimation uncertainty gives about 20 and 5 times larger failure probability, respectively.
- These effects are rapidly increasing with increasing load ratio and reaching a relatively stable level after ratio of 0.3.

Although Table 3.6 indicates only minor differences in the characteristic values for the selected probabilistic models, the reliability indices in Figure 3.13 suggest that the model selection is a key issue for reliability analysis. Consequently, comparison of characteristic values seems to be insufficient to support decision about appropriate probabilistic model.

3.5 Application example: Eiffel-hall of Budapest

The Eiffel-hall of Budapest is selected to demonstrate the effect of statistical uncertainties on a real life example. The structure is introduced in Annex B.2, here only the essential

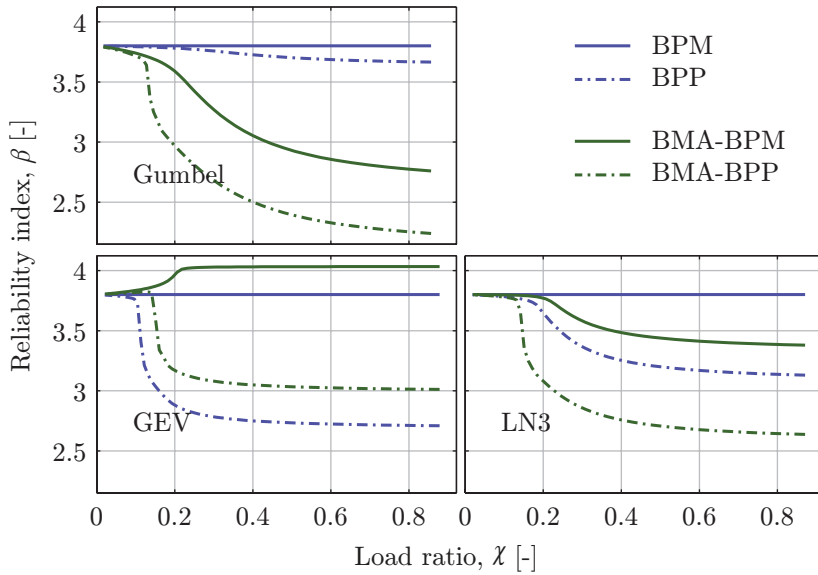


Figure 3.13 Load ratio—reliability index plots for models with (dash-dot) and without parameter estimation uncertainty (solid).

details, which are required to interpret the results, are provided. Maximum likelihood method is applied to infer the parameters of annual ground snow maxima of the site. Two-parameter Lognormal, three-parameter Lognormal, Gumbel, and Generalized extreme value distributions are considered for the analysis. The results in terms of reliability indices and normalized failure probabilities are given in Table 3.7. 50-year reference period is used for all calculations of the structure.

Table 3.7 Summary of the reliability measures of the selected purlin.

	Gumbel	GEV	LN2	LN3
β	3.27	2.88	1.42	2.86
$P_f/P_{f,Gumbel}$	1.00	3.68	145	3.96

As the site has Fréchet-like distribution with shape parameter greater than zero, all models yield to larger failure probability than that of the Gumbel. The LN3 and GEV failure probabilities are similar and four times larger than that of the Gumbel. The underestimation of Gumbel distribution is more salient for the LN2 distribution that leads to two order of magnitude difference and well represents the significant effect of model selection uncertainty.

3.6 Discussion

The main focus of this chapter is the quantification and propagation of statistical uncertainties. From a broader engineering perspective that views reliability analysis as a tool for decision making, the model selection uncertainty problem is recommended to be resolved

by agreeing on a conventional distribution type (Ditlevsen, 1994; Melchers, 2002). We support this approach; however, the decision on the selected distribution should be backed by appropriate techniques for model uncertainty analysis. For safety-critical facilities and actions it still might be desirable to analyze this source of uncertainty in detail. The Generalized extreme value distribution is recommended to represent annual maxima of ground snow extremes. This is not a novel recommendation as multiple studies considered GEV or members of GEV family, but for standardization they often settled with other types (Ellingwood and Redfield, 1984; Sanpaolesi et al., 1998).

Regarding parameter estimation uncertainty it is argued that it is often advisable to be considered in reliability studies by using the posterior predictive distribution. The main arguments are that reliability analysis is inherently predictive, the failure probability is governed by the very uncertain distribution tails, and after the selection of distribution function it is unambiguous to construct the posterior predictive estimates. The presented uncertainty interval construction techniques require no or several additional limit state function evaluations as compared to the standard reliability methods such as FORM, and thus are applicable to complex problems as well.

It is argued that in structural reliability every random variable should be represented by its posterior predictive distribution and for critical cases model averaging should be adopted. This is not a novel in-sight, treatment of statistical uncertainties is well developed in the statistical literature (Aitchison and Dunsmore, 1980; Wit et al., 2012) and also advocated in relation to probabilistic engineering analysis (Coles et al., 2003; Der Kiureghian, 2008; Van Gelder, 2000).

The treatment of uncertainties is always related to the considered “model universe”, i.e. the physical and mathematical framework (model) adopted to describe the reality. If point estimates are used the models derived from 5 realizations would convey the same confidence as those based on 1000 data. In contrast, the Bayesian posterior predictive distribution automatically penalizes the small sample size based predictions. Both presented model averaging (MA) techniques depend on the considered models (the weights in Eq.C.11), thus can be interpreted only in respect of the space of selected models.

It should be noted that the results are based on the analysis of few locations with fixed number of observations. For other phenomenon, such as wind extremes, which are typically following Weibull distribution, the effects are anticipated to be smaller. However, smaller number of observations can considerably increase statistical uncertainties. Moreover, it is expected that these uncertainties can be reduced by taking into account more informative priors, which are often available.

To support future snow maxima related studies the posterior distributions of GEV parameters related to lowlands, and mountains and highlands of the Carpathian Region are calculated and given in Annex A.2. These can be used as prior information for regions with similar climatic conditions.

3.7 Summary and conclusions

The current practice in civil engineering prevalently overlooks parameter estimation and model selection uncertainties in probabilistic calculations. To assess the effect of this simplification frequentist and Bayesian statistics along with reliability analyses are utilized and the following conclusions are drawn:

- The effect of parameter estimation uncertainty within the Gumbel model is small; however, the model uncertainty has substantial effect, considerably exceeding an order of magnitude in failure probability.
- The distribution choice may lead to 50 times increase in failure probability (GEV vs. Gumbel).
- For the Generalized extreme value and three-parameter Lognormal distributions the consideration of parameter estimation uncertainty can yield to about 20 and 5 times increase in failure probability, respectively.
- The use of “best” point estimates such as maximum likelihood estimator is not conservative and can have practically significant effect on calculated failure probability.

The following practical recommendations and observations are made based on completed analyses:

For common structures and standardization:

- Consensus on the conventional distribution type is needed.
- The commonly applied Gumbel model for annual maxima is often inadequate, this means that it underestimates failure probability and has deceptively narrow uncertainty interval, this model assumption should be revisited.
- Bayesian approach is recommended to handle parameter estimation uncertainties.

For structures that require fully probabilistic risk assessment framework:

- Bayesian statistics is promoted to incorporate both model selection and parameter estimation uncertainties.
- Generalized extreme value distribution is recommended for probabilistic modeling of extremes.
- Inclusion of all available data and prior information is recommended; however, guidance on priors is needed.

The consideration of statistical uncertainties can be especially important for predicting extremes under changing climate for which one cannot rely on historical observations.

Chapter 4

Effect of measurement uncertainty

Observations are inevitably contaminated with measurement uncertainty, which is a predominant source of uncertainty in some cases. In reliability analysis, probabilistic models are typically fitted to measurements without considering this uncertainty. Hence, this chapter intends to explore the effect of this simplification on structural reliability and to provide recommendations on its treatment. Statistical and interval-based approaches are used to quantify and to propagate measurement uncertainty. They are critically compared by analyzing ground snow measurements, which are often affected by large measurement uncertainty. It is propagated through the mechanical model of a generic structure to investigate its effect on reliability. The results indicate that measurement uncertainty may lead to significant (order of magnitude) underestimation of failure probability and should be taken into account in reliability analysis. Ranges of the key parameters are identified where measurement uncertainty should be considered. For practical applications, the lower interval bound and predictive reliability index are recommended as point estimates using interval and statistical analysis, respectively. The point estimates should be accompanied by uncertainty intervals, which convey valuable information about the credibility of results.

4.1 Problem statement and the state of the art

Models accounting for all uncertainties are of a considerable interest in structural reliability since these are the bases of design specifications, hence impacting the building and structure stocks of large regions. Snow is particularly important for light-weight structures for which it is typically the governing action. To our knowledge, the effect of snow measurement uncertainty on structural reliability has not yet been studied and other probabilistic models are treated similarly in civil engineering. For instance, neither the joint European research on snow actions ([Sanpaolesi et al., 1998](#)) or the JCSS Probabilistic Model Code ([JCSS, 2000a](#)) provides any information on the treatment of measurement uncertainty and its effect. Therefore, the aim of this chapter is to explore the effect of this simplification on structural reliability and to provide recommendations on its treatment.

Observations are inevitably contaminated with measurement uncertainty (MU), which is a predominant source of uncertainty in some cases. Uncertainty is understood here as the lack of knowledge (epistemic) and natural variability (aleatory)¹ not including known systematic error, which are assumed to be adjusted. In reliability analysis, probabilistic models are typically fitted to measurements without considering their uncertainty. This is the case for snow measurements where often only the snow depth is measured and the applied techniques makes the derived loads highly uncertain, for example, the uncertainty range can reach 50% of the measured depth².

The World Meteorological Organization conducted a comprehensive comparative study on the then available solid precipitation measurement techniques and experimentally confirmed that measurements should be adjusted for wetting loss, evaporation loss, and wind induced undercatch (Goodison et al., 1998). They found that the snow catch ratio of the four most widely used gauges ranges from 20% to 70% at 6 m/s wind speed. Even for automated systems, measurement error in solid precipitation can vary from 20% to 50% due to undercatch in windy conditions (Rasmussen et al., 2012). Although these mainly contribute to systematic error they indicate uncertainties in snow measurements as these errors cannot be exactly corrected. For instance coefficient of determination (R^2) values vary from 0.40 to 0.80 for the fitted wind correction equations at certain sites; these are associated with about 10% standard error in catchment ratio. Additional uncertainty may be introduced if no site specific auxiliary data, e.g. wind speed measurements, are available (Goodison et al., 1998). These issues are not limited to snow measurements but valid for all evidence based models – that is for every model – although their importance may vary.

4.2 Solution strategy

4.2.1 Adopted approaches

We assume that measurements are corrected for known systematic errors. Additionally, the following model is assumed to describe the connection between observed (Y) and real, true, physical (X) values, i.e. the variable of interest:

$$(\text{true, real}^3)X \xrightarrow{h(X,E)} Y(\text{observed}). \quad (4.1)$$

The $h(X, E)$ function represents the mathematical relationship between the true and observed random variables referred hereinafter as reality-observation link. E covers the unknown processes contributing to measurement uncertainty. The recommended probabilistic models – typically distributions – in the literature are almost exclusively

¹This division is subjective as conditioned on the selected “model universe”.

²Based on a personal correspondence with a meteorologist.

³Herein we tacitly assume the existence of some objective reality independent of the observer.

given for the true variable and not for the observed, potentially contaminated one. Possible reasons for this are that:

- The contamination is commonly site- and measuring technique-dependent, thus no general recommendations can be given for the distribution of Y .
- The model type is often selected based on theoretical arguments considering the physical phenomena generating X , for example Normal distribution if X is the result of summation; Lognormal if X is the product of random variables; extreme value distribution if X is related to extremes.
- Structural reliability ultimately depends on X and not on Y , although we are limited to access only Y .

The last point is especially important since structures are subjected to actions coming from X and not from Y ; the latter is affected by our ignorance or inability to make accurate measurements (epistemic uncertainty). In a broader sense this also applies for X , but for now we remain in the commonly accepted model universe of engineering and treat X as a random variable. If the distribution type of X is known or agreed, then the reality-observation link uniquely determines the distribution of Y . Hence, if any measurement uncertainty is present, its distribution type almost certainly differs from the distribution of X . This is prevalently neglected while fitting distributions in civil engineering – Y is assumed to be distributed as X . This simplification is acceptable in some practical cases. This method is termed hereinafter as Approach 1 while it is referred to as Approach 2 when the difference between distributions is appreciated:

Approach 1 Use the probabilistic model of true random variable (X) and treat the observations – contaminated with measurement uncertainty – (\mathbf{y}) as the realizations of this model: $\mathbf{y} \sim X$.

Approach 2 Differentiate between the distribution of true and observed random variables. Within this, the following two sub-approaches are considered:

Approach 2a Representation of measurement uncertainty with intervals at the level of observations and propagating them to the derived parameters via interval analysis. As interval representation by nature contains no information about the reality-observation link, the decontamination of observations is not possible.

Approach 2b Representation of measurement uncertainty with a probability distribution. Use a mathematical model ($h(X, E)$) to describe the connection between measurement uncertainty (E), true phenomenon (X), and observed phenomenon (Y). Based on this model and on observations (\mathbf{y}), infer the parameters of the true random variable (X). These issues are referred to as *measurement error problems* in the literature (Kondlo, 2010).

Additional assumptions for all considered approaches:

- $\mathbf{y} = \{y_1, y_2, \dots, y_n\}$ and $\mathbf{x} = \{x_1, x_2, \dots, x_n\}$ each are independent, identically distributed realizations; \mathbf{y} is contaminated with measurement uncertainty.
- The realizations of the true phenomenon (\mathbf{x}) and measurement uncertainty ($\boldsymbol{\epsilon}$) are mutually independent.
- The true phenomenon (X) follows arbitrary, but known distribution type.
- Only for Approach 2b: the measurement uncertainty (E) follows arbitrary, but known distribution type, and the reality-observation link is also known.

4.2.2 Uncertainty representation and propagation

Interval analysis

Interval representation is one possible approach to quantify uncertainty in an observed variable: the width of the interval expresses our uncertainty (Figure 4.1). In this concept the true value is certainly within the interval but we know nothing about how likely it takes a particular value from that. In other words no probability distribution function is assumed over the interval, thus it expresses greater ignorance than probability distributions can (Huber, 2010). The basic objective of interval analysis is to propagate the interval uncertainty of input variables to the outputs. Its main challenge is to calculate the interval bounds without overestimating them. This typically occurs if floating point computations are simply replaced by intervals and caused by interval dependency (Moore et al., 2009). Since the operators are typically not known explicitly and are non-monotonic, special algorithms are needed to obtain sufficiently narrow approximate interval bounds. Interval analysis is traditionally used to model floating point truncation error in numerical computations; however, it is also successfully applied to various civil engineering issues, for instance, reliability of structures (Qiu et al., 2008) and systems (Qiu et al., 2007). Rao et al. (2015) analyzed the effect of incorrect fitting on trusses and frames using mixed interval finite element formulation, using intervals to model fabrication errors. Muhamma et al. (2015) demonstrated the feasibility of non-linear interval finite element analysis for beam-column structures. In their study geometric, material and load uncertainties are modeled with intervals. In this study the general definition of interval variables is used and constrained numerical optimization is applied to find the interval endpoints. This is motivated by the readily available optimization algorithms, and its feasibility due to the analyzed simple, computationally cheap examples. For computationally demanding models more efficient algorithms are available (Alibrandi and Koh, 2015; Muhamma et al., 2015; Zhang et al., 2010). Intervals in this study are defined by midpoint and radius (ϵ_r), the midpoint is taken as the observed value, y_i , see Figure 4.1. In this approach, the true value is assumed to be certainly within the interval given the modeling assumptions are valid.

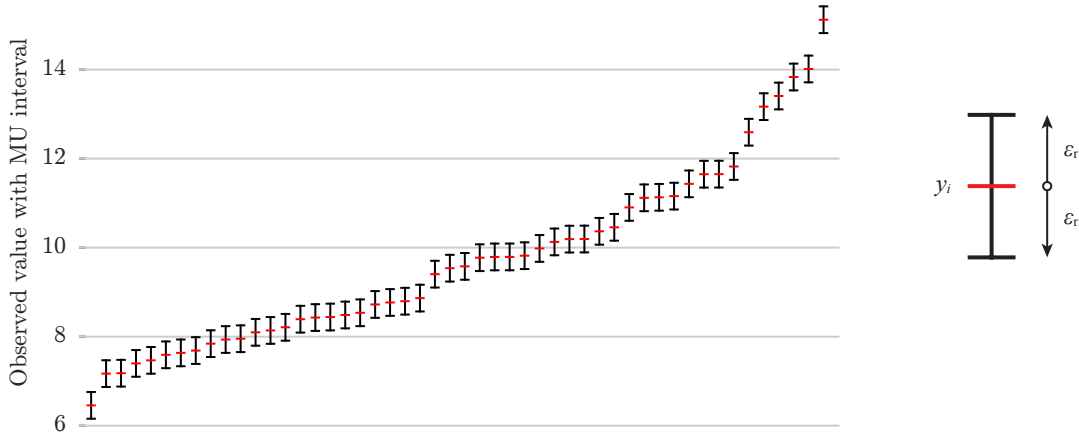


Figure 4.1 Interval representation of measurement uncertainty (black) on a sorted random sample (red). The sample is generated from Q_1 with properties given in Table 4.1 and $CV_{Q_1} = 0.2$.

Statistical analysis

An alternative approach to represent measurement uncertainty is statistical by means of probability distributions. The likelihood function depends on the reality-observation link (Eq.4.1). This connection is also uncertain, but for simplicity, known relationship is assumed here and a possible treatment of this uncertainty is discussed in Section 4.5. Algebra of random variables can be used to obtain the likelihood function reflecting the distribution of involved random variables and the reality-observation link:

$$L(\boldsymbol{\theta}_X, \boldsymbol{\theta}_E | \mathbf{x}, \boldsymbol{\epsilon}) = \prod_{i=1}^n p(h(x_i, \epsilon_i) | \boldsymbol{\theta}_X, \boldsymbol{\theta}_E) \quad (4.2)$$

where $\boldsymbol{\theta}_X$ and $\boldsymbol{\theta}_E$ are the parameters of true and measurement uncertainty random variables, respectively. In Approach 1, this means no additional complication because the observations are assumed to be distributed as the true random variable since the reality-observation link is neglected. However, in Approach 2b the likelihood function should be constructed to remove the effect of measurement uncertainty (E) from the variable of interest (X). The *measurement error problem* arises in many areas where only the contaminated values are attainable to the observer but the interest lays in the inference of true, uncontaminated values. Among others, these areas include astronomy, econometrics, biometrics, medical statistics, and image reconstruction (Koen and Kondlo, 2009; Meister, 2009; Stefanski and Bay, 2000). A straightforward solution is to construct the likelihood function (Eq.4.2) and to infer the parameters of the variable of interest (X) by a selected method. To our knowledge this approach has not been applied in civil engineering yet. Maximum likelihood method is used herein to infer the parameters in the statistical formulation of the measurement uncertainty problem. Additive and multiplicative reality-observation links are considered. For the additive relationship: $Y = X + E$, the density function of the sum of two independent, continuous random variables is obtained by

convolution:

$$f_Y(y) = (f_X * f_E)(y) = \int_{-\infty}^{\infty} f_X(y-x) \cdot f_E(x) \cdot dx. \quad (4.3)$$

Here, for convenience the $p(\cdot)$ notation of density functions is replaced with one that identifies the function elsewhere than in the argument, $f_X(x) \equiv p(x)$. The integral can be efficiently solved by utilizing Fourier transformation since afterwards it reduces to a point-wise multiplication. Here, the fast-Fourier transformation is used to accomplish this task. For the multiplicative relationship: $Y = X \cdot E$, the density function of the product of two independent, continuous random variables is obtained by computing the following integral:

$$f_Y(y) = \int_{-\infty}^{\infty} f_X(x) \cdot f_E\left(\frac{y}{x}\right) \cdot \frac{1}{|x|} \cdot dx. \quad (4.4)$$

This can be efficiently solved by Mellin transformation but here the integral is directly calculated due to the small computational burden. Sampling variability (parameter estimation uncertainty) is accounted for by using the predictive reliability index, $\tilde{\beta}$ (Der Kiureghian, 1989):

$$\tilde{\beta} = \frac{\text{mean}_B}{\sqrt{1 + \text{std}_B^2}} \approx \frac{\text{median}_B}{\sqrt{1 + (1.483 \cdot \text{mad}_B)^2}} \quad (4.5)$$

where B is the posterior reliability index, std and mad are the standard deviation and median absolute deviation of B , respectively. The formulation with median and mad are used in this chapter, as that is more robust to outliers. Eq.4.5 is an approximation as it is valid only for Normal distributed B . Additionally, the statistics are estimated from repeated analyses, and no Bayesian formulation of the reliability problem is used, even though that was used to derive the formula. For this study it is deemed sufficiently accurate to indicate tendencies and to identify critical cases.

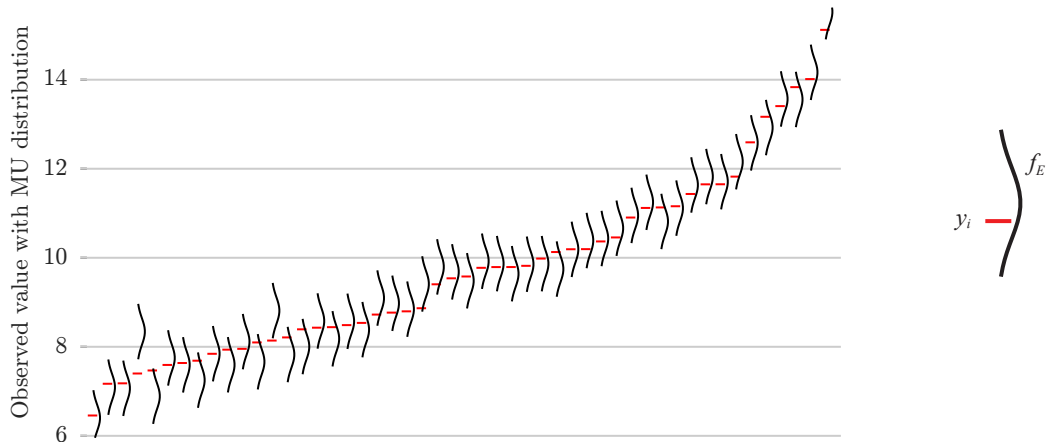


Figure 4.2 Illustration of probability distribution representation of measurement uncertainty (black) on a sorted random sample (red). The sample is generated from Q_1 with properties given in Table 4.1 and $CV_{Q_1} = 0.2$.

4.3 Example: reliability of a generic structure

4.3.1 Model description

The reliability of a simple structural member is analyzed using a generic limit state function:

$$g(\mathbf{X}) = R - (G + Q_{50}). \quad (4.6)$$

It represents a structure subjected to permanent (G) and variable (Q_{50}) actions, where the subscript 50 indicates 50-year reference period (common design working life). The probabilistic model of involved random variables are based on the recommendations of (JCSS, 2000a) and summarized in Table 4.1. For simplicity only the variable action is assumed to be affected by measurement uncertainty; it could be easily extended to more variables. Coefficient of variations 0.2, 0.4 for Q_1 represent annual snow maxima of mountains, highlands, while 0.6 characterizes lowlands in the Carpathian Region. The Lognormal model for snow maxima is typically adopted in the USA (ASCE, 2010), while the Gumbel model is widespread in Europe (JCSS, 2001; Sanpaolesi et al., 1998). The Normal and Gumbel distributions are light-tailed while the Lognormal is heavy-tailed. The adopted distributions and parameter ranges cover also other variable actions such as wind and thermal actions, thus the results can be readily generalized.

The annual maxima are assumed to be independent:

$$F_{50}(q) = F_1(q)^{50} \quad (4.7)$$

where $F(\cdot)$ is the cumulative distribution function.

Table 4.1 Probabilistic models.

Variable name (symbol)	Distribution	Mean	CV
Resistance (R)	Lognormal	*	0.10
Permanent action (G)	Normal	8	0.10
Variable action (Q_1) [†]	Normal, Lognormal, Gumbel	10	[0.20, 0.40, 0.60]

* set to reach $\beta_{\text{target}} = 3.8$ for each combination of inputs.

† the specified parameters are used to generate 50-element sample and the parameters of the model used in reliability analysis are inferred from it.

4.3.2 Interval and reliability analysis

To model the effect of measurement uncertainty, 50 random observations are generated from Q_1 , these are treated as observed (Y) values as the reality-observation link by definition is unknown in interval representation (Figure 4.3). Then intervals are centered at observations and various interval radiiuses are considered. Using these interval variables, the distribution of Q_1 is fitted by the method of moments, which is a widely used approach

in civil engineering (Sanpaolesi et al., 1998) and was proved to be robust e.g. for modeling hydrological extremes (Madsen et al., 1997). The hybrid interval-probabilistic reliability problem is solved using optimization and first order reliability method (FORM). An outcome of the analysis is an interval reliability index.

The upper bound of it is irrelevant from safety point of view and the lower bound is recommended for practical applications (Qiu et al., 2007). This is due to the special nature of intervals and how they represent uncertainty: the real value can be anything within the interval but one cannot assume that all points are equally likely (principle of indifference) at least because the consequence of specific values are not equal. Hence we chose the recommended, careful engineering approach and use the lower endpoint of the reliability index interval as representative value.

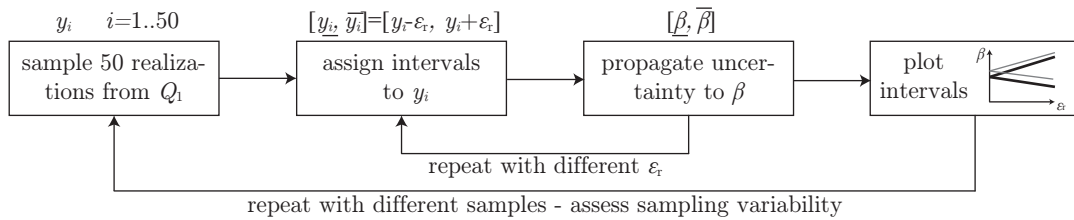


Figure 4.3 Algorithm of analyzing the effect of interval measurement uncertainty on reliability.

Full and approximate propagation of interval uncertainty

As measurement uncertainty is expressed at the level of individual observations its full propagation yields to two distinct 50-dimensional constrained optimization problems that can be computationally demanding if each iteration step involves fitting a distribution function and solving a reliability problem. The computational burden can be considerably lessened by a two-step approximate technique where first the distribution parameters are fitted to the interval observations. Then only the interval representation of distribution parameters are used in further reliability analysis. Thus, the optimization with reliability analysis is reduced to a two-dimensional search space. Moreover, our experience show that the optimum is at the bounds so as it can be found by considering only the possible permutations of the parameter bounds. The accuracy of full and two-step approximate uncertainty propagations are compared using Gumbel distributed Q_1 . The results in terms of reliability indices are presented in Figure 4.4. The interval uncertainty is expressed as the ratio of interval radius and mean of annual maxima (Q_1). 0-10% range is covered and it is assumed that all observations are contaminated with the same radius. For each coefficient of variation the mean of the resistance is set to reach the 3.8 target reliability level. This is performed by considering no measurement uncertainty ($\epsilon_r = 0$) and using the parameters given in Table 4.1, thus sampling variability has no effect. The calculated upper and lower reliability index endpoints are presented in the plots with solid and dashed lines for two-step and full propagations, respectively. Figure 4.4 shows also the reliability

index obtained by Approach 1. This is illustrated with a dotted line and is not affected by the assumed measurement uncertainty interval.

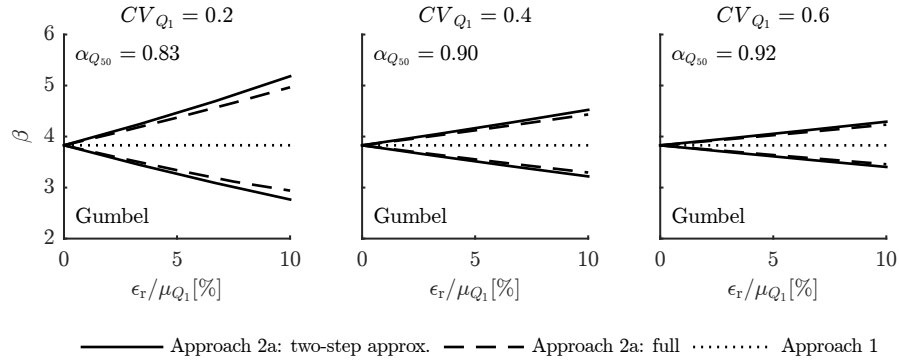


Figure 4.4 Reliability index intervals as the function of normalized measurement uncertainty radius (ϵ_r/μ_{Q_1}) with full and approximate propagation of interval uncertainty.

The plots show that the approximate technique slightly overestimates the accurate (full) reliability intervals, the largest difference is observed for $CV_{Q_1} = 0.2$ with large measurement uncertainty. Since in general the overestimation of the approximate technique is small, it is used in all further analysis. The sensitivity factor of the 50-year reference period maxima ($\alpha_{Q_{50}}$) is also displayed on the plots. It corresponds to a model without uncertainty in measurement and parameters. The decreasing interval range of β with increasing CV_{Q_1} is explained by the decreasing contribution of interval uncertainty to the full uncertainty of Q_1 , i.e. aleatory uncertainty becomes dominating. Figure 4.5 illustrates this shrinkage of uncertainty interval by comparing the transformed cumulative distribution functions with different coefficient of variations. The plots correspond to 50 particular random realizations; the same pattern is observed for other sets of random realizations.

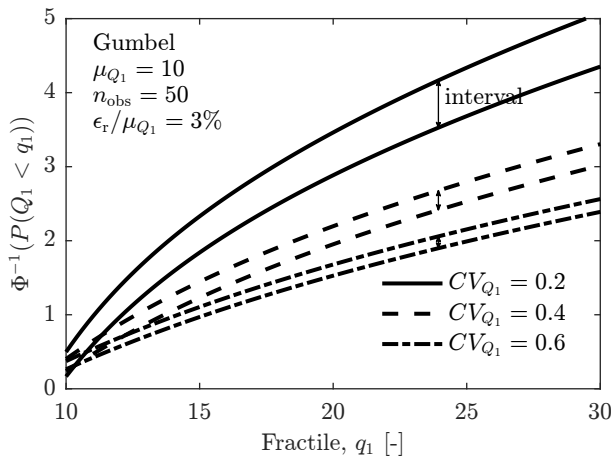


Figure 4.5 Illustration of the shrinkage of uncertainty interval with increasing coefficient of variation but constant measurement uncertainty interval.

Effect on reliability index and required resistance

Eq.4.7 is solved for Normal, Lognormal and Gumbel distributed variable action (Q_1) using the two-step approximation technique. The results are summarized in Figure 4.6; they have the same rationale as is given for Figure 4.4. The light gray lines show the opening reliability interval with increasing measurement uncertainty for 20 random samples, each with 50 realizations. These are indicative of the effect of sampling variability: in this case this is entirely parameter estimation uncertainty due to the finite sample size. The results show that sampling variability – with 50 realizations, which is typical for maxima model of climatic actions – has significant effect on reliability. It is dominating over measurement uncertainty for small interval radiiuses and comparable for larger values. The thick black lines are the median of the 20 sample sets. The reliability index without considering measurement uncertainty can be seen at the common starting point of the lower and upper bound lines. The difference of this value and the lower bound is of interest here as it indicates the extent of the non-conservative neglect of measurement uncertainty. Based on our experience, the difference is deemed significant if it is larger than 0.5. This level is indicated by a dashed horizontal line while the significant range with a red half line. With the selected target reliability level, this corresponds to more than six-fold increase in failure probability.

The results suggest that moderate $\pm 4\%$ measurement uncertainty can lead to significant reduction of reliability level for mountains and highlands represented by $CV_{Q_1} = 0.2 - 0.4$. For the largest considered value of $CV_{Q_1} = 0.6$, the Gumbel model does not reach the limiting value. This indicates that for lowlands even a quite large $\pm 10\%$ measurement uncertainty has no practically significant effect. The reliability interval ranges indicate that even a small $\pm 2\%$ measurement uncertainty can lead to an order of magnitude uncertainty in the failure probability, see for instance the Lognormal distribution with $CV_{Q_1} = 0.2$. For larger measurement uncertainties, the width of the reliability intervals can be larger than 2.0; the widths are quite considerable for large $CV_{Q_1} = 0.6$ models too. Measurement uncertainty thus seems to have a marked effect on structural reliability. The practical question then arises: what are its implications on design and how it should be accounted for? To examine this, we calculated the mean resistance (μ_R) required to reach the target reliability with the lower bound of the reliability interval (Approach 2a). Then this value is compared to the μ_R required to reach the target reliability without explicit consideration of measurement uncertainty (Approach 1). The ratios of the mean values (with interval MU/without explicit MU) are illustrated in Figure 4.7. These indicate how large adjustment might be needed in representative resistance values to meet target reliability in the presence of measurement uncertainty. The plots are structured and have the same rationale as Figure 4.6. Based on our expertise, the ratio is deemed practically significant if it is larger than 1.1. This level is indicated by a dashed horizontal line while the significant range with a red half line. The small effect of sampling variability for Normal distribution is likely due to the small sensitivity factor of Q_{50} . On the contrary, sampling

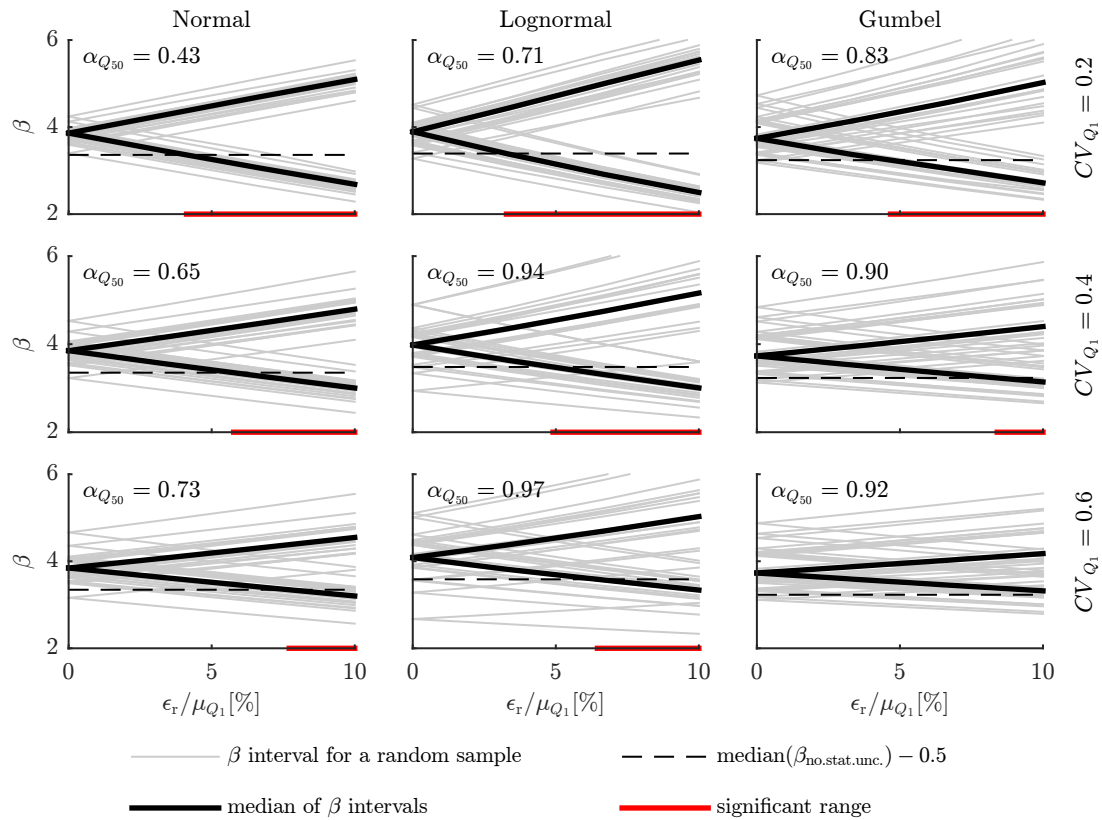


Figure 4.6 Reliability index intervals as the function of the normalized measurement uncertainty radius (ϵ_r / μ_{Q_1}). The gray lines represent 20 random samples, indicating sampling variability. The black lines are the median lower and upper interval endpoints of the reliability index. The red half line indicates the range where the lower endpoint of the reliability interval is significantly lower (> 0.5) than the reliability calculated without measurement uncertainty ($\epsilon_r = 0$).

variability is quite considerable for Lognormal distribution. The selected threshold is reached for all distributions. The Lognormal model shows opposite trend, this might be attributed to its heavy tail. For this distribution the 1.1 threshold is reached at about 4% normalized radius and the ratio can be over 1.4 for larger radii, which is a huge potential adjustment. The Gumbel distribution illustrates decreasing ratio with increasing coefficient of variation. For $CV_{Q_1} = 0.2$ (mountains), moderate $\pm 4\%$ measurement uncertainty can lead to significant μ_R ratio. For lowlands ($CV_{Q_1} = 0.6$), the ratio is over the selected threshold only for excessive measurement uncertainty $\pm 9\%$, which suggests that measurement uncertainty can be neglected for large values of CV_{Q_1} .

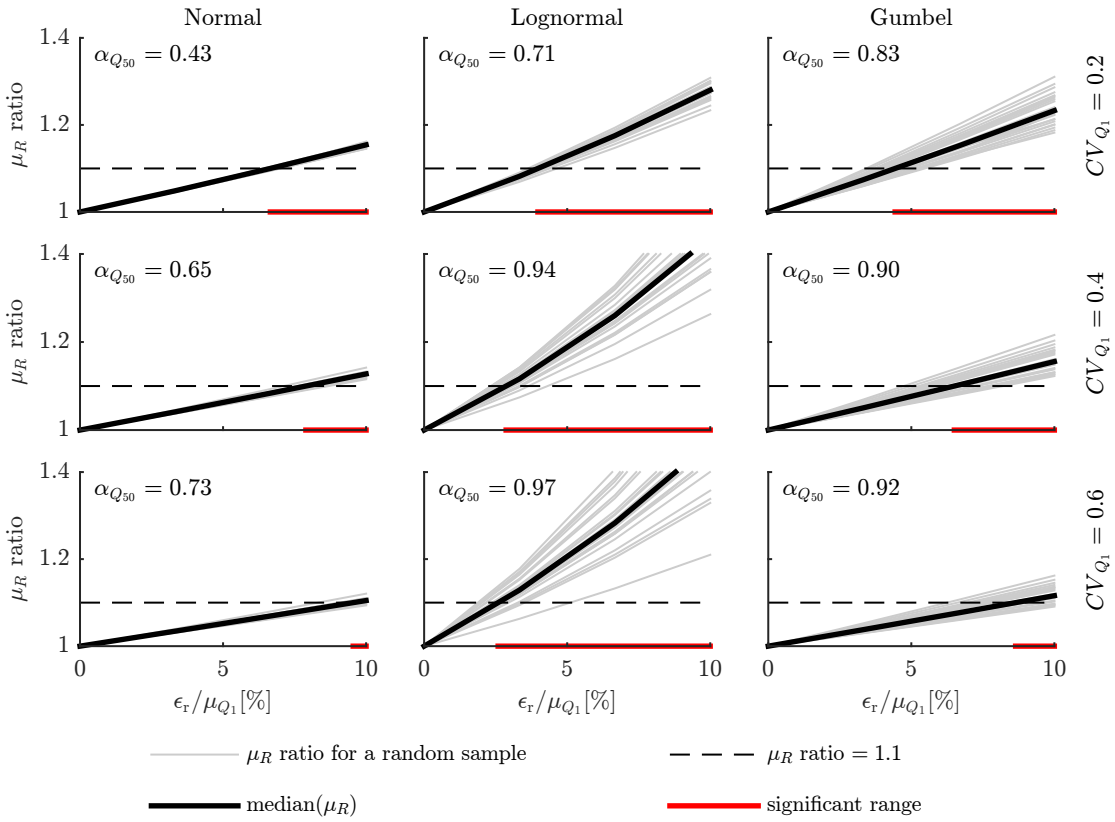


Figure 4.7 Mean resistance (μ_R) ratio for the variable action with and without measurement uncertainty as the function of the normalized measurement uncertainty radius (ϵ_r/μ_{Q_1}). The red half line indicates the significant range where the ratio is larger than 1.1.

4.3.3 Statistical and reliability analysis

This section presents the statistical approach to quantify and propagate measurement uncertainty (Approach 2b). To model the effect of measurement uncertainty, 50 random observations are generated from Q_1 and treated as true (X) values. Then by using the assumed reality-observation link they are contaminated with measurement uncertainty. This is generated from a known, independent distribution (E). The algorithm is outlined in Figure 4.8. Additive and multiplicative reality-observation links are assumed and the measurement uncertainty is taken as normally distributed with zero mean (unbiased).

After the contamination of data, the information about the parameters of the underlying generating models – with the exception of the zero mean of measurement uncertainty – is disregarded and the maximum likelihood method is applied to decouple true values from measurement uncertainty. Finally, the model of decontaminated observations is used in reliability analysis. The sampling variability is again indicated by 20 samples and taken into account in an approximate manner through the predictive reliability index (Eq.4.5). The median and mean absolute deviation are calculated.

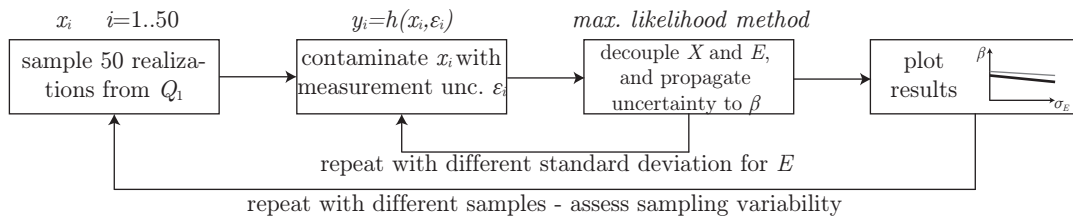


Figure 4.8 Algorithm of analyzing the effect of measurement uncertainty on reliability using statistical technique.

Decontamination of observations

To illustrate the technique and the effect of decontamination, random realizations are generated from Gumbel distribution – with parameters given in Table 4.1 – and contaminated with measurement uncertainty (Figure 4.9). First, additive reality-observation relationship is assumed and Approach 1 and Approach 2b are used to infer the model parameters. The maximum likelihood method is used to obtain point estimates and the delta method is applied to construct 90% confidence intervals to illustrate parameter estimation uncertainty (Coles, 2001). The results for three cases of Gumbel distribution and two cases of measurement uncertainty with varying standard deviation are discussed only. The realizations and the fitted models are shown in Figure 4.9. It comprises return value-return period plots transformed to Gumbel space where the Gumbel distribution appears as a straight line. Though the plots are corresponding to a particular set of realizations, they convey reliably the trends and expected differences: (i) Approach 1 typically overestimates the fractiles thus leading to lower reliability level and being conservative; (ii) the difference between models increases with increasing return period. Due to the small sample size, the difference is affected by large sampling variability. The calculations are repeated with multiplicative measurement uncertainty (Figure 4.10). The results correspond well with those obtained for the additive format. Furthermore, wider confidence intervals of Approach 2b compared with Approach 1 are observed. This is due to the larger model space where the same sample size allows less certain inference. This effect is less pronounced for the additive model. For both models, Approach 1 is inherently biased since it is not using the correct likelihood function, while Approach 2b asymptotically converges to the true model. Thus, in the long run – from theoretical point of view – Approach 2b is better; however, Approach 1 seems to be generally conservative

for the considered reality-observation links. This latter aspect is analyzed in more detail in the following section focusing on reliability index as a quantity of practical interest.

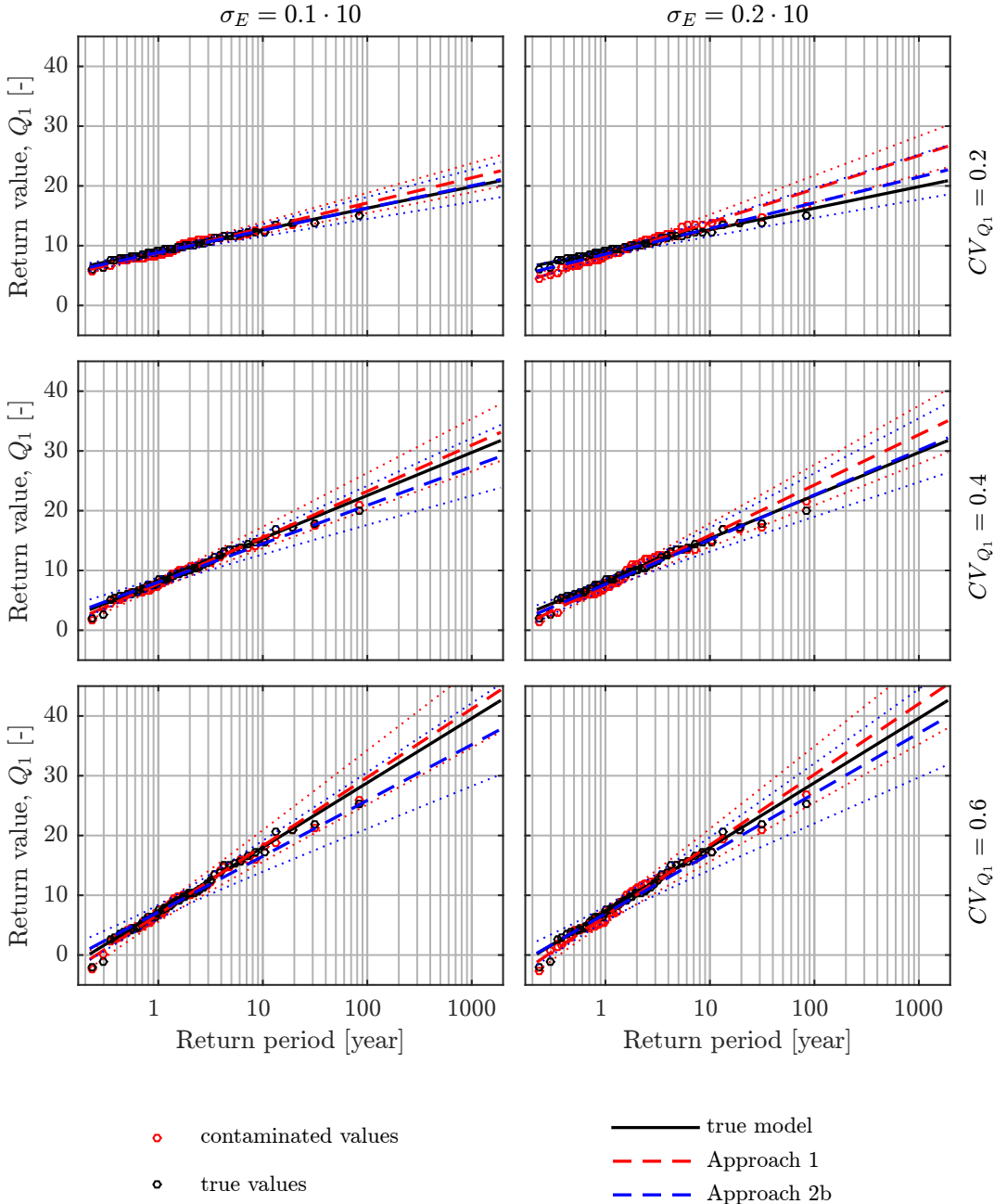


Figure 4.9 Gumbel distributions fitted to random realizations contaminated with additive measurement uncertainty using Approach 1 and Approach 2b. The point estimates (dashed lines) are accompanied by 90% confidence intervals (dotted lines).

Effect on reliability index

The effect of measurement uncertainty on reliability index is analyzed for the additive relationship considering Normal, Lognormal and Gumbel distributed true values and with coefficient of variation ranging from 0.2 to 0.6. The measurement uncertainty has Normal distribution with known zero mean and varying standard deviation. Consistently with the

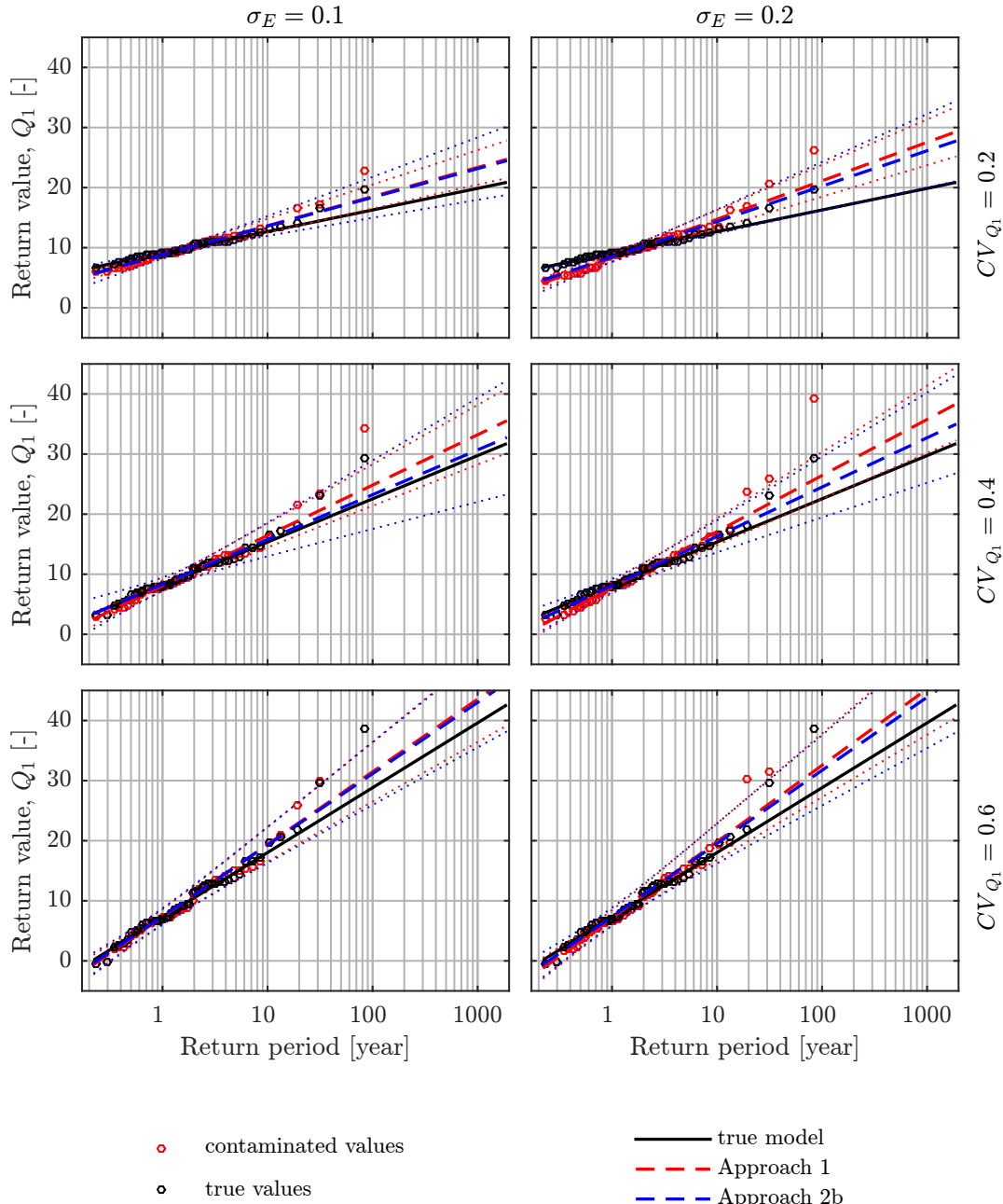


Figure 4.10 Gumbel distributions fitted to random realizations contaminated with multiplicative measurement uncertainty using Approach 1 and Approach 2b. The point estimates (dashed lines) are accompanied by 90% confidence intervals (dotted lines).

interval analysis in Section 4.3.2, the mean value of the resistance is determined to reach the target reliability without measurement uncertainty and parameter estimation uncertainty. Then the algorithm presented in Figure 4.8 is applied to generate contaminated observations, to decontaminate them, and to calculate the reliability index using the inferred parameters. The calculations are repeated for 20 samples with sample size of 50. The results in terms of reliability indices are shown in Figure 4.11 and in Figure 4.12. Grey and light blue solid lines are representing the 20 samples, and the corresponding thick solid and dashed lines are the median and predictive reliability indices, respectively. The difference between these latter two lines expresses the effect of parameter estimation uncertainty. For Normal distribution, this effect is small compared to Lognormal and Gumbel for which it is increasing with increasing standard deviation of measurement uncertainty. For Approach 2b it is typically larger than Approach 1 as the larger model space allows less certain inference with the same sample size. In case of Lognormal and Gumbel models, the ratio of the predictive and median failure probabilities can be as large as an order of magnitude or larger. Additionally, the plots show that the reliability index can considerably be overestimated when parameter estimation uncertainty is neglected. The salient large scatter of Approach 2b might be partially attributed to the unstable maximum likelihood estimators for small samples (Hosking et al., 1985; Martins and Stedinger, 2000).

Comparing Approach 1 with Approach 2b for Normal and Gumbel distributions, the former approach yields to systematically lower reliability indices. The opposite trend observed for Lognormal distribution might be attributed to its heavy-tail. For Normal distribution, Approach 1 seems to be overly conservative, the median is well below the target reliability level. For all distributions, Approach 1 is reasonably conservative with the exception of Lognormal distribution and coefficient of variation of 0.6. However, even in this case the predictive reliability index corrects the overestimation. Though for Normal distribution it is too conservative, the currently prevalent Approach 1 appears to be safely applicable to measurement uncertainty problems in case of additive reality-observation relationship. Approach 2b is sound from theoretical point of view; however, its median overestimates reliability level, thus the predictive reliability index is to be used to avoid underestimation of failure probability. Its larger parameter estimation uncertainty can lead large reduction in reliability index for small sample sizes.

4.4 Application example: Turbine hall of Paks Nuclear Power Plant

The turbine hall of Paks Nuclear Power Plant is selected to demonstrate the effect of measurement uncertainty on a real life example. The structure is introduced in Annex B.1, here only the essential details, which are required to interpret the results, are provided. The interval approach is used to represent measurement uncertainty and the two-step approximation is applied to propagate interval uncertainty. Annual ground snow maxima

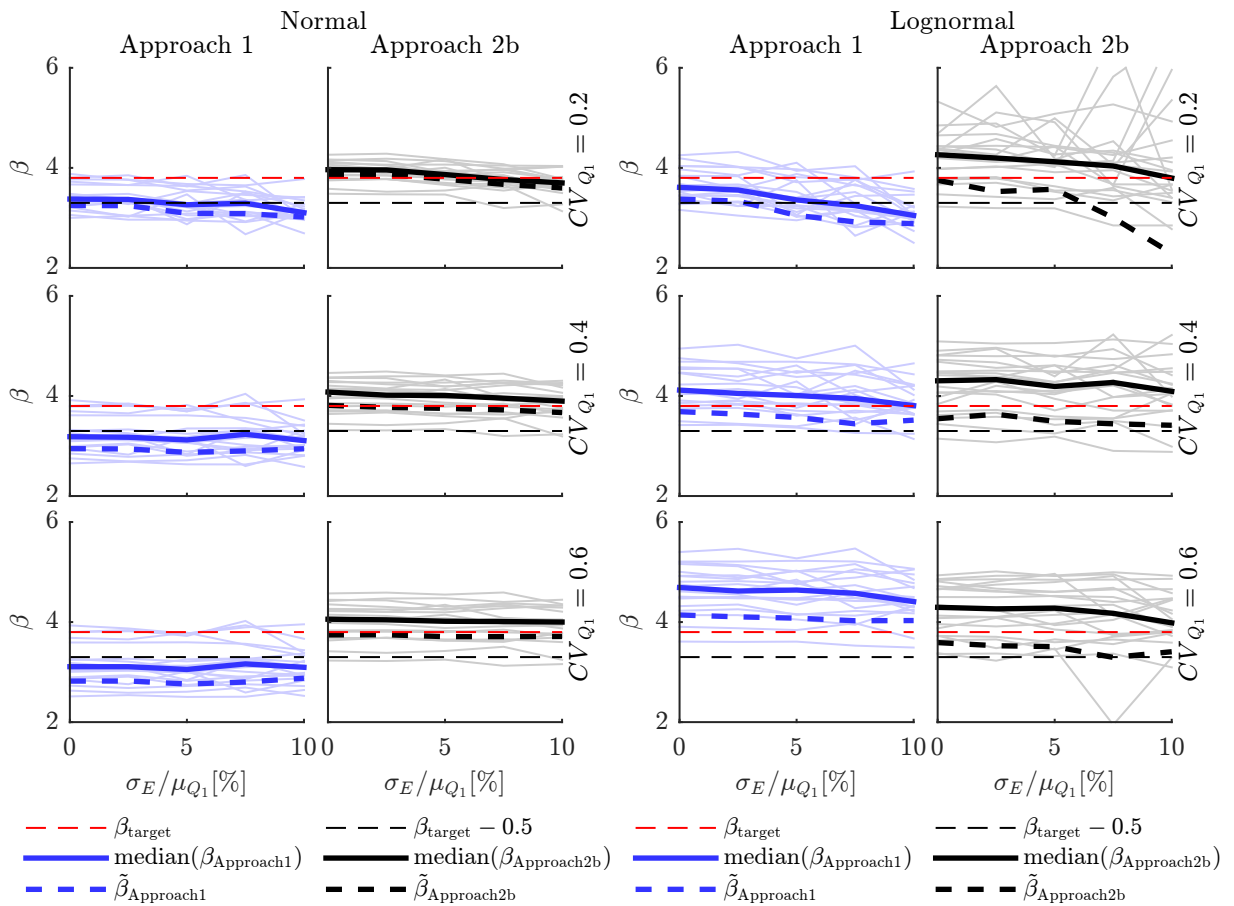


Figure 4.11 Reliability indices as the function of the normalized standard deviation of measurement uncertainty (σ_E/μ_{Q_1}). The thick solid lines are the median of the reliability indices while the thick dashed lines are the approximate predictive reliability indices.

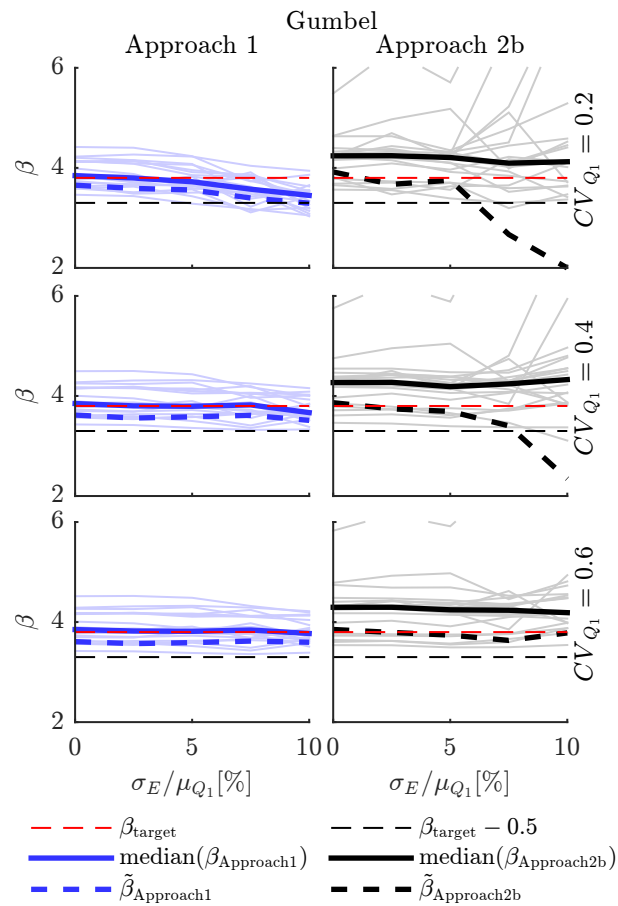


Figure 4.12 Reliability indices as the function of the normalized standard deviation of measurement uncertainty (σ_E / μ_{Q_1}). The thick solid lines are the median of the reliability indices while the thick dashed lines are the approximate predictive reliability indices.

related to the location are contaminated with measurement uncertainty, the rest of random variables are represented by probability distributions. The results in terms of reliability indices and failure probabilities are given in Figure 4.13. One year reference period is used for all calculations of the frame.

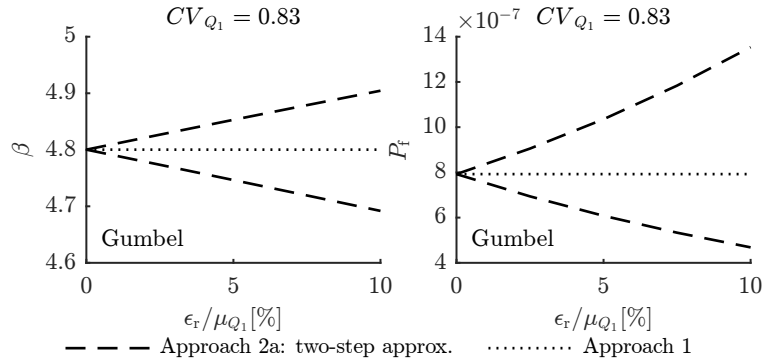


Figure 4.13 Reliability index and failure probability intervals as the function of normalized measurement uncertainty radius (ϵ_r / μ_{Q_1}). Comparison of Approach 1 and Approach 2a for the turbine hall of Paks Nuclear Power Plant.

The widest reliability index interval is 0.2, which is obtained for the largest measurement uncertainty error radius. This small value is in agreement with the trend observed in the previous example (Figure 4.6). It is attributed to the large coefficient of variation of annual ground snow load that is dominating over measurement uncertainty. In this example, neglect of measurement uncertainty leads to 70% underestimation of failure probability at worst; hence, the effect is negligible.

4.5 Discussion

One can distinguish two components of measurement uncertainty: the reality-observation link and the nature of the contamination E . The three approaches considered here differ in how they treat these two components. The present prevalent approach (Approach 1) neglects both components, thus entirely ignores the possibility that the real values are greater or smaller than the observed due to measurement uncertainty.

The interval approach (Approach 2a) expresses full ignorance in respect of reality-observation link and represents measurement uncertainty with intervals. Therefore, no decoupling of true values from measurement uncertainty is possible. Intervals should be used with caution because by definition values outside of the interval are impossible. This assumption is rarely met in civil engineering. Measurement uncertainty is often described on the basis of expert judgment and wide intervals are applied to almost surely capture real, unobserved values.

The statistical approach (Approach 2b) requires the knowledge of the reality-observation link and represents measurement uncertainty with distribution function. This is the only approach that can decontaminate the observations and can directly infer the variable of

interest, true variable. This is important since structural reliability is dependent on the true variable. The statistical and interval analysis based approaches are conceptually different, thus they are only comparable on that level but not quantitatively. Their uncertainty representation is inherently distinct, thus there is no equivalency between interval and distribution based representations.

Additionally, it must be emphasized that another type of uncertainty – statistical uncertainty in parameter estimation and selection of distribution function – often needs to be taken into account in reliability analysis as it may be even more important as measurement uncertainty investigated here (Rózsás and Sýkora, 2015b,c). Bayesian paradigm is a natural choice to incorporate this uncertainty, consequently that is recommended for practical applications. For example, in real-life situations, the reality-observation link cannot be established with certainty. Yet, this uncertainty can be captured by using multiple models and averaging them with respect their goodness of describing the data, this can be achieved for example by Bayesian model averaging (Hoeting et al., 1999).

Although this study is limited by the considered distribution types, reality-observation functions, and parameter range, it is believed to cover many practically relevant random variables. The presented approaches and algorithms can be easily used for other distribution types and measurement error structure. An additional limitation of this study is that measurement uncertainty is considered only for the dominant variable action. However, it is anticipated that for other random variables the effect is smaller due to their typically smaller sensitivity factor. Moreover, measurement uncertainty is much smaller for other than climatic actions such as resistance and permanent actions. Furthermore, the effect of sample size should be analyzed in later works. It is believed that the outcomes would be similar for sample sizes ranging from 20 to couple of hundreds, which cover the majority of cases in civil engineering. More data would allow more certain model identification.

4.6 Summary and conclusions

The current practice in probabilistic engineering treats observed data contaminated with measurement uncertainty as realizations of the true distribution, thus neglecting the contamination mechanism. Statistical and interval-based analyses are thus conducted to investigate the effect of this simplification on structural reliability. Extensive parametric analyses – based on 50 realizations, which is a typical length of records for climatic actions – reveal that:

If interval representation of measurement uncertainty is used:

- Sampling variability (parameter estimation uncertainty) has significant effect on reliability: it is dominant over measurement uncertainty for small interval radiiuses and comparable for large radiiuses.

- For mountains and highlands, moderate $\pm 4\%$ measurement uncertainty – relative to value of an observed variable – can lead to significant reduction of reliability level. For lowlands, even a large $\pm 10\%$ measurement uncertainty has no significant effect. An effect is deemed significant if it yields to greater than six fold increase in failure probability compared with Approach 1 (neglect of measurement uncertainty).
- Reliability interval ranges indicate that a small $\pm 2\%$ measurement uncertainty can lead to reduction of 0.6 in reliability index. For larger measurement uncertainties, the width of the reliability intervals can be larger than 2.0.
- The effect of measurement uncertainty is more pronounced for low variability random variables where its contribution to the total uncertainty increases.
- Parameter ranges where Approach 1 often overestimates the reliability index are identified.

If statistical (distribution function) representation of measurement uncertainty is used:

- It is demonstrated that the statistical approach can be used to decontaminate the observations, thus to access the variable of interest.
- The ratio of the predictive and median failure probabilities can be as large as an order of magnitude or larger (~ 30 for Lognormal distribution).
- If parameter estimation uncertainty is disregarded, the reliability index can be considerably overestimated.
- For all considered distributions with additive measurement uncertainty, Approach 1 is reasonably conservative in most cases.

Practical recommendations:

- Figure 4.6 and Figure 4.7 can be used to identify cases when Approach 1 significantly overestimates reliability index. In such cases and when no or very limited information on measurement uncertainty is available, then interval analysis could be used, considering the lower bound of the reliability interval.
- If the reality-observation link is known then the statistical approach is recommended. For small and moderate sample sizes (< 100), the predictive reliability index is recommended. For additive measurement uncertainty, Approach 1 is conservative.
- For point estimates, such as median, the reliability index should be accompanied by uncertainty intervals to indicate the credibility of results.
- For ground snow extremes at lowlands, Approach 1 provides a reasonable approximation, thus the effect of measurement uncertainty can be neglected. Otherwise more advanced analysis is recommended.

Assessment of measurement uncertainty should be region- and case-specific accounting for measuring techniques, and applied correction equations, thus involvement of meteorologists, analysts or other experts is beneficial. Moreover, the selected approach to propagate measurement uncertainty should always be based on the particular issue in question, acknowledging “the degree of precision to which the nature of the subject admits”.

Chapter 5

Long-term trends in annual ground snow maxima

The current structural design provisions are prevalently based on experience and on the assumption of stationary meteorological conditions. However, the observations of past decades and advanced climate models show that this assumption is debatable. Therefore, this chapter examines the historical long-term trends in ground snow load maxima and their effect on structural reliability. Annual maxima snow water equivalents are taken and univariate generalized extreme value distribution is adopted as a probabilistic model. Stationary and five non-stationary distributions are fitted to the observations utilizing the maximum likelihood method. Statistical and information theory based approaches are used to compare the models and to identify trends. Finally, reliability analyses are performed on a simple structure to explore the practical significance of the trends. The calculations show decreasing trends in annual maxima for most of the region. Although statistically significant changes are detected at many locations, the practical significance – with respect to structural reliability – is considerable only for a few, and the effect is favorable. The results indicate that contrary to the widespread practice in extreme event modeling, the exclusive use of statistical techniques on the analyzed extremes is insufficient to identify practically significant trends. This should be demonstrated using practically relevant examples, such as reliability of structures.

5.1 Problem statement and the state of the art

The provisions of current structural standards are based on the assumption that the underlying natural phenomena – generating the actions on structures, and determining their working environment – are stationary. However, observations of the past decades and advanced meteorological analyses show that this assumption does not represent accurately the present, either the future world (Herring et al., 2015; IPCC, 2012; Milly et al., 2008).

Hence, the aim of this chapter is to analyze the long-term trends in snow events and their implications on structural reliability. The Carpathian Region is selected for the study and the database presented in Section 3.2.1 is used.

Previous studies indicate that there is a statistically significant time-trend in snow events for the region. Birsan and Dumitrescu (2014) have analyzed historical observations from Romania and detected decrease in snowfall days (82% of stations) with substantial decrease in snow depth (18% of stations) and also in snow coverage (29% of stations).

To our knowledge the long-term trends in extreme snow loads, e.g. annual maxima, for the Carpathian Region have not been sufficiently analyzed yet. Moreover, we are not aware of any study quantitatively analyzing the effect of time-trends in snow loads on structural reliability. Although Pecho et al. (2009) and Sadovský et al. (2007) examined time-trends in snow precipitation for the Slovakian Alps, their study is insufficiently documented, which makes it difficult to evaluate the merit and value of their work. From the available information it appears that their approach is not able to answer the main questions of this chapter.

An excellent study is available for the Swiss Alps where Marty and Blanchet (2012) detected statistically significant negative, long-term trends in annual snow depth. However, their analysis is focused on statistical significance testing and on return values. Thus, although indicating interesting tendencies, the practical significance of their results, e.g. with respect to structural reliability cannot be judged. This is partially inevitable since practical significance differs by end-users. Therefore, in this chapter a more pragmatic approach is promoted in which after the statistical analysis the practical significance of the findings is examined. The main interest here is the impact of snow trends on structural reliability, particularly on the probability of structural failure. Only historical observations are considered but a worthwhile extension would be to incorporate the projections of global climate models. In a recent study O’Gorman (2014) showed that no considerable change is expected in the 20-year return period extreme snow events for the North American region up to the end of the 21st century, though the impact on structural reliability is inconclusive since that is governed by rarer events.

5.2 Solution strategy

Univariate generalized extreme value (GEV) distribution is selected as it is widely accepted in extreme value analysis (Klein Tank et al., 2009) and was successfully applied for modelling extreme precipitations (Coles and Pericchi, 2003), temperatures (Guttorp and Xu, 2011), discharges (Hao et al., 2015), wind speeds (Hundecha et al., 2008) and waves (Caires et al., 2006). Stationary and non-stationary models are compared based on how likely the data are generated by each model. The considered non-stationary distributions with time-dependent parameters are summarized in Table 5.1. The shape parameter is constant in all presented models, this is explained by that models with shape parameter

linearly varying in time yielded to considerably worse fit than the others and often lead to unrealistic fractiles. The adopted block length is one year, covering a whole winter season. Furthermore, to account for seasons without snow the cumulative distribution function of annual maxima is expressed as follows:

$$P(X < x) = P(\text{snowfall}) \cdot P(X < x | \text{snowfall}) \quad (5.1)$$

where the former event has Bernoulli, while the latter has GEV distribution.

Maximum likelihood method is selected for parameter estimation due to the large number of locations. According to Hosking et al. (1985) and Martins and Stedinger (2000) the maximum likelihood method can lead to unstable parameter estimation for small sample size; however, it is deemed to be sufficient for this exploratory analysis. Bayesian approach might be used to overcome the issue of instability for further detailed studies.

Table 5.1 Summary of the considered non-stationary GEV distributions.

Model ID	Location par. (μ)	Scale par. (σ)	Shape par. (ξ)
$\mu 1$	$a_0 + a_1 \cdot t$	constant	constant
$\mu 2$	$b_0 + b_1 \cdot t + b_2 \cdot t^2$	constant	constant
$\sigma 1$	constant	$d_0 + d_1 \cdot t$	constant
$\sigma 2$	constant	$e_0 + e_1 \cdot t + e_2 \cdot t^2$	constant
$\mu 1\sigma 1$	$g_0 + g_1 \cdot t$	$g_2 + g_3 \cdot t$	constant

Likelihood ratio (LR) test and Akaike information criterion (AIC) are used to compare the stationary and non-stationary models. The former is a standard frequentist hypothesis test for comparing nested models (Wilks, 1938). The latter is an asymptotic information criterion that is based on the premise that the model with smallest information loss (Kullback-Leibler divergence) should be preferred (Wit et al., 2012). In the absence of the true model, the information loss cannot be calculated in absolute terms; however, the models can be compared and their relative “strength” can be expressed by the difference in AICs or by using Akaike weights (Eq.C.10). Herein the corrected form of Akaike information criterion (AICc, Eq.C.9) is applied that takes into account the effect of a finite sample size. The goodness-of-fit of the models is visually checked using Q–Q, P–P, and return-period—return value plots (Coles, 2001). These plot types are defined in Annex C.3. Additionally, at some locations the GEV model is compared to other commonly applied distributions for diagnostic purposes, i.e. Gumbel and three-parameter Lognormal. Due to the limitations of statistical significance testing (Carver, 1993) the effect size, power of the test, and confidence intervals are also utilized to compare the models. The conclusions are based on the practical bearing of these models on structural reliability.

5.3 Stationary model

Stationary GEV distribution is fitted to each of the 5895 grid points using the ML method; the corresponding shape parameters are plotted in Figure 5.1. This map and all the others in the following are created using equidistant conic projection and linear interpolation. In Figure 5.1, the areas bounded by black contours indicate Weibull distribution, it can be seen that the high mountainous areas have dominantly this upper bounded distribution type. Considerable part of the studied area has Fréchet distribution with relatively large shape parameter ($\xi > 0.2$), which is in conflict with the Gumbel assumption widely accepted in Europe (Sanpaolesi et al., 1998), EN 1991-1-3:2003 and ISO 4355:2013. Additional limitation of the Gumbel distribution is that it yields to artificially narrower confidence intervals than the Fréchet as its parameters span smaller space, see Chapter 3 and Coles and Pericchi (2003).

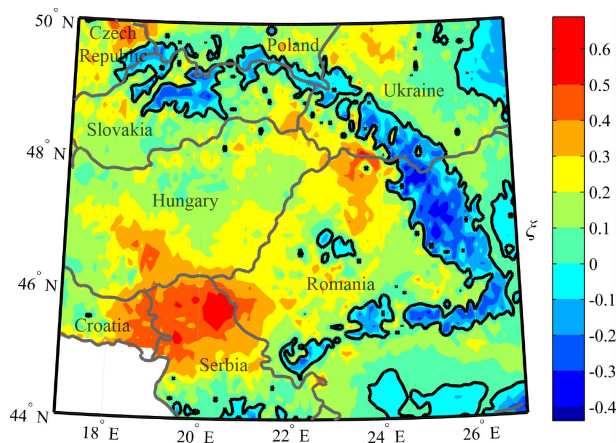


Figure 5.1 Shape parameter (ξ) of the fitted, stationary GEV distributions, the black contour surrounds the Weibull type.

The unfavorable deviation from Gumbel distribution is the most pronounced in the northern part of Serbia. It is interesting that some locations exhibit shape parameter larger than 0.5, which means that the distribution has infinite variance. If this is deemed to be unrealistic, it might be avoided by adopting constraints in ML or by using Bayesian approaches with appropriate priors.

5.4 Long-term trends, non-stationary models

First, a straight line is fitted to the annual maxima (Figure 5.2a) at every grid point in the least-squares sense, while the snow-free years are discarded from the analysis. The associated slope parameters are illustrated in Figure 5.2b, where the negative values are referring to decreasing trends in time. At 97% of the locations decreasing trend is identified, whereas a mild increase is observed in the northern part of the region – Slovakia, the Czech Republic, and Poland. The small regions with strong, increasing trends next to

decreasing ones (orange areas surrounded by dark blue ones) in Slovakia and Ukraine imply discrepancy in the database. Areas with the most pronounced decreasing trend are matching well with the Weibull regions with the exception of the southern part. Based on the linear trend the average change in annual maxima for the entire region during observation period is -42%, compared to the 1962 level.

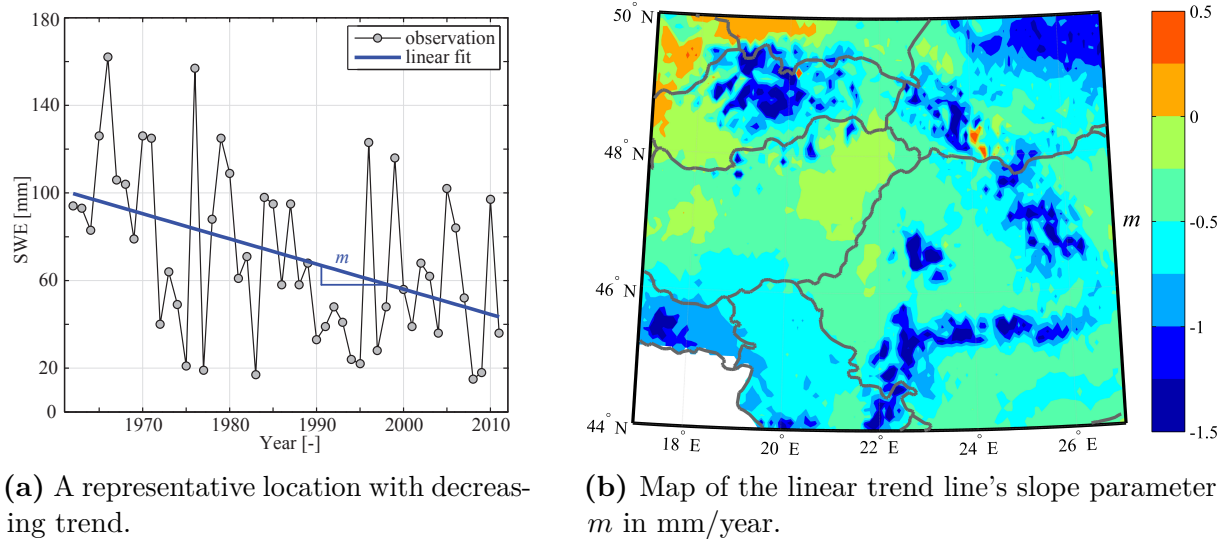


Figure 5.2 Fitting linear line to the annual maxima ground snow loads.

A more involved, LR and Akaike weight based comparisons of the stationary and five non-stationary GEV distributions show that the models with time-variant location parameters fit better the observations than those with time-variant scale parameter. Comparison between the models with time-variant location parameter reveals that the μ_1 model performs the best for most of the area. The LR and Akaike weight based results, comparing the μ_1 and stationary models are presented in Figure 5.3a and 5.3b. Albeit both figures are showing probabilities (P), their interpretation is substantially different. In case of the LR test it expresses the probability that if the null hypothesis is true (stationary model) the difference between the log-likelihoods is at least as large as the one observed. This probability is typically referred as the p -value, and Figure 5.3a is showing the complementer of it ($P = 1 - p$). On the other hand, the Akaike weights — illustrated in Figure 5.3b — express the probability that μ_1 model is better than the stationary one in the Kullback-Leibler divergence sense. In respect of these probabilities, the selected threshold is 90% in both cases. Locations above this value are marked with a dot and considered as statistically significant. The vast majority of the statistically significant trends identified by the LR test are decreasing (black dots), only two locations in the Czech Republic show significant increase (white dots in the upper left corner in Figure 5.3a). The Akaike weight based comparison shows solely decreasing trends. The LR test is identified much more locations with significant trend, although the probabilities are not directly comparable. In addition, 65% of these locations are statistically significant

even with 95% threshold level as well. The trends might be explained by the diminishing number of snow days as a consequence of increasing mean global temperature.

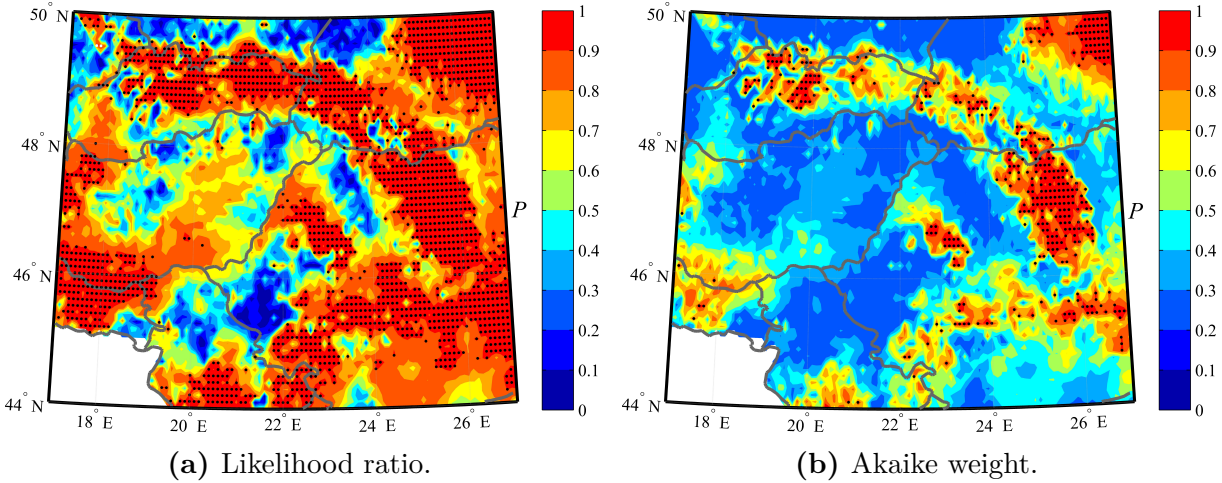


Figure 5.3 Comparison of μ_1 and stationary models, grid-points with $P > 0.90$ are marked with dots: black for decreasing and white for increasing trends.

A more pragmatic comparison of time-trends is presented in Figure 5.4, where the 50-year return values for stationary and non-stationary μ_1 models are compared. The 50-year return value is referred as characteristic value in structural engineering and serves as the basis of everyday design. All the selected locations, shown in Figure 5.4, exhibit significant negative trend in AICc sense.

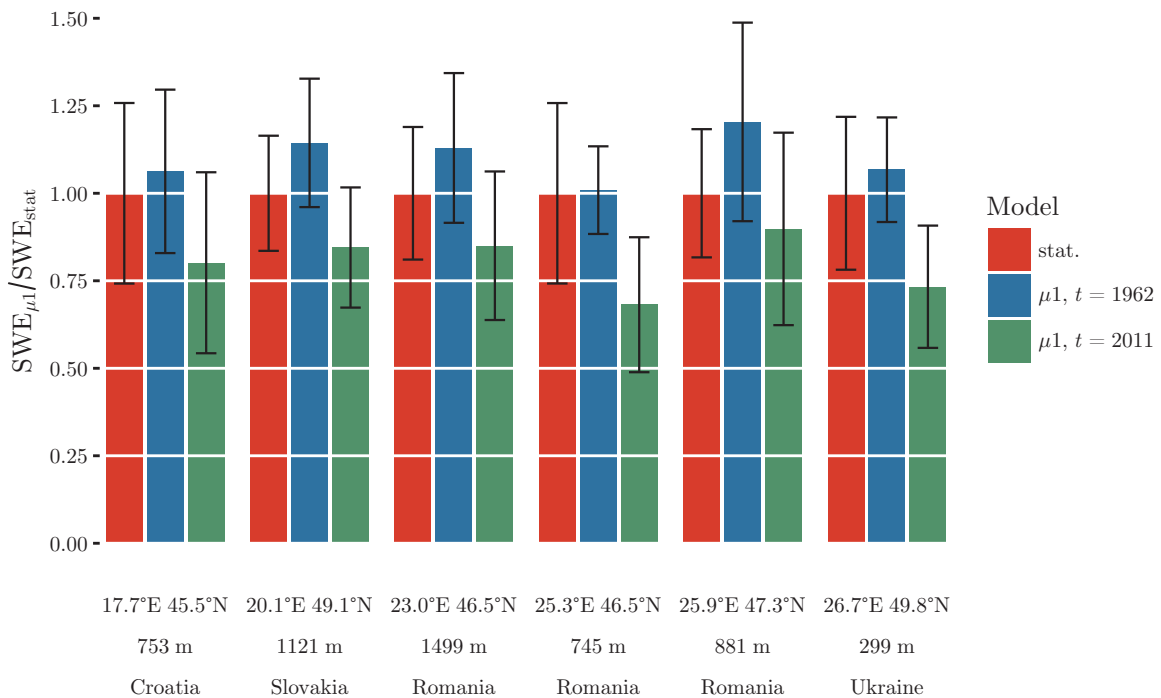


Figure 5.4 Normalized 50-year return value SWE with 90% confidence intervals (black) for selected locations that have significant negative trends as identified by Akaike weights .

Figure 5.4 also shows that even for the locations where the AICc based criterion identified significant trends, in respect of 50-year return value with 90% confidence interval, the difference is not always practically significant. The time-trend is deemed practically significant if the stationary estimate is outside of the non-stationary confidence interval. For the entire region, the average change characteristic values between 1962 and 2011 is -10% , using the μ_1 model and 1962 as reference. For locations with statistically significant trends the changes are -19% and -26% for LR test and Akaike weights respectively.

5.5 Impact on structural reliability

Although the focus of this chapter is the statistical characterization of snow loads and identification of trends in annual maxima, the key question from an engineering point of view is the effect of the changes on structural reliability and the adequacy of current provisions. The simple statistical, information theory (LR, AICc), and representative fractile based comparisons cannot answer this question, since the failure probability of a structure is dominantly determined by the tail of the distribution functions, well above or below the characteristic value. Thus, a simple, illustrative example is selected to explore this question. The related limit state function and the properties of the random variables are given in Eq. 5.2 and in Table 5.2, respectively. For simplicity, the distribution functions of annual snow maxima are used and annual failure probabilities are calculated. Exceptional snow loads and accidental load combinations are not covered in the analysis.

$$g(\mathbf{X}) = R - (G + \mu \cdot S) \quad (5.2)$$

Table 5.2 Summary of the considered non-stationary distributions.

Variable	Distribution	Mean	CV	Reference
Resistance, R	Lognormal	1000/350*	0.12	JCSS (2000b)
Ground snow, S	GEV	†	†	—
Ground to roof conversion factor, μ	Lognormal	0.75	0.15	JCSS (2001)
Permanent action, G	Normal	50	0.10	JCSS (2001)

* 1000 for the Hungarian, and 350 for the Ukrainian locations to achieve realistic and comparable reliability level.

† varies according to the selected model.

Reliability analyses are performed for two representative locations using standard, first order reliability analysis (FORM). The first one is the Ukrainian location presented in Figure 5.4. It has small, scattered settlements and it represents the significant negative trend even in respect of 50-year return values. The second is the fifth most populous city in Hungary (Pécs), it is identified by the LR test with statistically significant negative trend. It represents the moderate negative trend, which reflects well the majority of the region. These two locations are referred hereinafter as Ukrainian and Hungarian. Reliability is

analyzed considering a reference period of one year. The location parameter is obtained from the non-stationary model for each of the selected years: 1962, 2011 and 2062. The delta method is used to construct approximate confidence intervals for these indices, and the results are summarized in Figure 5.5.

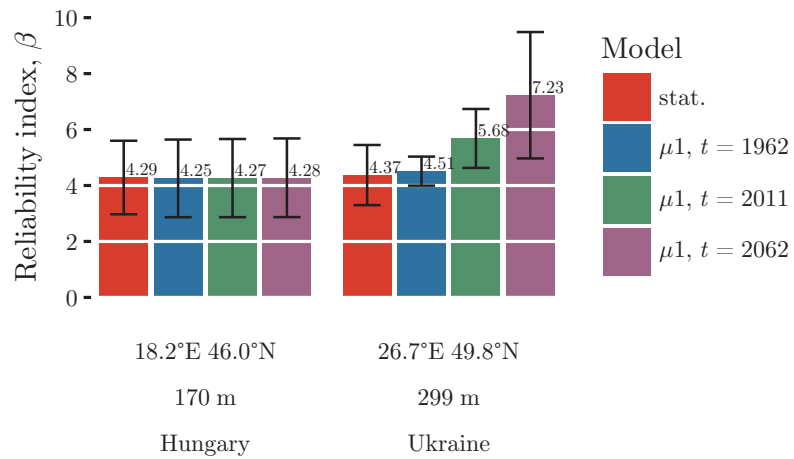


Figure 5.5 Reliability indices with 75% confidence intervals (black) from ground snow parameter estimation uncertainty.

From Figure 5.5 it is clear that the moderate decreasing trend has almost no effect on structural reliability, it is dwarfed by the parameter estimation uncertainty. For the Ukrainian location the increase in reliability level is practically significant, although the uncertainty is large here as well. From safety point of view, the change is clearly favorable, and whether the current provisions will provide economical design for these locations in the future is a different issue. The most important factor in the difference of the results for the Hungarian and Ukrainian locations is that the former has Fréchet while the latter has Weibull distribution. The extrapolation of the non-stationary model to 2062 should be handled with care, it is provided only for illustrative purposes. It introduces additional uncertainty for non-stationary models as illustrated for the Ukrainian location in Figure 5.6. This should be reduced by use of physical models or further explanations.

5.5.1 Application example: Turbine hall of Paks Nucelar Power Plant

Non-stationary extreme value analyses of annual ground snow maxima are conducted for the site of the turbine hall of Paks Nuclear Power Plant. The structure is introduced in Annex B.1, here only the essential details, which are required to interpret the results, are provided. Table 5.3 summarizes the Akaike weights and some representative fractiles for the selected models; the parameters are estimated using maximum likelihood method. The Akaike weights favor the stationary model, while the second best model is the one

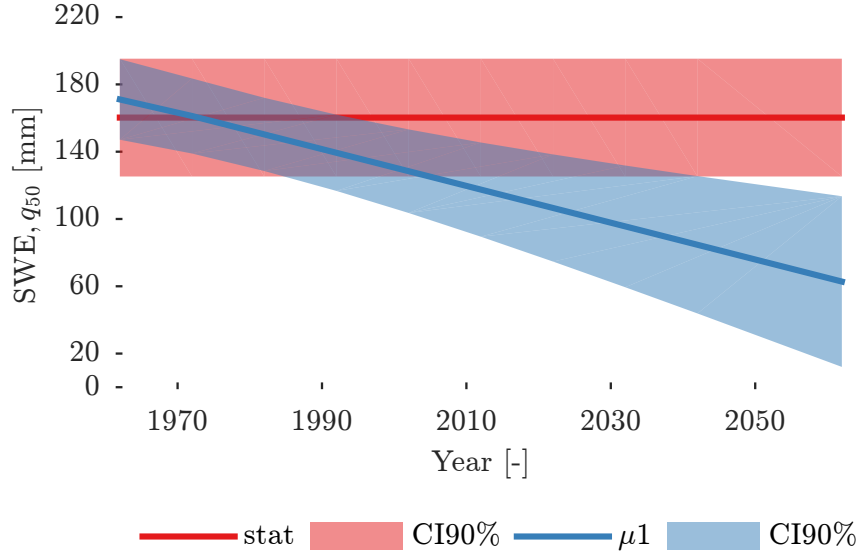


Figure 5.6 Ukrainian location, 50-year return value SWE (q_{50}) with 90% confidence bands (CI90%) for stationary (stat) and μ_1 models.

with linearly varying location parameter (μ_1). The fractiles of non-stationary models show small decrease in time.

The stationary and μ_1 models are used to calculate the annual reliability index of the structure in three distinct years (1962, 2011, and 2062). Furthermore, the parameter estimation uncertainty of ground snow load model is propagated to reliability index by using the delta method. The results are presented in Table 5.4, from which it is salient that parameter estimation uncertainty dominates over the time-trend caused change in reliability index.

Table 5.3 Akaike weights and representative fractiles of the fitted stationary and non-stationary GEV distributions for the site of Paks Nuclear Power Plant. Fractiles are given for the years of 1962 and 2011.

Model ID	w^*	q_{50} [kN/m ²]		q_{1000} [kN/m ²]	
		1962	2011	1962	2011
stat.	0.439	1.53	1.53	4.83	4.83
μ_1	0.190	1.55	1.49	4.82	4.76
μ_2	0.092	1.57	1.50	4.64	4.56
σ_1	0.139	1.56	1.41	4.74	4.25
σ_2	0.054	1.75	1.53	4.99	4.29
$\mu_1\sigma_1$	0.085	1.80	1.11	5.38	3.35

* Akaike weight.

5.6 Discussion

The results are dependent on the number of observations and on the reference period used in the reliability analyses. More data would yield to narrower confidence intervals and

Table 5.4 Annual reliability indices for the turbine hall considering stationary and non-stationary GEV distributed ground snow maxima. Reliability indices are accompanied by 90% confidence intervals and they are given for the years of 1962, 2011 and 2062.

Model ID	1962	2011	β^* 2062
stat.	3.37 (2.35,4.41)	3.37 (2.35,4.41)	3.37 (2.35,4.41)
μ_1	3.38 (2.33,4.43)	3.39 (2.33,4.45)	3.40 (2.33,4.46)

* Maximum likelihood point estimate of annual reliability index with 90% confidence interval in brackets.

allow sharper/stronger conclusions, while an extended reference period would level out the differences in annual failure probabilities.

The adopted, practical-significance oriented approach could be applied for other issues as well and not restricted to snow extremes and structural reliability. A limitation of this study is that only GEV distributions are considered. This can have an important effect on the failure probability, since that is governed by the tail of the distribution, i.e. very rare, not even observed events. This is known in structural reliability as distribution arbitrariness (Ditlevsen, 1994). This effect could be investigated by more involved statistical techniques, but could be overcome only by using additional data or accurate physical models; these are rarely available.

In all analysis here, historical observations are used, though similar calculations are completed for the Carpathian Region considering climate projection until the end of the 21st century. The preliminary results indicate decreasing trend in ground snow load and negligible effect on structural reliability for some selected locations (Kámán, 2014). However, it requires further research to decide whether the results of global circulation models can reasonably predict such extremes that needed in structural reliability analyses.

In spite of limitations, it is believed that the present analysis provides an interesting insight and considering the current state of knowledge in structural engineering it can support decision-making process.

5.7 Summary and conclusions

The following main conclusions are drawn from the statistical and information theory based time-trend analysis of annual ground snow maxima:

- Based on the shape parameter of Generalized extreme value distribution, for the majority of lowland and highland locations Fréchet distribution seems to be appropriate, while Weibull distribution fits the data better for mountains.
- A decreasing trend in annual snow maxima is found for 97% of the studied region.

- The LR test identified numerous locations with statistically significant ($p < 0.05$) decreasing trends. However, the power of the test on average is low, and the effect size compared to confidence intervals regarding the 50-year return value reveals substantial uncertainty.
- The likelihood ratio test and Akaike weights suggest that the trend in the annual maxima is better captured by allowing trend in the location parameter than in the scale parameter.
- The reliability analyses show that the practical significance of time trends is not implied by the statistical significance. This is largely due to the substantial uncertainty in the parameter estimation, dominating structural reliability.
- The reliability analyses indicate that for most locations in the region that are characterized by Fréchet distribution the negative trend in annual snow maxima has a minor effect on structural reliability, the uncertainty in parameter estimation is governing. Moreover, it is deemed unjustified to extrapolate trends based on about 50 years to thousands of years, which represent a relevant return periods for the ultimate limit states.
- For locations with a strongly decreasing trend and Weibull distribution, the effect of the trend on structural reliability is practically significant, although it is favorable.

Chapter 6

Effect of dependence structure

In structural reliability the dependence structure between random variables is almost exclusively modeled by Gauss (normal or Gaussian) copula, however, this implicit assumption is typically not corroborated. Some studies – from various disciplines – indicate that the adopted copula function can have significant effect on the outcomes. This chapter focuses on time-variant reliability problems with continuous stochastic processes, which are collection of dependent random variables, and to our knowledge they are overwhelmingly modeled using Gauss copula in structural reliability. Therefore, the aim of this chapter is to quantify the impact of this copula assumption on failure probability. Three simple examples are studied considering bivariate Gauss, t, rotated Clayton, Gumbel, and rotated Gumbel copulas. The time-variant actions are modeled as stationary, ergodic, continuous stochastic processes, and the PHI2 method is adopted for the analyses. The calculations show that the copula function has significant effect on the failure probability. In the studied examples, application of Gauss copula can four times underestimate or even ten times overestimate the failure probabilities obtained by other copulas. The findings imply that the copula function should be inferred from observations or if not available, multiple copula functions and Bayesian model averaging is advocated to explore this uncertainty.

6.1 Problem statement and the state of the art

The problems in structural reliability require the integration of multidimensional joint probability distribution functions (Eq.2.1). Due to the scarcity of available information, the joint distribution is overwhelmingly given by its marginals and by a single parameter dependence measure between any two random variables. The typical dependence measure is the Pearson correlation coefficient, however, this single parameter does not uniquely determine the joint distribution function. This means that infinitely many joint distributions can be found to the prescribed marginals and correlation coefficient.

In structural reliability until recently it was a prevalent, implicit assumption that the dependence structure follows Gauss copula. However, some studies imply that this

assumption is not justified by data, and can lead to severe under- or overestimation of failure probability. Tang et al. (2013a) showed that in geotechnical problems the function adopted to describe the dependence structure between cohesion and friction angle has significant effect on the failure probability. They demonstrated that the measurements are best described by Plackett copula, and the copula type might lead to an order of magnitude difference in the failure probability for slope stability. Further geotechnical engineering related studies arrived to similar conclusions (Li et al., 2013; Tang et al., 2015). A study on the impact of copulas on two-component parallel systems concluded that the tail dependence of copulas has significant effect on system reliability (Tang et al., 2013b). These results are particularly important for the current study, since the herein adopted PHI2 method formulates the time-variant reliability problem as a parallel system. Yet, there are important differences due to the nature of time-variant reliability problems, in this chapter: (*i*) the system reliability calculation is only one step in the analysis; (*ii*) the components have substantially different probabilities (failure and survival too); and (*iii*) the component's failure probability is typically much lower than that of considered in the mentioned study.

Copulas are also widespread in many other fields, they are applied for instance for correlated stress-strength models (Domma and Giordano, 2013), for risk assessment of dam overtopping considering bivariate distribution of flood peak and volume (Requena et al., 2013), for describing joint distribution of drought indices (Madadgar and Moradkhani, 2011), for economic time series (Patton, 2012), and for modeling multivariate random variables in financial risk (Donnelly and Embrechts, 2010; Romano, 2002). All the referred studies draw attention to the importance of dependence structure modeling. Additionally, some show the grave consequences of Gauss copula assumption.

To our knowledge, the impact of copulas on time-variant reliability problems has not yet been studied. The referred works suggest that in many cases the Gauss copula assumption is severely biased, thus the aim of this chapter is to quantitatively investigate the effect of copulas on time-variant reliability problems. We restrict our attention to stationary, ergodic stochastic processes and adopt the PHI2 method for the analysis. This method is well suited for time-variant reliability questions where continuous stochastic processes are involved, since it reduces the problem to classical time-invariant problems, for which effective methods are available see, e.g. Ditlevsen and Madsen (2007). The PHI2 method is an accurate, effective, and versatile compared to other time-variant techniques (Andrieu-Renaud et al., 2002, 2004; Baroth et al., 2011). It has been successfully applied among others for the analysis of aging marine structures (Mejri et al., 2011), for degrading reinforced concrete beams (Sudret, 2008b), for steel catenary riser subjected to extreme wave loading (Perdrizet and Averbuch, 2008), for adhesive bonded assemblies (Mejri and Cognard, 2009), and for floating wind turbines too (Perdrizet and Averbuch, 2011).

In Section 6.2, the concept of stochastic processes and copula functions is briefly introduced and the adopted types are described. Thereafter, the PHI2 method and

applied numerical techniques are outlined. Then, three simple examples are presented: (*i*) parametric analysis of a minimal problem with a single stochastic process; (*ii*) a simply supported beam with degrading resistance that also subjected to stochastic loading; and (*iii*) a snow related stochastic problem, where copulas are fitted to observations.

6.2 Stochastic processes

Stochastic process is a sequence of random variables that are typically dependent and the strength of this dependence is the function of their distance. Here only time-continuous stochastic processes are considered where the distance is measured in time. Furthermore, the focus is restricted to stationary and ergodic processes. Under these assumptions, the stochastic process is fully characterized by its marginal distribution, autocorrelation function, and dependence (copula) function. The former describes the distribution of intensity in an arbitrary point in time. The autocorrelation function specifies the strength of dependence between random variables separated by a given time interval (Δt). This function applies only to the parameter that measures dependence, and the copula function is required to fully specify the dependence structure.

6.2.1 Autocorrelation function

Gaussian type autocorrelation function is the common choice in the literature. Herein, it is accompanied by Cauchy function to explore the effect of changing function type (Figure 6.1). These two are applied in this work and defined as:

$$\rho_{\text{Gauss}}(\Delta t) = \exp\left(-\left(\frac{\Delta t}{\tau_F}\right)^2\right) \quad \text{and} \quad (6.1)$$

$$\rho_{\text{Cauchy}}(\Delta t) = \left(1 + \left(\frac{\Delta t}{\tau_F}\right)^2\right)^{-2} \quad (6.2)$$

where:

τ_F correlation length;

ρ Pearson correlation coefficient.

Albeit the latter can express only linear dependence, it is applied here due to its ubiquity in the literature. Kendall's tau and Spearman's rho are more general single parameter measures. For instance, they are sensitive to any monotonic dependence, thus better candidates for dependence measure.

To allow direct comparison with published results and to utilize the more general Kendall's tau measure, the functions given in Eq.6.1 and 6.2 are kept and the following transformation is used:

$$\tau(\Delta t) = \frac{2}{\pi} \cdot \arcsin(\rho(\Delta t)). \quad (6.3)$$

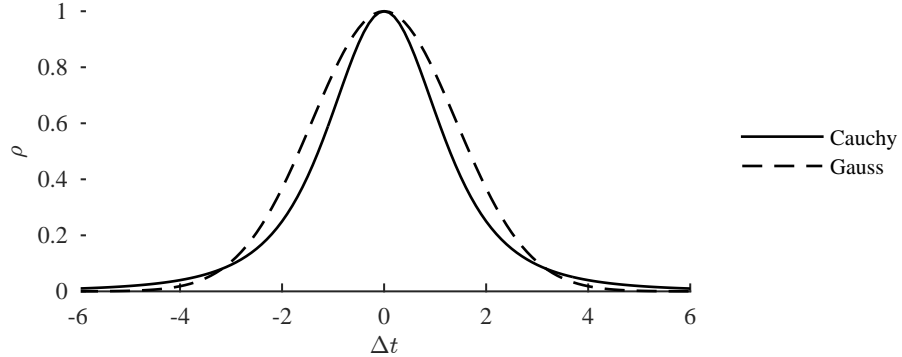


Figure 6.1 Illustration of the considered autocorrelation functions.

The equivalence of copulas is then set in terms of Kendall's tau values. Formula 6.3 transforms between Pearson's rho (ρ) and Kendall's tau (τ) for Gaussian and t copulas, thus the connection to literature is established while allowing for easy extension to other copulas.

6.2.2 Copula based dependence structure

Copula is a multivariate probability distribution function with uniformly distributed marginals. It can be used to model the dependence between random variables with arbitrary marginal distributions (Joe, 2014). In this chapter, we deal mostly with bivariate distributions – the formulas are given for that case – though their extension to higher dimensions is straightforward. The copula function is expressed as:

$$C(u_1, u_2; \theta) = P\{U_1 \leq u_1, U_2 \leq u_2\} \quad (6.4)$$

where:

$C(\cdot)$ copula function;

θ copula parameter;

U_1, U_2 uniformly distributed random variables.

The copula function uniquely describes the dependence structure and it is independent of the marginals if those are continuous. Sklar's theorem establishes the connection between marginals, copula, and joint distribution (Marshall, 1996; Nelson, 2006):

$$F_{X_1 X_2} = C(F_{X_1}, F_{X_2}; \theta) \quad (6.5)$$

where:

F_{X_1}, F_{X_2} cumulative distribution functions of the marginals;

$F_{X_1 X_2}$ the bivariate joint distribution.

Copulas describe only the dependence structure of random variables, this separation of marginal and dependence is beneficial since in practice one has rarely full information about the joint distribution function, and it makes possible to separately infer the marginals and the copula.

In this chapter, Gauss, t , rotated Clayton, Gumbel, and rotated Gumbel copulas are adopted, all has a single parameter (Joe, 1997; Nelson, 2006). The copula functions with the range of the parameters are summarized in Table 6.1. Furthermore, they are compared in Figure 6.2.

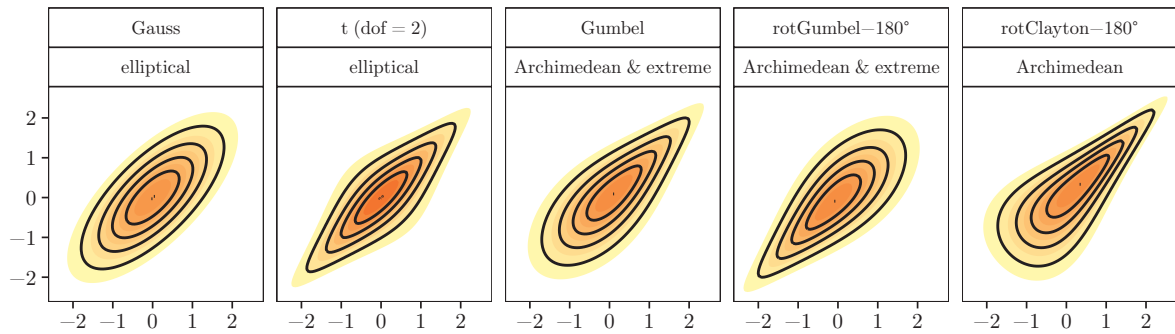


Figure 6.2 Illustration of considered copula functions using bivariate density function contours. For all functions standard normal marginal distributions are used with 0.5 Kendall' tau.

The copula selection is partially motivated by their widespread use. Additionally, it is anticipated that these types cover broad range of possible functions, thus provide a representative picture about the impact of copulas on reliability. Theoretical upper and lower bounds exist for the copula functions, these are referred to as Fréchet-Hoeffding bounds (Nelson, 2006) and they are also given in Table 6.1.

Gauss (normal) and t copulas belong to the elliptical family. Copulas within this family have density contours as concentric, constant eccentricity ellipses. Gumbel and Clayton copulas and their rotated alternatives belong to the Archimedean family. These are widely used due to their simple formulation and their great variety (Nelson, 2006). The Gumbel copula also belongs to the extreme copula family, which arises from extreme value theory, thus it can be used to model dependence between rare events (Joe, 1997). With the exception of Gauss copula, all considered copulas has tail-dependence, which roughly means that joint extremes are more likely than joint moderate values. Gumbel and rotated Clayton copulas have right-tale dependence, while rotated Gumbel copula has left-tail dependence. Both tails of t copula exhibit tail dependence. These are also observable on the density contour plots in Figure 6.2, and might be of particular importance in structural reliability, which is governed by extremely rare events.

6.3 PHI2 method

PHI2 method is an algorithm to solve time-variant reliability problems where (*i*) a random variable is monotonically changing in time, e.g. degradation of material properties; and/or (*ii*) a continuous time-varying process is involved. The algorithm originates from Hagen and Tvedt (1991), who formulated the calculation of the out-crossing rate as a two-component,

Table 6.1 List of the considered copula functions, parameter ranges, and parameters as function of Kendall's tau (τ).

Name	Copula function, $C(u_1, u_2; \theta)$	Range of θ	$\theta(\tau)$
Gauss	$\Phi_2(\Phi^{-1}(u_1), \Phi^{-1}(u_2); \theta)$	$[-1, 1]$	$\sin(\pi/2\tau)$
t	$t_2(t^{-1}(u_1; \nu), t^{-1}(u_2; \nu); \theta)$	$[-1, 1]$	$\sin(\pi/2\tau)$
Gumbel	$\exp\left(-\left(-\log(u_1)^\theta + -\log(u_2)^\theta\right)^{1/\theta}\right)$	$[1, \infty]$	$1/(1-\tau)$
rotGumbel-180°	$u_1 + u_2 - 1 + \exp\left(-\left(-\log(1-u_1)^\theta + -\log(1-u_2)^\theta\right)^{1/\theta}\right)$	$[1, \infty]$	$1/(1-\tau)$
rotClayton-180°	$u_1 + u_2 - 1 + \left(\max\left\{(1-u_1)^{-\theta} + (1-u_2)^{-\theta} - 1; 0\right\}\right)^{-1/\theta}$	$[1, \infty] \setminus \{0\}$	$2 \cdot \tau / (1-\tau)$
lower bound, C_{\sup}	$\max\{1 - 2 + u_1 + u_2; 0\}$	—	—
upper bound, C_{\inf}	$\min\{u_1; u_2\}$	—	—

$\Phi_2(\cdot)$ and $\Phi(\cdot)$ are the bi- and univariate standard normal cumulative distribution functions.

$t_2(\cdot)$ and $t(\cdot)$ are the bi- and univariate t cumulative distribution functions with $\nu = 2$ degrees of freedom.

— Not applicable/not available.

parallel system reliability problem (Eq.6.6). Out-crossing occurs if a random variable or stochastic process is passing the limit state function from safe- to failure region. By definition, the out-crossing rate in time is given as (Hagen and Tvedt, 1991):

$$\nu^+(t) = \lim_{\Delta t \rightarrow 0} \frac{P(\{g(t) > 0\} \cap \{g(t + \Delta t) \leq 0\})}{\Delta t} \quad (6.6)$$

where:

ν^+ out-crossing rate;

$g(\cdot)$ limit state function;

t monotonically increasing parameter, typically time.

Since in structural engineering out-crossings occur rarely, it is generally assumed that they can be described with a Poisson process (Cramer and Leadbetter, 1967). After some algebra and simplification one can derive the formula that is widely used in structural reliability to calculate time-variant failure probability (Melchers, 2002):

$$P_f(t) = P_f(0) + \int_0^t \nu^+(\tau) \cdot d\tau. \quad (6.7)$$

The nominator in Eq.6.6 expresses the failure probability of a parallel system with correlated components. This system reliability problem inherits the copula assumption of the stochastic process. The correlation is typically estimated from the sensitivity factors obtained by first order reliability analysis (FORM) and then bivariate normal distribution is used to calculate the system failure probability (Andrieu-Renaud et al., 2004). Likely this is why the method is coined as PHI2 by Andrieu-Renaud et al. (2002). However, the method is more general and not restricted to bivariate normal distribution, thus the naming is not fortunate. Nevertheless, it reflects well the overwhelming use of Gauss copulas in structural reliability. The application of Gauss copula in classical reliability methods such as FORM is usually referred to as Nataf transformation (Liu and Der Kiureghian, 1986; Nataf, 1962).

It is known that the out-crossing rate given by Eq.6.6 is sensitive to the size of the time step (Δt), thus Sudret (2008a) derived an improved formula, which considerably mitigates this. Since it also relies on the Gauss copula assumption, the original, numerical derivation (Eq.6.6) version is adopted here. To minimize the error, Sudret recommends the time step to be taken as 10% of the correlation length (τ_F). Our analysis confirms this recommendation for Gauss copula with double precision calculation. However, for other copulas the results can be greatly sensitive to the chosen time step. To alleviate this problem multiprecision calculation – quad or larger (Advanpix, 2016) – is adopted that yields to numerically stable results even for small time steps. For the examples in this chapter the range $\Delta t = (10^{-5} \div 10^{-3}) \cdot \tau_F$ is found to have stable convergence: (i) the time step is sufficiently small to accurately estimate the derivative (Eq.6.6); and (ii) the floating point representation is accurate enough to keep truncating errors low. Thus,

for all calculations time step in this range is applied, the convergence and sensitivity to discretization are checked in each cases.

The system reliability problems emerging in PHI2 method are formulated with different copulas and solved by direct, numerical integration (DI). This approach is suited only for simple problems, such those considered in this chapter. For more complicated problems computationally more efficient methods would be needed such as FORM or SORM. Note, that these methods are almost solely implemented with Nataf transformation (Gauss copula) in the currently available research and commercial applications. They can be extended to elliptical copulas, since for these the physical variables can be transformed to a space where the search for the most probable point reduces to minimal distance search (Lebrun and Dutfoy, 2009). However, to date, for other copula types no generalization of these methods is available, thus the application of non-elliptical copulas might be unmanageable.

6.4 Example 1: simple time-variant problem

First, a simple example is analyzed with a single continuous stochastic process ($S(t)$) and deterministic resistance (R). The limit state function is linear and expressed by Eq.6.8:

$$g(t) = R - S(t). \quad (6.8)$$

Using Eq.6.6, the system failure probability ($P_{f,sys}$), required in PHI2 method can be written as:

$$P_{f,sys} = P \left(\{R - S_1 > 0\} \cap \{R - S_2 \leq 0\} \right). \quad (6.9)$$

Where S_1 and S_2 are correlated random variables defined as:

$$S_1 = S(t) \quad \text{and} \quad S_2 = S(t + \Delta t). \quad (6.10)$$

Using Eq.6.9 and 6.5, the failure probability of the parallel system can be expressed as:

$$\begin{aligned} P_{f,sys} &= F_S(R) - F_{S_1 S_2}(R, R) \\ &= P_{s,comp} - C(P_{s,comp}, P_{s,comp}; \theta) \end{aligned} \quad (6.11)$$

where $P_{s,comp}$ stands for the survival probability of a component and it corresponds to $1 - P_f(0)$. It can be seen from Eq.6.11 that for a given $P_{s,comp}$ the system's failure probability is independent of the marginal distributions. Therefore, the stochastic process is sufficiently characterized by the autocorrelation function and by the copula, for the current purposes.

By specifying $P_{s,comp}$ and the copula type, the system's failure probability can be calculated. Then by the finite difference formulation of Eq.6.6 and using Eq.6.7 the time-variant reliability can be obtained. For this example, the time interval is taken as 50

years, and the autocorrelation length is $\tau_F = 1/365$ year. First, Gaussian autocorrelation function is used.

The analyses are completed for various initial/component failure probabilities ranging from 10^{-10} to 10^{-6} with all five copulas having the same Kendall's tau for a particular set of input parameters. The results are represented as reliability indices in Figure 6.3. Moreover, Figure 6.4 summarizes the time-variant failure probabilities and their normalized values.

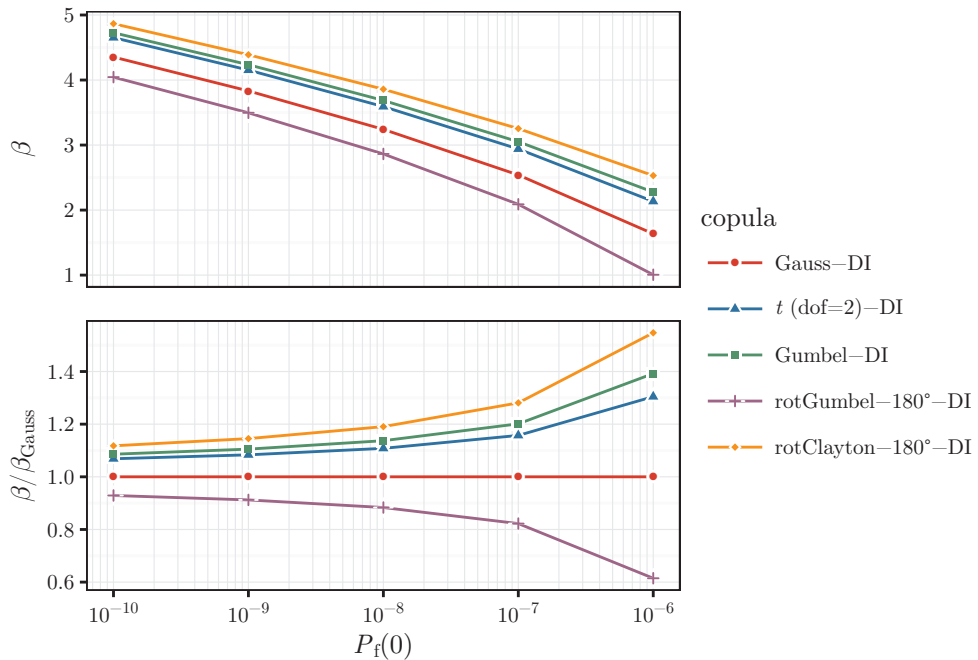


Figure 6.3 Reliability indices (β) and normalized reliability indices plotted against initial failure probability ($P_f(0)$) for various copulas. DI refers to direct integration.

From the figures it is clear that the copula type has significant effect on the failure probability. Compared with the widely used Gauss, the rotated Gumbel copula gives 3.1-3.9 times higher failure probability, the ratio is decreasing with decreasing initial failure probability. On the other hand, t , Gumbel, and rotated Clayton copulas yield to 0.09-0.33 times lower results than the Gauss copula; here too the ratio is decreasing with decreasing initial failure probability. Irrespectively of the copula type, the initial failure probability has no significant effect on the normalized results.

The calculations are repeated with other correlation lengths ranging from $0.1/365$ to $100/365$. It is found that the normalized results are only slightly affected by this change, even at maximum less than 2% change is observed in failure probability. This can be explained by that (i) the correlation between S_1 and S_2 is independent of τ_F because Δt is chosen as a fixed percentage of that; and (ii) $P_f(0)$ is typically much smaller than the second term in Eq.6.7. Indeed, the largest difference is observed when $P_f(0)$ is comparable to the time-variant failure probability. In case of $\tau_F = 1000/365$ for Gumbel copula,

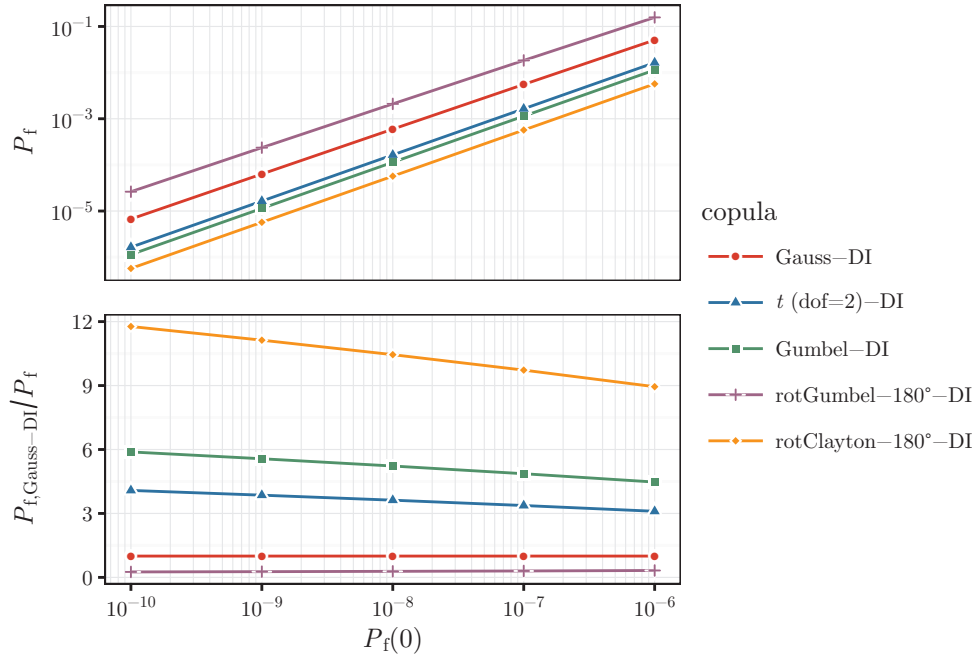


Figure 6.4 Failure probabilities (P_f) and normalized failure probabilities plotted against initial failure probability ($P_f(0)$) for various copulas. DI refers to direct integration.

the normalized time-variant failure probability increases by 7% compared to 1/365 year correlation length. The increase is 15% for rotated Clayton copula.

Up to this point, all presented calculations correspond to Gaussian autocorrelation function. Switching to Cauchy function, the normalized time-variant failure probabilities – with $\tau_F = 1/365$ year correlation length – change irrespectively of initial failure probability and of copula type. The ratio of normalized time-variant Cauchy and Gaussian failure probabilities is uniformly 1.41. It is solely influenced by the autocorrelation function.

In our case, the upper Fréchet-Hoeffding bound yields to zero up-crossing rate, while the lower bound gives infinitely large value. These can be shown using Eq.6.11 and Table 6.1:

$$\begin{aligned} P_{f,sys,inf} &= P_{s,comp} - C_{sup}(P_{s,comp}, P_{s,comp}) = 3 \cdot P_{s,comp} - 1 \xrightarrow{\frac{dP_{f,sys}(t)}{d\Delta t}} \nu_{inf}^+ = \infty \\ P_{f,sys,sup} &= P_{s,comp} - C_{inf}(P_{s,comp}, P_{s,comp}) = 0 \xrightarrow{\frac{dP_{f,sys}(t)}{d\Delta t}} \nu_{sup}^+ = 0. \end{aligned} \quad (6.12)$$

This means that the copula bounds convey no useful information; however, more importantly it implies that there are copula functions that yields to arbitrary large or arbitrary small out-crossing rates. Hence, compared with Gauss copula, arbitrary large error could be produced.

6.5 Example 2: corroding beam

The following example is adopted from Sudret (2008a). It is a simply supported, corroding steel beam subjected to a time-variant load that is described by a continuous stochastic

process (Figure 6.5). The original example is intended to illustrate the application of PHI2 method to solve a time-variant reliability problem and it implicitly adopted Gauss copula. Herein we extend the example by investigating the effect of copula function on out-crossing rate and reliability.

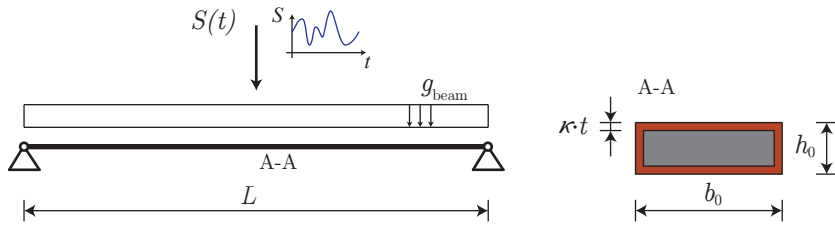


Figure 6.5 Illustration of the corroding beam example.

The mechanical and probabilistic models (Table 6.2) are the same as in the original example, solely the copula is varied that describes the dependence between the survival and failure of the structure between two “close” time instants.

Table 6.2 Probabilistic models for corroding beam example.

Variable name	Distribution	Mean	CV
Concentrated load, $S(t)$ [N]	Normal	3500	0.20
Yield strength, σ_R [MPa]	Lognormal	240	0.10
Beam width, b_0 [mm]	Lognormal	200	0.05
Beam height, h_0 [mm]	Lognormal	40	0.10
Unit weight, ρ_{st} [kN/m ³]	constant	78.5	–
Span, L [m]	constant	5	–

– Not applicable.

The autocorrelation function of the stochastic process is Gaussian (Eq.6.1), with correlation length of 1 day. The corrosion occurs uniformly on the surface of the beam and propagates linearly in time:

$$b(t) = b_0 - 2 \cdot \kappa \cdot t \quad \text{and} \quad h(t) = h_0 - 2 \cdot \kappa \cdot t \quad (6.13)$$

where:

t time;

κ corrosion rate, 0.05 mm/year.

Taking into account the self-weight of the beam and the time-variant load ($S(t)$) the limit state function corresponding to the formulation of a plastic hinge at midspan is given by Eq.6.14:

$$\begin{aligned} g(t) &= M_R(t) - (M_G + M_S(t)) \\ &= \frac{b(t) \cdot h(t)^2 \cdot \sigma_R}{4} - \left(\frac{\rho_{st} \cdot b_0 \cdot h_0 \cdot L^2}{8} + \frac{S(t) \cdot L}{4} \right). \end{aligned} \quad (6.14)$$

In accordance with the original example, the self-weight is assumed to be time-invariant, although the cross-section's dimensions are decreasing in time. The design life of the beam is assumed to be 20 years.

The time-variant reliability problem is solved with copulas listed in Table 6.1; the corresponding out-crossing rates and normalized out-crossing rates in time are shown in Figure 6.6. In case of Gauss copula, besides the direct numerical integration (DI) the calculations are also carried out by FORM. In the latter, the correlation between the two components (Eq.6.6) is estimated from the angle between corresponding FORM hyperplanes (Ditlevsen, 1979). The small difference between FORM and numerical integration outcomes is attributed (*i*) to the non-linearity of limit state function; and (*ii*) to the approximate correlation coefficient used in FORM. The results confirm the applicability of FORM to approximate the reliability.

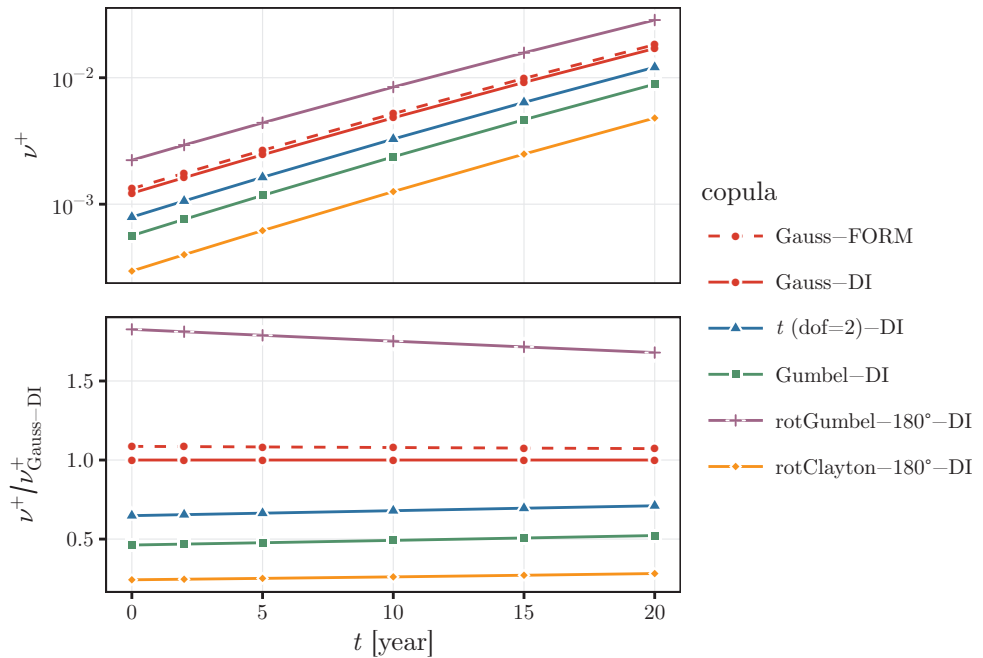


Figure 6.6 Out-crossing rates (ν^+) and normalized out-crossing rates in time for various copulas. DI refers to direct integration.

Figure 6.6 shows considerable differences in out-crossing rates for different copulas. Compared with the Gauss-DI solution, the rotated Gumbel copula gives about 1.8 times larger rates, while other copulas lead to smaller rates. The largest reduction is observed for rotated Clayton copula, which is 0.25 times that of the Gauss copula. It can be also observed that normalized out-crossing rates vary only slightly in time.

Figure 6.7 and Figure 6.8 illustrate the time-variant failure probabilities and reliability indices, respectively. The former follows well the trend observed in out-crossing rates, which is as quasi-constant ratio in time. In Figure 6.7, it can be seen that the normalized ratios per copula function is very close to that of the out-crossing rates, with the exception of $t = 0$ time instant, where the out-crossing rate is not taken into account. The figures

also indicate that the two degrees of freedom t copula leads to similar results as of Gumbel copula. Compared with the Gauss copula with direct integration, the largest ratios in failure probabilities are 1.1 and 1.8 for Gauss-FORM and rotated Gumbel copulas, respectively. The smallest ratios are 0.7, 0.5, and 0.3 for t , Gumbel, and rotated Clayton copulas, respectively. The increasing difference in reliability indices with increasing time is attributed to the nonlinear transformation between failure probability and reliability index.

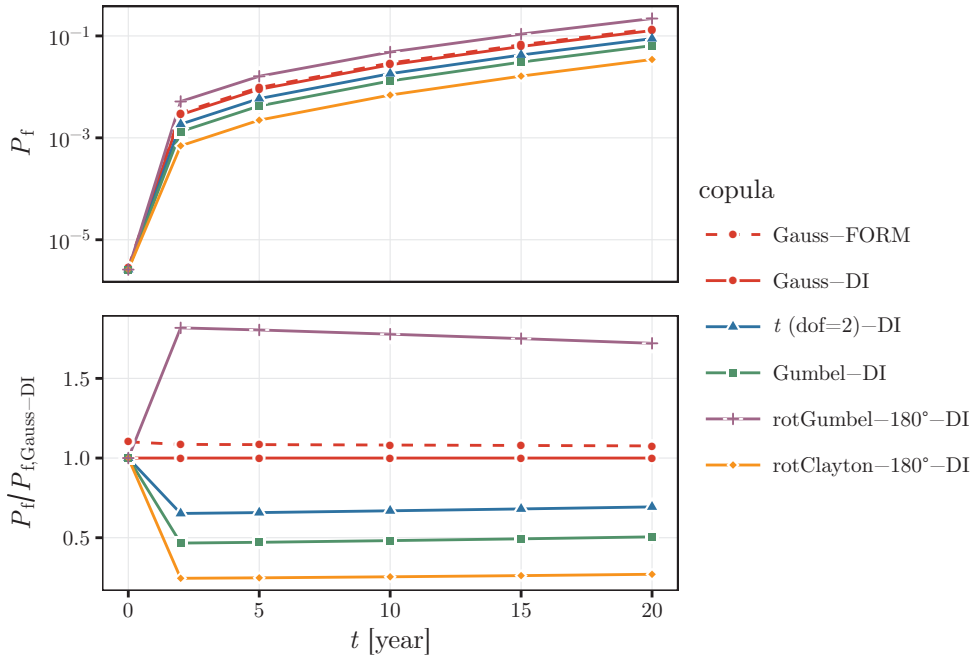


Figure 6.7 Failure probabilities (P_f) and normalized failure probabilities in time for various copulas. DI refers to direct integration.

All the presented results are from analyses using Gaussian autocorrelation function. The calculations are repeated with Cauchy autocorrelation function and the outcomes show that the change in out-crossing rate is independent of the copula type and time. The ratio of out-crossing rate obtained by using Cauchy and Gaussian autocorrelation functions is 1.41. This considerable effect is also rarely acknowledged in the literature, where the Gaussian autocorrelation function is prevalent. This ratio is inherited by the time-variant failure probability since the initial failure probability is negligible compared to the term involving the out-crossing rate (Eq.6.7).

6.6 Example 3: generic structure subject to snow load

In this example a time-variant reliability problem is studied, where the stochastic process is inferred from observations. Maximum likelihood method (Section C.1.1) is chosen for

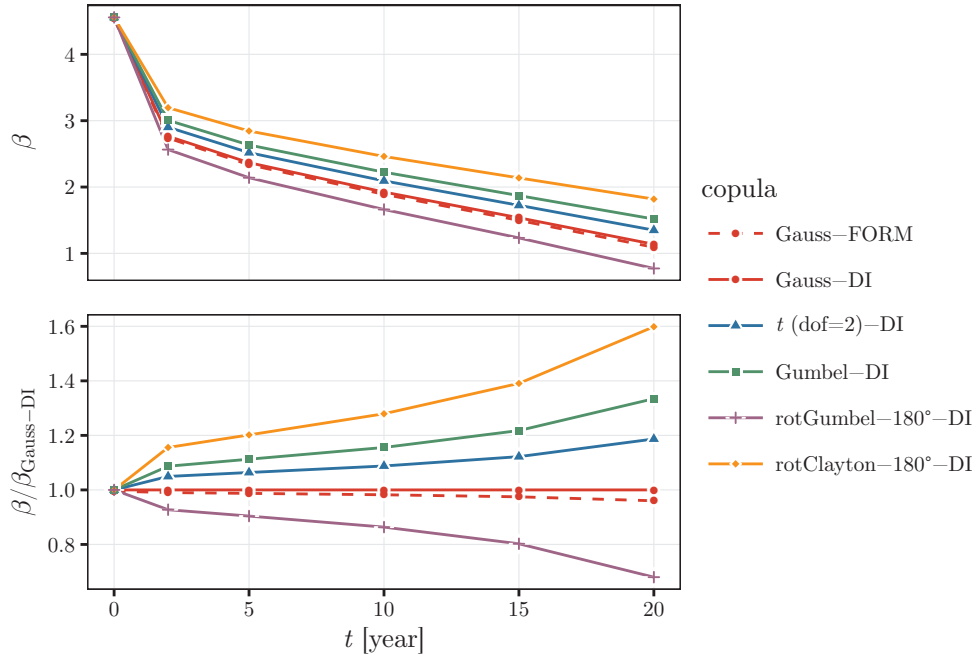


Figure 6.8 Reliability indices (β) and normalized reliability indices for various copulas. DI is referring to direct integration.

parameter estimation. However, the calculation of the full likelihood is computationally demanding – often numerically intractable – even for moderately large datasets due to the need to evaluate high-dimensional, multivariate distributions. Thus, it is often replaced with pairwise likelihood that requires only bivariate distributions and shares the same properties as the full likelihood based estimator except its loss of efficiency (Padoan et al., 2010). This pairwise approach is also applied for spatial modeling such as temperature extremes in Switzerland (Ribatet and Sedki, 2012) and adopted herein too. The formulation of the pairwise likelihood function is given as:

$$L_p(\mathbf{x}; \theta) = \prod_{i < j} p([x_i, x_j]; \theta). \quad (6.15)$$

Ground snow observations in the form of snow water equivalent are selected for the representative lowland location of Budapest in the Carpathian Region. The data are from the CarpatClim database and available in 10 km spatial and 1-day maxima temporal resolution (Szalai et al., 2013). Budapest (19.1°E, 47.5°N) is characterized by intermittent snow cover, i.e. couple of snowfalls followed by often complete melting. The analyzed sample is extracted using the following principles:

- peaks are extracted from daily maxima;
- from two peaks separated by four or less days the smaller one is removed;
- each winter season is treated as a single unit because snowfalls are clustered over a few months;

- if only a single peak occurs in a season its likelihood is calculated from the univariate marginal.

This means that a sequence of peaks is obtained for each winter seasons that are assumed to be independent. However, peaks within the same season are treated as realizations of a time-continuous stochastic process, thus they are dependent. The extracted sequence of peaks along with daily maxima are illustrated in Figure 6.9 for five consecutive years.

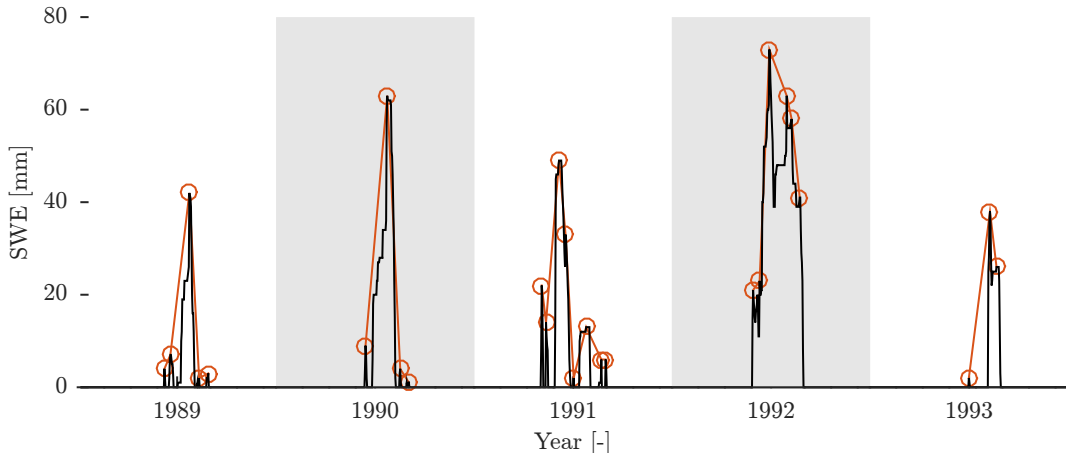


Figure 6.9 Illustration of extracted peaks from daily snow water equivalent (SWE) maxima over five consecutive years.

Note that this is a somewhat arbitrary approach and the sample could be extracted many different ways. However, this deemed sufficient to illustrate the effect of copulas inferred from data. In average five peaks are present for a given winter season and in total there are 249 peaks for the 49 seasons. Gauss and Cauchy autocorrelation functions, and Gauss, *t*, Gumbel, rotated Gumbel, and rotated Clayton copulas are considered. Additionally, three marginal distributions are used: Gauss, Lognormal, and Gumbel.

For each autocorrelation-marginal-copula triplet three parameters are inferred: two parameters of the marginal and the correlation length. Separate inference of the marginal and copula is not possible due to nature of the problem, thus the parameters are estimated simultaneously.

Akaike information criterion (AIC, Eq.C.8) is calculated for each triplet. Then pooling is made for each autocorrelation-marginal sets, where a set is composed of the copulas as candidate models. This pooling is explained by the large difference in AIC (>100) between models with different marginal function. The related Akaike weights (w , Eq.C.10) are visually compared in Figure 6.10. It shows that – with the exception of Gauss autocorrelation-Gumbel marginal pair – Gumbel copula performs significantly better than the other considered copulas.

In most cases, the Cauchy autocorrelation function provides significantly better fit ($\Delta\text{AIC} > 5$) than the Gauss using the same type of copula and type of marginal. The only exception is the rotated Clayton copula for which Gauss autocorrelation function is slightly better. The marginal distribution type has substantial effect on the fit, it can

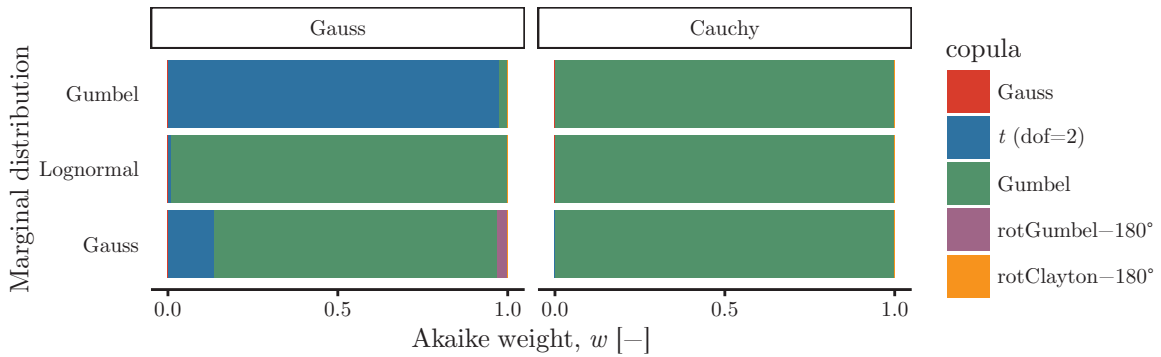


Figure 6.10 Akaike weights for autocorrelation-marginal pools. A pool is formed by a particular autocorrelation function (Gauss, Cauchy) and by a particular marginal distribution (Gauss, Lognormal, Gumbel), and the six copula functions provide the candidate models.

yield to over 100 difference in AIC. Lognormal provides the best fit, followed by Gumbel and Gauss. The outstanding performance of Gumbel copula implies that extreme copulas might suit better for describing dependent extremes, this conjecture is also supported by the extreme value theory. Furthermore, by using extreme t copula with two degrees of freedom even better fit is obtained than that of Gumbel.

To explore the effect on time-variant reliability the inferred stochastic models are used in a simple reliability problem characterized by the following limit state function:

$$g(t) = R - (G + S(t)). \quad (6.16)$$

The properties of the involved probabilistic models are summarized in Table 6.3.

Table 6.3 Marginal distribution of random variables for stochastic snow load example.

Variable name	Distribution	Mean	CV
Resistance, R	Lognormal	250	0.10
Permanent action, G	Normal	60	0.07
Snow maxima, $S(t)$	Normal, Lognormal, Gumbel	*	*

* Depends on the applied autocorrelation-marginal-copula triplet.

For comparison, the out-crossing rates are calculated for each triplet and presented in a normalized form in Figure 6.11. For each marginals the out-crossing rates are normalized with that of the corresponding Gauss copula. The same trend is observed for all marginals. Using Gauss copula the largest underestimation of out-crossing rate is 8 times, while the largest overestimation is 3 times. Neither of these are corresponding to Gumbel copula, which yields to 4.2, 2.9, and 3.5 times smaller out-crossing rates for Gauss, Lognormal, and Gumbel marginals, respectively. Figure 6.11 conceals the multiple order of difference between out-crossing rates of different marginals. Although it is low importance now as we are interested in the effect of copula functions. The effect of replacing the Gauss autocorrelation with Cauchy function yields to similar results as observed in previous

examples. The ratio of corresponding Cauchy and Gauss out-crossing rates is uniformly about 1.4.

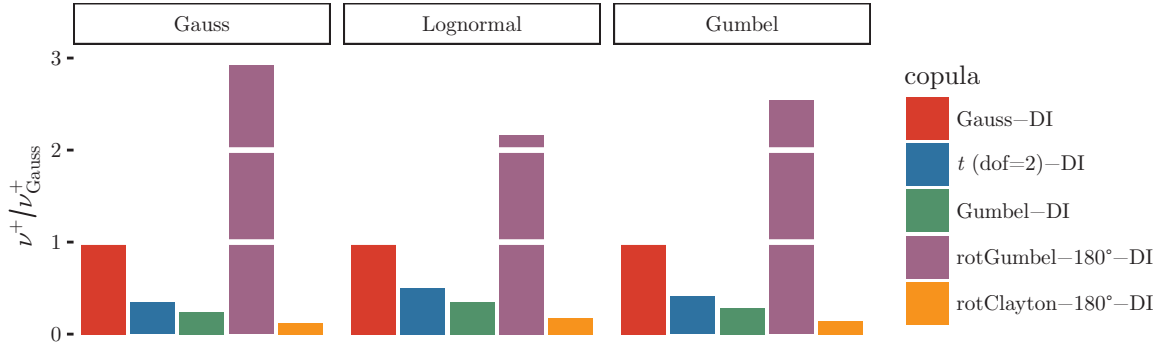


Figure 6.11 Normalized out-crossing rates for Gauss autocorrelation function. For each marginals (Gauss, Lognormal, Gumbel) the out-crossing rates are normalized with that of the corresponding Gauss copula. DI refers to direct integration.

6.7 Application example: Eiffel-hall of Budapest

In Section 6.6 a generic structure is analyzed, which is located at the site of Eiffel-hall. Herein the same location – thus same snow action – but the structure of the Eiffel-hall is investigated. The structure is introduced in Annex B.2, here only the essential details, which are required to interpret the results, are provided. The stochastic snow models fitted in the preceding section is used in the analysis. Only Gaussian autocorrelation function and Gumbel marginal distribution are considered. The wind action is represented by a distribution function corresponding to 50 years reference period. The out-crossing rates – calculated by direct numerical integration – are summarized in Table 6.4. Compared with Gauss copula, the largest difference is observed for Gumbel copula, which yields to about three times smaller out-crossing rate. Figure 6.10 shows that for the inputs the t copula provides the best fit, which leads to 40% smaller out-crossing rate than that of the Gauss. The effect of copula function type is smaller than in previous examples, though it is still considerable.

Table 6.4 Out-crossing rates for Eiffel-hall considering Gauss autocorrelation function and Gumbel marginal distribution.

Parameter	Gauss	t (dof=2)	Gumbel	rotGumbel-180°	rotClayton-180°
$\nu^+ [\cdot 10^{-3}]$	1.18	0.737	0.403	2.22	0.794
$\nu^+/\nu^+_{\text{Gauss}}$	1.00	0.622	0.340	1.87	0.671

6.8 Discussion

Dependence structure (or copula function) uncertainty belongs to probability model selection uncertainty. Thus, from mathematical point of view the issue is very similar to distribution selection uncertainty, which is treated in Chapter 3. The same considerations apply here as well: typically there are insufficient data to identify the true model, copula function. Hence, for normal structures agreement on the copula function is recommended, and for safety critical structures Bayesian model averaging is advocated to account for copula type uncertainty.

For non-Gaussian copulas direct integration is used here and typically quad or larger precision calculation is required to achieve convergence. Efficient algorithms, such as FORM, are currently only available for elliptical copulas, additional research would be needed to extend existing or develop new methods for other copulas. Thus, this poses a limitation on incorporation of copula function uncertainty in probabilistic analysis.

6.9 Summary and conclusions

In this chapter the effect of the dependence structure between random variables is analyzed on the failure probability of structures. Copula function is adopted to describe the dependence and the emphasis is placed on time-variant reliability using PHI2 method. The analysis of three simple examples – considering Gauss, t , rotated Clayton, Gumbel, and rotated Gumbel copulas – reveal:

- The applied dependence structure has significant effect on time-variant reliability. The prevalently applied Gauss copula assumption can 4 times underestimate or even 10 times overestimate failure probabilities obtained by other adopted copulas.
- For a simple case (Example 1), it is demonstrated that by an appropriate choice of copula function arbitrary large error can be produced in out-crossing rate, compared with that of the Gauss copula.
- The correlation length of stochastic process and initial failure probability have minor effect on the ratio of the Gauss and other copula results.
- The autocorrelation function has considerable effect on the time-variant failure probability. The ratio of normalized time-variant Cauchy and Gaussian failure probabilities is uniformly 1.41. It is solely influenced by the autocorrelation function.
- Analysis of ground snow observations implies that extreme copulas, such as Gumbel, fit significantly better to dependent snow extremes than Gauss copula. The Gumbel copula can yield to 4 times lower out-crossing rate than that of Gauss.

To our knowledge the copula and autocorrelation effects have not yet been studied previously and the findings provide a novel insight into time-variant problems. The results

also give indication about whether a particular part of the mechanical or probabilistic model is worth of refinement, if the actual dependence structure is largely unknown.

If observations are available, the actual dependence structure should be inferred, and in case of limited information, multiple copula functions should be used to quantify the related uncertainty. Model averaging (Annex C.1.5) provides a viable approach to rigorously account for this uncertainty. In reporting of reliability analyses, the dependence structures, namely the adopted copulas should also be reported to give full description of the probabilistic model and to allow reproducibility.

Chapter 7

Summary and conclusions

This final chapter provides a summary and it recapitulates the main conclusions along with practical recommendations. Furthermore, theses are formulated, and novelties and limits of the study are highlighted.

7.1 Purpose and significance of the study

The aim of this thesis is to subtly adjust the existing imbalance between probabilistic and physical models in civil engineering. To this end, it deals with issues related to probabilistic models and it aims to explore neglected effects and to provide improved probabilistic analysis to capture them. Extreme ground snow load is selected as a vehicle of illustration, though the investigated issues are present for most random variables. The main contributions are as follows:

- This study explores commonly neglected or underappreciated effects in structural reliability; these are: statistical uncertainty, measurement uncertainty, long-term trends, and dependence structure.
- Existing methods are transferred, adapted and applied from other fields to solve civil engineering issues. Some of these are rarely or have not been used before for issues considered here. These serve as reference since they are able to capture the neglected effects in current approaches.
- It is demonstrated that the neglect of the examined factors can lead to an order of magnitude underestimation of failure probability. Recommendations are made on how and when to incorporate them in probabilistic analysis.

The results are applicable to probabilistic analysis of structures and to codification as well. They bear significance especially for safety critical structures, such as nuclear power plants, where probabilistic risk analysis is prescribed. The findings provide improved insight into probabilistic analysis of snow extremes and into their effect on structural reliability.

7.2 Recapitulation of main conclusions

The main conclusions emphasizing the contributions¹ of this work are presented as responses to the questions posed in Section 1.2. The responses are identically structured and divided into subsections: previous works and current practice, methods, novelty, scope and limit, and thesis. Although the proposed practical recommendations constitute novelties they are not listed among them as they are presented at the theses. The assertions about current practice, previous works, and novelty of the answers are not absolute statements. The expression: *to the best knowledge of the candidate* should be put in front of each.

7.2.1 Distribution of annual ground snow maxima

Which distribution function is the “best” to model ground snow extremes? What constitutes an appropriate model?

Previous works, current practice

Consensus is missing on the appropriate model for annual ground snow maxima among reliability experts. Gumbel and three-parameter Lognormal distributions are widespread in Europe, while two-parameter Lognormal is typical in the USA. Often instead of a general rationale, prescriptions are provided thus adaptation to local conditions can be cumbersome.

Methods

Method of moments, frequentist, and Bayesian techniques are adopted for inference of distribution parameters. Visual checks and information theory based goodness-of-fit measures are used to identify the “best” performing distribution type. Gumbel, Generalized extreme value, two-parameter Lognormal, and three-parameter Lognormal distributions are considered.

Novelty

Advanced statistical analyses are performed on snow water equivalent annual maxima in the Carpathian Region, for example information theory based measures are used for model comparison. Application of many of these are novel compared with the typically adopted approaches and it allows for judging the merits and performance of the latter. In the spirit of open and successive research, posterior distributions and an online, open-source, interactive snow map are provided to facilitate cooperation between neighboring countries.

¹In accordance with the requirements of the Vásárhelyi Pál Doctoral School, the contributions of the candidate are organized into theses. These are formulated to comply with the unwritten rules of the School. One of which is that the theses are to be written in first person singular.

Scope and limits

The used methods, developed codes and applications are easily adaptable to other climatic actions. Limitations are that solely annual block maxima, limited number of distribution functions, and only three statistical techniques are considered.

Thesis I

I statistically analyzed the ground snow water equivalent data of about 6000 grid points in the Carpathian Region covering 49 winter seasons from 1961 to 2010. I fitted multiple distribution types to the annual snow maxima that are extracted from daily observations. Based on extensive statistical analysis:

- I/a** I demonstrated that mountains and highlands are better represented by Weibull, while lowlands by Fréchet distribution compared with the currently standardized Gumbel model recommended in Eurocode and used in Hungary. I showed that the Gumbel model often appreciably underestimates the snow maxima of lowlands and thus overestimates structural reliability. The Lognormal model typically performs even worse than the Gumbel. From the considered distributions, based on reliability, empirical (data-driven), and theoretical considerations Weibull distribution is recommended for mountains and highlands, and Fréchet for lowlands.
- I/b** I determined the posterior distribution of the characteristics of snow maxima for representative areas in the region. These can be used as prior information for regions with similar conditions. Furthermore, I created an open-source, online, interactive snow map for the Carpathian Region. It can be used to obtain characteristic ground snow load and to check exceptional ground snow load with 10 km spatial resolution.

(Rózsás and Sýkora, 2015b,c; Rózsás et al., 2016b; Vigh et al., 2016)

7.2.2 Effect of statistical uncertainties

How large is the effect of statistical uncertainties on structural reliability? Is their neglect reasonable? How should these uncertainties be taken into account?

Previous works, current practice

Statistical uncertainties are routinely neglected in reliability analyses, i.e. point estimates of distribution parameters are used for representative fractiles and in probabilistic models. For example the background research document on snow loads of Eurocode completely ignores this uncertainty.

Methods

Frequentist and Bayesian approaches are applied to quantify parameter estimation and model selection uncertainties. The former is accounted for by uncertainty intervals and the latter is by model averaging. Bayesian posterior predictive distribution is used to integrate parameter estimation uncertainty into failure probability. Multiple examples with extensive parametric analyses are performed to explore the effect of neglecting statistical uncertainties.

Novelty

Systematic, rigorous analysis on the effect of statistical uncertainties on representative fractiles and on structural reliability has not yet been performed. Drawing attention to the severe underestimation of failure probability using current approaches provides novel insights.

Scope and limits

Although the numerical results and conclusions are confined to limited parameter range and are mainly focused on ground snow extremes, the adopted techniques are not restricted to the considered problem and can be utilized for other random variables, phenomena as well, such as floods and wind loads.

Thesis II

I analyzed the effect of statistical uncertainties (parameter estimation and model selection uncertainties) in annual ground snow maxima on representative fractiles and on reliability. These are prevalently neglected in current civil engineering practice though inevitably present due to data scarcity.

II/a I showed that the neglect of parameter estimation uncertainty can lead to considerable (20%) underestimation of representative fractiles. Furthermore, the applied distribution type (model selection uncertainty) has larger effect on representative fractiles than the parameter estimation uncertainty. Two-parameter Lognormal, three-parameter Lognormal, Gumbel, and Generalized extreme value distributions are considered.

II/b Using reliability analyses, I demonstrated that the neglect of statistical uncertainties can even lead to multiple order of magnitude underestimation of failure probability. I illustrated that the use of “best” point estimates, such as maximum likelihood or method of moments estimates, are not conservative from reliability point of view. They can lead to practically significant underestimation of failure probability.

Based on these findings, I made recommendations on the treatment of statistical uncertainties for normal and safety critical structures. Furthermore, I recommend the use of Bayesian posterior predictive distribution in reliability analysis and I advocate model averaging to account for model selection uncertainty.

(Rózsás et al., 2016a; Rózsás and Sýkora, 2015a,b,c,d; Rózsás and Vigh, 2014)

7.2.3 Effect of measurement uncertainty

How measurement uncertainty should be taken into account and propagated to structural reliability? Is the current practice, which neglects it, acceptable from reliability point of view? Is its effect on failure probability practically significant?

Previous works, current practice

Observations are inevitably contaminated with measurement uncertainty, which is a significant source of uncertainty in some cases. In reliability analysis, probabilistic models are typically fitted to measurements without considering this uncertainty. The statistical approach to this problem is applied in astronomy, econometrics, biometrics, etc., however, not in civil engineering.

Methods

Statistical and interval based approaches are proposed to quantify and to propagate measurement uncertainty. These are critically compared by analyzing ground snow measurements, which are often affected by large measurement uncertainty. It is propagated through the mechanical model of a generic structure to investigate its effect on reliability.

Novelty

The conducted measurement uncertainty analyses represent novelty both in methods and in results, i.e. demonstrating their practical significance and the inadequacy of current practice. Mathematically sound statistical and interval based approaches are adapted from statistics and computational science. Their application to measurement uncertainty in civil engineering is novel.

Scope and limits

Although the study is limited by the considered distribution types (Normal, Lognormal, Gumbel), reality-observation links (additive, multiplicative), and parameter ranges (coefficient of variation 0.2-0.6), it covers many practically relevant random variables. The presented approaches and algorithms can be easily used for other distribution types and measurement error structures. An additional limitation of the study is that measurement

uncertainty is considered only for the dominant variable action. Furthermore, the effect of sample size should be analyzed in future studies.

Thesis III

I analyzed the effect of measurement uncertainty in annual ground snow maxima on structural reliability, which is typically neglected in civil engineering. I proposed statistical and interval analysis based approaches and concluded that:

III/a Measurement uncertainty may lead to significant (order of magnitude) underestimation of failure probability. Ranges of the key parameters are identified where measurement uncertainty should be considered. I derived these from analysis of Normal, Lognormal, and Gumbel distributions with coefficient of variation ranging from 0.2 to 0.6 and with various extents of measurement uncertainty (0-10% of mean of annual maxima).

III/b If the contamination mechanism is known then the statistical approach is recommended, otherwise the interval approach is advocated. For ground snow extremes at lowlands, the neglect of measurement uncertainty is acceptable. Otherwise, statistical or interval approaches are recommended.

For practical applications, the lower interval bound and predictive reliability index are recommended as point estimates using interval and statistical analysis, respectively. The point estimates should be accompanied by uncertainty intervals, which convey valuable information about the credibility of results.

(Rózsás and Sýkora, 2016b)

7.2.4 Long-term trends in annual ground snow maxima

Is the stationary assumption tenable for snow extremes? What are the practical implications of time-trends for structural reliability?

Previous works, current practice

The current structural design provisions are prevalently based on experience and on the assumption of stationary meteorological conditions. However, the observations of past decades and advanced climate models show that this assumption is debatable. Non-stationary extreme value analyses are regularly performed by statisticians and meteorologists, but rarely considered or applied by civil engineers.

Methods

Annual maxima snow water equivalents are taken and univariate Generalized extreme value distribution is adopted as a probabilistic model. Stationary and five non-stationary distributions are fitted to the observations utilizing the maximum likelihood method. Statistical and information theory based approaches are used to compare the models and to identify trends. Finally, reliability analyses are performed on a simple structure to explore the practical significance of trends.

Novelty

Quantitative analysis on the effect of time-trends in ground snow loads on structural reliability has not yet been undertaken. Furthermore, long-term trends in extreme ground snow loads, e.g. annual maxima, for the Carpathian Region have not been sufficiently analyzed before.

Scope and limits

The presented approach can be applied for other basic variables too that suspected to exhibit practically significant time-trends. The adopted annual block maxima approach yields to only 49 observations, which allow poor extrapolation to the future. It is dominated by parameter estimation uncertainty. Additional limitation of this study is that only Generalized extreme value distribution is considered. This can have an important effect on the failure probability, since that is governed by the tail of the distribution.

Thesis IV

Using non-stationary extreme value analysis, I investigated the long-term time-trends in annual ground snow maxima of the last 49 years for the Carpathian Region. By statistical and information theory based analyses I showed that:

IV/a Decreasing time-trend is present in annual snow maxima for 97% of the Carpathian Region. Statistically significant ($p < 0.05$) decreasing time-trend is found for 65% of the studied region. The hypothesis test is accompanied by effect size and power analysis too. Furthermore, the practical significance of change is demonstrated in respect of characteristic values for several locations. The time-trends are confirmed by information theory based analysis as well.

IV/b For most locations in the region that are characterized by Fréchet distribution the negative trend in annual snow maxima has a minor effect on structural reliability. The uncertainty in parameter estimation is governing. For locations with a strongly decreasing trend and Weibull distribution, the effect of the trend on structural

reliability is practically significant, although the change is favorable from a safety point of view as it increases the reliability.

(Rózsás et al., 2016a,b; Sýkora et al., 2016)

7.2.5 Effect of dependence structure

How large is the effect of copula assumption on time-variant structural reliability? Is the current practice conservative for snow loads? How can the copula function uncertainty be treated?

Previous works, current practice

In structural reliability the dependence structure between random variables is almost exclusively modeled by Gauss copula; however, this implicit assumption is typically not corroborated. Some studies – from various disciplines – indicate that the adopted copula function can have significant effect on the outcomes. Still, time-variant problems with continuous stochastic processes are not modeled by other than Gauss copula in civil engineering.

Methods

Time-variant reliabilities are calculated and compared using Gauss, t , Gumbel, rotated Gumbel, and rotated Clayton copulas. Since analytical solutions are in general not available, finite difference formulation of out-crossing rate is used. Three simple examples are considered to investigate the effect of copula assumption. In the third one, the copula function is inferred from observations.

Novelty

The effect of copula and autocorrelation functions on time-variant reliability has not yet been studied previously and the findings provide a novel insight into these problems.

Scope and limits

The raised questions are valid and the proposed approach is applicable for all types of time-continuous stochastic processes, not limited to snow actions. Although, the numerical findings may vary based on the variable in question.

Thesis V

I investigated the effect of widespread Gauss copula assumption on time-variant reliability with continuous stochastic processes and demonstrated that:

V/a The applied dependence structure has significant effect on time-variant reliability.

The prevalently applied Gauss copula assumption can four times underestimate or even ten times overestimate failure probabilities obtained by other adopted copulas (t , Gumbel, rotated Gumbel, and rotated Clayton). For a simple case, I demonstrated that by an appropriate choice of copula function, arbitrary large error can be produced in out-crossing rate compared with that of the Gauss copula.

V/b The autocorrelation function has considerable effect on the time-variant failure probability. The ratio of normalized time-variant failure probabilities obtained using Cauchy and Gauss autocorrelation functions is uniformly 1.41. It is solely influenced by the autocorrelation function type.

V/c Analysis of ground snow observations implies that extremes copulas, such as Gumbel, fit significantly better to dependent snow extremes than Gauss copula. The Gumbel copula can yield to four times lower out-crossing rate than that of Gauss.

If observations are available, the actual dependence structure should be inferred from them. In case of limited information, multiple copula functions should be used to quantify the related uncertainty. In the latter case, the sole use of Gauss copula is not justified and may not err on the safe side. Model averaging is proposed as a viable approach to rigorously account for this uncertainty.

(Rózsás and Mogyorósi, 2016)

7.3 Concluding remarks

The findings imply that the investigated – in the current practice prevalently neglected – factors, such as selection of appropriate distribution type, effect of statistical uncertainty, measurement uncertainty, long-term trends, and dependence structure, often have practically significant bearing on structural reliability. Their neglect can lead to an order of magnitude underestimation of failure probability.

Neglecting uncertainties violates a basic requirement of probability calculation, namely that all information should be incorporated and all uncertainties accounted for². However, incorporation of all uncertainties can easily lead to reliability estimates that are difficult to interpret. This is due to the scarcity and often complete lack of observations in the region governing reliability.

Given that structural reliability analysis is a tool in engineering decision making process rather than an exact science, agreement on the applied models can overcome these difficulties. An agreed model can provide the mathematical structure to extrapolate into unobserved regions and can ensure the common ground to make probabilistic analyses

²This is one of Jaynes' fundamental desiderata: "consistency" (Jaynes, 2003) and known in structural reliability as "completeness" requirement (Der Kiureghian, 1989).

comparable, thus avoiding the arbitrariness of fully data-driven analysis in the presence of data scarcity.

Reliability analysis and standardization are a delicate balancing between these two opposing demands: capturing more uncertainty and prescribing models to serve practical utility. The uncertainty modeling should be extended if practically significant aspects are neglected. It is believed that many of the presented findings belongs to this category and the related factors should be incorporated into probabilistic analyses. Moreover, the proposed approaches are devoid of arbitrariness, thus allow comparison and practical applicability.

The tackled challenges are general and relevant for most random variables such as wind, traffic, and earthquake actions. Therefore the findings can be applied for these as well and they can help to draft more consistent standards and to build safer structures.

Bibliography

- Advanpix (2016). Multiprecision computing toolbox for MATLAB (version 3.9.7.10723). (page 70)
- Aitchison, J. and Dunsmore, I. (1980). *Statistical Prediction Analysis*. Cambridge University Press, New York, USA. (page 29)
- Akaike, H. (1973). Information theory and an extension of the maximum likelihood principle. In Petrov, B. and Csáki, F., editors, *2nd International Symposium on Information Theory*, pages 267–281. Budapest: Akadémiai Kiadó. (page 118)
- Alibrandi, U. and Koh, C. (2015). First-order reliability method for structural reliability analysis in the presence of random and interval variables. *ASCE-ASME Journal of Risk and Uncertainty in Engineering Systems, Part B: Mechanical Engineering*, 1(4):041006. (page 34)
- Andrieu-Renaud, C., Lemaire, M., and Sudret, B. (2002). The PHI2 method: a way to assess time-variant reliability using time-invariant reliability tools. pages 472–479. (page 65, 70)
- Andrieu-Renaud, C., Sudret, B., and Lemaire, M. (2004). The PHI2 method: a way to compute time-variant reliability. *Reliability Engineering & System Safety*, 84(1):75–86. (page 65, 70)
- Ang, A. H.-S. and Tang, W. H. (2006). *Probability Concepts in Engineering: Emphasis on Applications to Civil and Environmental Engineering*. Wiley. (page 5)
- ASCE (2010). Minimum design loads for buildings and other structures. ASCE/SEI 7-10. (page 14, 37)
- Ayyub, B. M. and Klir, G. J. (2006). *Uncertainty Modeling and Analysis in Engineering and the Sciences*. Taylor & Francis Group. (page 6)
- Barnett, V. (1999). *Comparative Statistical Inference*. Wiley Series in Probability and Statistics. John Wiley & Sons Ltd., 3rd edition. (page 8)
- Baroth, J., Breysse, D., and Schoefs, F. (2011). *Construction Reliability: Safety, Variability and Sustainability*. Wiley-ISTE. (page 65)
- Birsan, M.-V. and Dumitrescu, A. (2014). Snow variability in Romania in connection to large-scale atmospheric circulation. *International Journal of Climatology*, 34(1):134–144. (page 54)
- Bjørnstad, J. F. (1990). Predictive likelihood: A review. *Statistical Science*, 5(2):242–254. (page 117)
- Box, G. E. P. and Cox, D. R. (1964). An analysis of transformations. *Journal of the Royal Statistical Society. Series B (Methodological)*, 26(2):211–252. (page 115)

- Breitung, K. (1984). Asymptotic approximations for multinormal integrals. *Journal of Engineering Mechanics*, 110(3):357–366. (page 9)
- Burnham, K. P. and Anderson, D. R. (2002). *Model Selection and Multimodel Inference. A Practical Information-Theoretic Approach*. Springer-Verlag, New York, 2nd edition. (page 118, 119)
- Burnham, K. P. and Anderson, D. R. (2004). Multimodel inference: Understanding AIC and BIC in model selection. *Sociological Methods & Research*, 33(2):261–304. 10.1177/0049124104268644. (page 118)
- Caires, S., Swail, V. R., and Wang, X. L. (2006). Projection and analysis of extreme wave climate. *Journal of Climate*, 19(21):5581–5605. (page 54)
- Carver, R. P. (1993). The case against statistical significance testing, revisited. *The Journal of Experimental Education*, 61(4):287–292. (page 55)
- Casella, G. and Berger, R. L. (2001). *Statistical inference*. Cengage Learning, 2nd edition. (page 114)
- CEN (2002). Eurocode 0: Basis of structural design. (page 9)
- Chang, W., Cheng, J., Allaire, J., Xie, Y., and McPherson, J. (2015). *shiny: Web Application Framework for R*. R package version 0.12.2. (page 105)
- Chaussé, P. (2010). Computing generalized method of moments and generalized empirical likelihood with R. *Journal of Statistical Software*, 34(11):1–35. (page 115)
- Coles, S. (2001). *An Introduction to Statistical Modeling of Extreme Values*. Springer-Verlag, London. (page 12, 15, 43, 55, 115)
- Coles, S. and Pericchi, L. (2003). Anticipating catastrophes through extreme value modeling. *Journal of the Royal Statistical Society. Series C (Applied Statistics)*, 52(4):405–416. (page 11, 54, 56)
- Coles, S., Pericchi, L. R., and Sisson, S. (2003). A fully probabilistic approach to extreme rainfall modeling. *Journal of Hydrology*, 273(1–4):35–50. (page 12, 29)
- Cornell, C. A. (1967). Bounds on the reliability of structural systems. *Journal of the Structural Division, ASCE ST1*, 93(1):171–200. (page 5)
- Cornell, J. and Benjamin, C. (1970). *Probability, Statistics, and Decision for Civil Engineers*. McGraw-Hill Companies. (page 7)
- Corotis, R. B. (2015). An overview of uncertainty concepts related to mechanical and civil engineering. *ASME Journal of Risk and Uncertainty in Engineering Systems, Part B: Mechanical Engineering*, 1(4):040801–040801–12. (page 6)
- Cramer, H. and Leadbetter, M. (1967). *Stationary and Related Stochastic Processes/ Sampling Function Properties and Their Applications*. John Wiley and Sons, New York. (page 70)
- Cunnane, C. (1978). Unbiased plotting positions — a review. *Journal of Hydrology*, 37(3–4):205–222. (page 115)
- de Finetti, B. (1974). *Theory of Probability*, volume 1. John Wiley & Sons. (page 6)

- Der Kiureghian, A. (1989). Measures of structural safety under imperfect states of knowledge. *Journal of Structural Engineering*, 115(5):1119–1140. (page 12, 36, 91)
- Der Kiureghian, A. (2008). Analysis of structural reliability under parameter uncertainties. *Probabilistic Engineering Mechanics*, 23(4):351–358. (page 29)
- Der Kiureghian, A., Haukaas, T., and Fujimura, K. (2006). Structural reliability software at the University of California, Berkeley. *Structural Safety*, 28(1–2):44–67. (page v)
- Ditlevsen, O. (1979). Narrow reliability bounds for structural systems. *Journal of Structural Mechanics*, 7(4):453–472. (page 75)
- Ditlevsen, O. (1994). Distribution arbitrariness in structural reliability. In Schuëller, G., Shinozuka, M., and Yao, J., editors, *ICOSSAR'93, Structural Safety and Reliability*. (page 29, 62)
- Ditlevsen, O. and Madsen, H. (2007). *Structural Reliability Methods*. Department of Mechanical Engineering, Technical University of Denmark, Online publication. (page 5, 65)
- Domma, F. and Giordano, S. (2013). A copula-based approach to account for dependence in stress-strength models. *Statistical Papers*, 54(3):807–826. (page 65)
- Donnelly, C. and Embrechts, P. (2010). The devil is in the tails: Actuarial mathematics and the subprime mortgage crisis. *ASTIN Bulletin*, 40(01):1–33. (page 65)
- Dorfman, R. (1938). A note on the δ -method for finding variance formulae. *The Biometric Bulletin*, 1:129–137. (page 115)
- Dunai, L., Armuth, M., Horváth, L., Kövesdi, B., Vigh, L. G., Visnovitz, Gy., Pap, Zs. B., Rózsás, Á., Ther, T., and Turán, P. (2016). Eiffel-csarnok. Részletes szakértői jelentés [Eiffel-hall. Comprehensive technical report]. Technical report, Department of Structural Engineering, Budapest University of Technology and Economics. in Hungarian. (page 111)
- Dunai, L., Rózsás, Á., and Vigh, L. G. (2014). Paksi Erőművi és szabadtéri létesítmények sérülékenységének jellemzésére kidolgozott módszertan: 1. Jelentés. módszertani elemzés, kritikai felülvizsgálat és a módszertan pontossítása [Methodology development for the fragility assessment of main and supporting facilities of Paks Nuclear Power Plant: Report I. Methodological analysis, critical appraisal and improvement of methodology]. Technical report, Department of Structural Engineering, Budapest University of Technology and Economics. in Hungarian. (page 108)
- Efron, B. (1979). Bootstrap methods: Another look at the jackknife. *The Annals of Statistics*, 7(1):1–26. (page 115)
- Efron, B. and Tibshirani, R. (1994). *An Introduction to the Bootstrap*. Chapman and Hall/CRC. (page 115)
- Elishakoff, I. (2004). *Safety Factors and Reliability: Friends or Foes?* Kluwer Academic Publishers, Dordrecht, Netherlands. (page 5)
- Ellingwood, B. and O'Rourke, M. (1985). Probabilistic models of snow loads on structures. *Structural Safety*, 2(4):291–299. (page 24)
- Ellingwood, B. and Redfield, R. K. (1984). Probability models for annual extreme water-equivalent ground snow. *Monthly Weather Review*, 112(6):1153–1159. (page 14, 29)

- Freudenthal, A. M. (1947). Safety of structures. *Transactions ASCE*, 112:125–180. (page 4)
- Galambos, J. (1978). *The asymptotic theory of extreme order statistics*. Wiley Series in Probability and Statistics - Applied Probability and Statistics Section. Wiley. (page 5)
- Geis, J., Strobel, K., and Liel, A. (2011). Snow-induced building failures. *Journal of Performance of Constructed Facilities*, 26(4):377–388. (page 2)
- Gelman, A., Carlin, J., Stern, H., and Rubin, D. (2003). *Bayesian Data Analysis*. CRC Press, USA, 2nd edition. (page 114, 116, 117)
- Goodison, B. E., Louie, P. Y. T., and Yang, D. (1998). WMO solid precipitation measurement intercomparison. WMO instruments and observing methods rep. 67, WMO/TD-872. Technical report, World Meteorological Organization. (page 32)
- Goodman, J. and Weare, J. (2010). Ensemble samplers with affine invariance. *Communications in Applied Mathematics and Computational Science*, 5(1):65–80. (page 120)
- Guttorp, P. and Xu, J. (2011). Climate change, trends in extremes, and model assessment for a long temperature time series from Sweden. *Environmetrics*, 22(3):456–463. (page 54)
- Habib, A. and Szántai, T. (2000). New bounds on the reliability of the consecutive k-out-of-r-from-n:f system. *Reliability Engineering & System Safety*, 68(2):97 – 104. (page 5)
- Hagen, Ø. and Tvedt, L. (1991). Vector process out-crossing as parallel system sensitivity measure. *Journal of Engineering Mechanics*, 117(10):2201–2220. (page 68, 70)
- Hall, A. (2005). *Generalized Method of Moments*. Oxford University Press, New York, United States. (page 114)
- Hao, Y., Huo, X., Duan, Q., Liu, Y., Fan, Y., Liu, Y., and Yeh, T.-C. (2015). A Bayesian analysis of nonstationary generalized extreme value distribution of annual spring discharge minima. *Environmental Earth Sciences*, 73(5):2031–2045. (page 54)
- Hasofer, A. M. and Lind, N. C. (1974). Exact and invariant second-moment code format. *Journal of Engineering Mechanics Division of the American Society of Civil Engineers*, 100:111–121. (page 9)
- Herring, S., Hoerling, M., Kossin, J., Peterson, T., and Stott, P. (2015). Explaining extreme events of 2014 from a climate perspective. *Bulletin of American Meteorological Society*, 96(12):1–172. (page 53)
- Hájek, A. (2012). Interpretations of probability. In Zalta, E. N., editor, *The Stanford Encyclopedia of Philosophy*. Winter 2012 edition. (page 6)
- Hoeting, J. A., Madigan, D., Raftery, A. E., and Volinsky, C. T. (1999). Bayesian model averaging: A tutorial. *Statistical Science*, 14(4):382–417. (page 50, 118)
- Holický, M. and Sýkora, M. (2009). *Failures of Roofs under Snow Load: Causes and Reliability Analysis*, pages 444–453. American Society of Civil Engineers. doi:10.1061/41082(362)45. (page 2)
- Honfi, D. (2013). *Design for Serviceability - A probabilistic approach*. PhD thesis, Faculty of Engineering, Lund University. (page 5)
- Hosking, J., Wallis, J., and Wood, E. (1985). Estimation of the generalized extreme-value distribution by the method of probability-weighted moments. *Technometrics*, 27(3):251–261. (page 46, 55)

- Huber, W. A. (2010). Ignorance is not probability. *Risk Analysis*, 30(3):371–376. (page 34)
- Hundecha, Y., St-Hilaire, A., Ouarda, T. B. M. J., El Adlouni, S., and Gachon, P. (2008). A nonstationary extreme value analysis for the assessment of changes in extreme annual wind speed over the Gulf of St. Lawrence, Canada. *Journal of Applied Meteorology and Climatology*, 47(11):2745–2759. (page 54)
- IPCC (2012). Managing the risks of extreme events and disasters to advance climate change adaptation. Report. (page 53)
- Jaynes, E. T. (1976). *Confidence intervals vs Bayesian intervals*, volume II, pages 175–257. Reidel Publishing Company, Dordrecht, Netherlands. (page 8)
- Jaynes, E. T. (2003). *Probability Theory: The Logic of Science*. Cambridge University Press. (page 7, 8, 91)
- JCSS (2000a). *JCSS Probabilistic Model Code. Part I - Basis of Design*. (page 31, 37)
- JCSS (2000b). *JCSS Probabilistic Model Code. Part III - Resistance Models*. (page 24, 59)
- JCSS (2001). *JCSS Probabilistic Model Code. Part II - Load Models*. (page 14, 24, 37, 59)
- Joe, H. (1997). *Multivariate Models and Dependence Concepts, Monographs on Statistics and Applied Probability* 73. Springer Science+Business Media Dordrecht. (page 68)
- Joe, H. (2014). *Dependence Modeling with Copulas*. Monographs on Statistics & Applied Probability. Chapman and Hall/CRC. (page 67)
- Kazinczy, G. (1921). A biztonság fokáról [on the degree of safety]. *Építőipar-Építőművészet*, 44:78–79, 86–87. in Hungarian. (page 4, 5)
- Křivý, V. and Stříž, M. (2010). Digital ground snow load map for the area of the Czech Republic. *Transactions of the VŠB – Technical University of Ostrava, Civil Engineering Series*, 10(1):1–9. (page 14)
- Klein Tank, A., Zwiers, F., and Zhang, X. (2009). Guidelines on analysis of extremes in a changing climate in support of informed decisions for adaptation. Report WMO-TD No. 1500, World Meteorological Organization. (page 54)
- Kámán, Cs. (2014). *Structural Reliability of Steel Frames. With emphasis on snow loads considering historical data and future projections*. M.sc. thesis, Budapest University of Technology and Economics, Department of Structural Engineering. (page 62)
- Koen, C. and Kondlo, L. (2009). Fitting power-law distributions to data with measurement errors. *Monthly Notices of the Royal Astronomical Society*, 397(1):495–505. (page 35)
- Kondlo, L. O. (2010). Estimation of Pareto distribution functions from samples contaminated by measurement errors. Master's thesis, Department of Statistics, University of the Western Cape. (page 33)
- Koris, K. (2009). *Durability-design of pre-cast concrete structural members*. PhD thesis, Department of Structural Engineering, Budapest University of Technology and Economics. (page 5)
- Lebrun, R. and Dutfoy, A. (2009). A generalization of the Nataf transformation to distributions with elliptical copula. *Probabilistic Engineering Mechanics*, 24(2):172–178. (page 71)

- Lógó, J., Rad, M. M., Knabel, J., and Tauzowski, P. (2011). Reliability based design of frames with limited residual strain energy capacity. *Periodica Polytechnica Civil Engineering*, 55(1):13–20. (page 5)
- Li, D.-Q., Tang, X.-S., Phoon, K.-K., Chen, Y.-F., and Zhou, C.-B. (2013). Bivariate simulation using copula and its application to probabilistic pile settlement analysis. *International Journal for Numerical and Analytical Methods in Geomechanics*, 37(6):597–617. (page 65)
- Liu, P.-L. and Der Kiureghian, A. (1986). Multivariate distribution models with prescribed marginals and covariances. *Probabilistic Engineering Mechanics*, 1(2):105–112. (page 9, 70)
- Madadgar, S. and Moradkhani, H. (2011). Drought analysis under climate change using copula. *Journal of Hydrologic Engineering*, 18(7):746–759. (page 65)
- Madsen, H., Rasmussen, P. F., and Rosbjerg, D. (1997). Comparison of annual maximum series and partial duration series methods for modeling extreme hydrologic events: 1. at-site modeling. *Water Resources Research*, 33(4):747–757. (page 38)
- Marshall, A. W. (1996). *Copulas, marginals, and joint distributions*, volume Volume 28 of *Lecture Notes–Monograph Series*, pages 213–222. Institute of Mathematical Statistics, Hayward, CA. (page 67)
- Martins, E. S. and Stedinger, J. R. (2000). Generalized maximum-likelihood generalized extreme-value quantile estimators for hydrologic data. *Water Resources Research*, 36(3):737–744. (page 46, 55)
- Marty, C. and Blanchet, J. (2012). Long-term changes in annual maximum snow depth and snowfall in Switzerland based on extreme value statistics. *Climatic Change*, 111(3–4):705–721. (page 54)
- Matlab (2015). *version 7.10.0 (R2015a)*. The MathWorks Inc., Natick, Massachusetts. (page v)
- Mayer, M. (1926). *Die Sicherheit der Bauwerke und ihre Berechnung nach Grenzkräften anstatt nach zulässigen Spanungen [Safety of Building Structures and their Calculation according to Limit Forces instead of Admissible Stresses]*. Springer, Berlin. in German. (page 4)
- McRobie, A. (2004). The Bayesian view of extreme events. (page 1)
- Meister, A. (2009). *Deconvolution Problems in Nonparametric Statistics*. Lecture Notes in Statistics. Springer-Verlag Berlin Heidelberg, 1st edition. (page 35)
- Mejri, M., Cazuguel, M., and Cognard, J. Y. (2011). A time-variant reliability approach for ageing marine structures with non-linear behaviour. *Computers & Structures*, 89(19–20):1743–1753. (page 65)
- Mejri, M. and Cognard, J.-Y. (2009). Time-variant assessment for adhesively bonded assemblies with non-linear behaviour in naval applications. *Ships and Offshore Structures*, 4(3):275–286. (page 65)
- Melchers, R. E. (2002). *Structural Reliability Analysis and Prediction*. John Wiley and Sons Ltd., Chichester, UK, 2nd edition. (page 5, 29, 70)
- Meløysund, V. (2010). *Prediction of local snow loads on roofs*. Ph.D. thesis, Norwegian University of Science and Technology, Department of Structural Engineering. (page 2)

- Menyhárd, I., Gábory, P., and Rózsa, M. (1951). *Vasbetonszerkezetek új méretezési módja. A biztonsági tényezőkön és a törései elméletben alapuló számítási módszer [New design method for reinforced concrete structures. Design method based safety factors and ultimate state theory]*. Építőipari Könyv- és Lapkiadó Vállalat. in Hungarian. (page 5)
- Milly, P. C. D., Betancourt, J., Falkenmark, M., Hirsch, R. M., Kundzewicz, Z. W., Lettenmaier, D. P., and Stouffer, R. J. (2008). Stationarity is dead: Whither water management? *Science*, 319(5863):573–574. (page 53)
- Mistéth, E. (2001). *Méretezéselmélet [Structural Reliability]*. Akadémiai Kiadó, Budapest. in Hungarian. (page 5)
- Moore, R. E., Kearfott, R. B., and Cloud, M. J. (2009). *Introduction to Interval Analysis*. Society for Industrial and Applied Mathematics, Philadelphia, PA, USA. (page 34)
- Muhanna, R. L., Mullen, R. L., and Rao, M. V. R. (2015). Nonlinear finite element analysis of frames under interval material and load uncertainty. *ASCE-ASME Journal of Risk and Uncertainty in Engineering Systems, Part B: Mechanical Engineering*, 1(4):041003. (page 34)
- Nataf, A. (1962). Détermination des distributions de probabilités dont les marges sont données. *Comptes Rendus de l'Académie des Sciences*, 225:42–43. (page 70)
- Nelson, R. B. (2006). *An Introduction to Copulas*. Springer Series in Statistics. Springer-Verlag New York, Inc., 2nd edition. (page 67, 68)
- Nowak, A. S. and Collins, K. R. (2000). *Reliability of Structures*. The McGraw-Hill Companies, Inc., USA. (page 4, 5)
- O’Gorman, P. A. (2014). Contrasting responses of mean and extreme snowfall to climate change. *Nature*, 512(7515):416–418. (page 54)
- Padoan, S. A., Ribatet, M., and Sisson, S. A. (2010). Likelihood-based inference for max-stable processes. *Journal of the American Statistical Association*, 105(489):263–277. (page 77)
- Patton, A. J. (2012). A review of copula models for economic time series. *Journal of Multivariate Analysis*, 110:4–18. (page 65)
- Pecho, J., Faško, P., Lapin, M., Mikulová, K., and Šťastný, P. (2009). Extreme values of precipitation and snow cover characteristics in Slovakia. In Pribullová, A. and Bičárová, editors, *Sustainable development and bioclimate: reviewed conference proceedings*, pages 24–25, Stará Lesná, Slovakia. Geophysical Institute of the Slovak Academy of Sciences. (page 54)
- Perdrizet, T. and Averbuch, D. (2008). Long term failure probability calculation method applied to riser design. In *27th International Conference on Offshore Mechanics and Arctic Engineering, OMAE 2008*, pages 847–852, Estoril, Portugal. (page 65)
- Perdrizet, T. and Averbuch, D. (2011). Short and long term extreme reliability analysis applied to floating wind turbine design. In *30th International Conference on Ocean, Offshore and Arctic Engineering, OMAE 2011*, pages 893–898, Rotterdam, Netherlands. (page 65)
- Prékopa, A. (1995). *Stochastic Programming*. Akadémiai Kiadó, Budapest. (page 5)
- Qiu, Z., Yang, D., and Elishakoff, I. (2007). Combination of structural reliability and interval analysis. *Acta Mechanica Sinica*, 24(1):61–67. (page 34, 38)

- Qiu, Z., Yang, D., and Elishakoff, I. (2008). Probabilistic interval reliability of structural systems. *International Journal of Solids and Structures*, 45(10):2850 – 2860. (page 34)
- R Core Team (2015). *R: A Language and Environment for Statistical Computing*. R Foundation for Statistical Computing, Vienna, Austria. (page v, 105)
- Rackwitz, R. and Fiessler, B. (1979). Structural reliability under combined random load sequences. *Computers and Structures*, 9:484–494. (page 9)
- Rad, M. M. (2011). *Extended Optimization Methods in Structural Plasticity with Uncertainties*. PhD thesis, Department of Structural Mechanics, Budapest University of Technology and Economics. (page 5)
- Ramachandran, K. and Tsokos, C. (2009). *Mathematical Statistics with Applications*. Elsevier Academic Press. (page 113)
- Rao, M. R., Muhanna, R. L., and Mullen, R. L. (2015). Geometric misfitting in trusses and frames: an interval-based approach. *International Journal of Reliability and Safety*, 9(2-3):132–153. (page 34)
- Rasmussen, R., Baker, B., Kochendorfer, J., Meyers, T., Landolt, S., Fischer, A. P., Black, J., Thériault, J. M., Kucera, P., Gochis, D., Smith, C., Nitu, R., Hall, M., Ikeda, K., and Gutmann, E. (2012). How well are we measuring snow: The NOAA/FAA/NCAR winter precipitation test bed. *Bulletin of the American Meteorological Society*, 93(6):811–829. (page 32)
- Reiss, R.-D. and Thomas, M. (2007). *Statistical Analysis of Extreme Values with Applications to Insurance, Finance, Hydrology and Other Fields*. Birkhäuser Basel, 3rd edition. (page 12)
- Requena, A. I., Mediero, L., and Garrote, L. (2013). A bivariate return period based on copulas for hydrologic dam design: accounting for reservoir routing in risk estimation. *Hydrology and Earth System Sciences*, 17(8):3023–3038. (page 65)
- Ribatet, M. and Sedki, M. (2012). Extreme value copulas and max-stable processes. *Journal de la Société Française de Statistique*, 153(3):138–150. (page 77)
- Rényi, A. (1970). *Probability Theory*. Akadémiai Kiadó, Budapest. (page 5)
- Romano, C. (2002). Applying copula function to risk management. (page 65)
- Rózsás, Á., Kovács, N., Vigh, L. G., and Sýkora, M. (2016a). Climate change effects on structural reliability in the Carpathian Region. *Időjárás*, 120(1):103–125. (page 87, 90, 125, 126)
- Rózsás, Á. and Mogyorósi, Zs. (2016). The effect of copulas on time-variant reliability with continuous stochastic processes. In *International Conference in Modelling in Mechanics and Structural Reliability*, pages 1–14, Ostrava, Czech Republic. (page 91, 127)
- Rózsás, Á. and Sýkora, M. (2015a). Effect of parameter estimation uncertainty on structural reliability. In Krejsa, M., editor, *Modelling in Mechanics*, pages 100–111, Ostrava, Czech Republic. (page 87, 125)
- Rózsás, Á. and Sýkora, M. (2015b). Effect of statistical uncertainties in ground snow load on structural reliability. In *IABSE Conference: Structural Engineering: Providing Solutions to Global Challenges*, pages 220–227, Geneva, Switzerland. (page 50, 85, 87, 124, 125)

- Rózsás, Á. and Sýkora, M. (2015c). Model comparison and quantification of statistical uncertainties for annual maxima of ground snow loads. In Podofillini, L., Sudret, B., Stojadinovic, B., Enrico, Z., and Kröger, W., editors, *Safety and Reliability of Complex Engineered Systems: ESREL 2015*, pages 2667–2674, Zürich, Switzerland. CRC Press. (page 50, 85, 87, 124, 125)
- Rózsás, Á. and Sýkora, M. (2015d). Neglect of parameter estimation uncertainty can significantly overestimate structural reliability. *Transactions of the VŠB – Technical University of Ostrava, Civil Engineering Series*, 15(2):1–10. (page 87, 125)
- Rózsás, Á. and Sýkora, M. (2016a). Effect of statistical uncertainties on predicted extreme wind speeds. In *7th International Workshop on Reliable Engineering Computing, REC2016. Computing with Polymorphic Uncertain Data*, pages 489–503, Bochum, Germany. (page 12)
- Rózsás, Á. and Sýkora, M. (2016b). Propagating snow measurement uncertainty to structural reliability by statistical and interval-based approaches. In *7th International Workshop on Reliable Engineering Computing, REC2016. Computing with Polymorphic Uncertain Data*, pages 91–110, Bochum, Germany. (page 88, 126)
- Rózsás, Á., Sýkora, M., and Vigh, L. G. (2016b). Long-term trends in annual ground snow maxima for the Carpathian Region. *Applied Mechanics and Materials*, 821:753–760. (page 85, 90, 124, 126)
- Rózsás, Á. and Vigh, L. G. (2014). On the reliability of steel frames exposed to snow load. Considering the effect of epistemic uncertainty. In Landorfo, R. and Mazzolani, F., editors, *7th European Conference on Steel and Composite Structures, Eurosteel 2014*, pages 1–6, Naples, Italy. (page 87, 125)
- Sadovský, Z., Bochníček, O., Faško, P., Mikolová, K., and Št'astný, P. (2007). Revision of snow load data for structural design in Slovakia. In Aven, T. and Vinnem, J., editors, *ESREL 2007, Risk, Reliability and Societal Safety*. Taylor & Francis Group. (page 54)
- Sanpaolesi, L., Currie, D., Sims, P., Sacré, C., Stiefel, U., Lozza, S., Eiselt, B., Peckham, R., Solomos, G., Holand, I., Sandvik, R., Gränzer, M., König, G., Sukhov, D., Del Corso, R., and Formichi, P. (1998). Scientific support activity in the field of structural stability of civil engineering works: Snow loads. Final report phase I. Report, Commission of the European Communities. DGIII-D3. (page 2, 12, 14, 29, 31, 37, 38, 56, 110, 112, 113)
- Sisson, S. A., Pericchi, L. R., and Coles, S. G. (2006). A case for a reassessment of the risks of extreme hydrological hazards in the Caribbean. *Stochastic Environmental Research and Risk Assessment*, 20(4):296–306. (page 12)
- Sýkora, M., Diamantidis, D., Retief, J., Viljoen, C., and Rózsás, Á. (2016). On risk-based design of structures exposed to changing climatic actions (accepted for publication). In *Proceedings of the Fifth International Symposium on Life -Cycle Civil Engineering IALCCE2016*, pages 1–9, Delft, The Netherlands. (page 90, 126)
- Spiegelhalter, D. and Rice, K. (2009). Bayesian statistics. *Scholarpedia*, 4(8):5230. (page 7)
- Stefanski, L. and Bay, J. (2000). Measurement error models. *Journal of the American Statistical Association*, 95(1353-1358). (page 35)
- Sudret, B. (2008a). Analytical derivation of the outcrossing rate in time-variant reliability problems. *Structure and Infrastructure Engineering*, 4(5):353–362. (page 70, 73)

- Sudret, B. (2008b). Probabilistic models for the extent of damage in degrading reinforced concrete structures. *Reliability Engineering & System Safety*, 93(3):410–422. (page 65)
- Szalai, K. and Kovács (2011). Verification of the ultimate limit state requirements for concrete members by the use of the global safety factor format. *Concrete Structures. Journal of the Hungarian Group of fib*, 12:58–65. (page 5)
- Szalai, S., Auer, I., Hiebl, J., Milkovich, J., Radim, T., Stepanek, P., Zahradnicek, P., Bihari, Z., Lakatos, M., Szentimrey, T., Limanowka, D., Kilar, P., Cheval, S., Deak, G., Mihic, D., Antolovic, I., Mihajlovic, V., Nejedlik, P., Stastny, P., Mikulova, K., Nabivyanets, I., Skyryk, O., Krakovskaya, S., Vogt, J., Antofie, T., and Spinoni, J. (2013). Climate of the greater Carpathian Region. Report. (page 13, 24, 77, 110, 111)
- Szántai, T. and Kovács, E. (2012). Hypergraphs as a mean of discovering the dependence structure of a discrete multivariate probability distribution. *Annals of Operations Research*, 193(1):71–90. (page 5)
- Tang, X.-S., Li, D.-Q., Rong, G., Phoon, K.-K., and Zhou, C.-B. (2013a). Impact of copula selection on geotechnical reliability under incomplete probability information. *Computers and Geotechnics*, 49(0):264–278. (page 65)
- Tang, X.-S., Li, D.-Q., Zhou, C.-B., and Phoon, K.-K. (2015). Copula-based approaches for evaluating slope reliability under incomplete probability information. *Structural Safety*, 52, Part A(0):90–99. (page 65)
- Tang, X.-S., Li, D.-Q., Zhou, C.-B., Phoon, K.-K., and Zhang, L.-M. (2013b). Impact of copulas for modeling bivariate distributions on system reliability. *Structural Safety*, 44(0):80–90. (page 65)
- Thoft-Cristensen, P. and Baker, M. (1982). *Structural Reliability Theory and Its Applications*. Springer-Verlag. (page 5)
- Van Gelder, P. (2000). *Statistical Methods for the Risk-Based Design of Civil Structures*. Thesis. (page 29)
- Vigh, L. G., Rózsás, Á., Zsarnóczay, Á., Balogh, T., Morais, E. C., and Simon, J. (2016). Megbízhatósági analízis alkalmazása extrém hatásoknak kitett szerkezetek vizsgálatára [Application of reliability analysis to the study of structures subjected to extreme actions]. In Hegedűs, I., Farkas, G., Dunai, L., and Kovács, T., editors, *A BME Hidak és Szerkezetek Tanszék Tudományos Közleményei: Tassi Géza és Orosz Árpád 90 éves*, pages 119–128. Department of Structural Engineering, Budapest University of Technology and Economics. in Hungarian. (page 85, 124)
- Vigh, L. G., Dunai, L., Völgyi, I., Rózsás, Á., Budaházy, V., Kámán, Cs., and Cserpák, T. (2014). Paksi Erőművi és szabadtéri létesítmények sérülékenységének jellemzésére kidolgozott módszertan: 2. Jelentés. kritikus szerkezetek és szerkezeti elemek sérülékenységi görbéi [Methodology development for the fragility assessment of main and supporting facilities of Paks Nuclear Power Plant: Report II. Fragility curves for safety critical structures and structural members]. Technical report, Department of Structural Engineering, Budapest University of Technology and Economics. in Hungarian. (page 108)
- Wagenmakers, E.-J., Lee, M. D., Lodewyckx, T., and Iverson, G. (2008). *Bayesian versus frequentist inference*, pages 181–207. Springer New York. (page 8)
- Wilks, S. (1938). The large-sample distribution of the likelihood ratio for testing composite hypotheses. *The Annals of Mathematical Statistics*, 9(1):60–62. (page 55)

- Wit, E., van den Heuvel, E., and Romeijn, J.-W. (2012). ‘All models are wrong...’: an introduction to model uncertainty. *Statistica Neerlandica*, 66(3):217–236. (page 29, 55, 118)
- WMO (2008). Guide to meteorological instruments and methods of observation, WMO/No. 8. Technical report, World Meteorological Organization. (page 13)
- Zhang, H., Mullen, R. L., and Muhanna, R. L. (2010). Interval estimates of structural reliability. In Beer, M., Muhanna, R. L., and Mullen, R. L., editors, *4th International Workshop on Reliable Engineering Computing. REC 2010*, pages 386–395. Research Publishing Services. (page 34)
- Zhang, Y. and Der Kiureghian, A. (1995). Two improved algorithms for reliability analysis. In Rackwitz, R., Augusti, G., and Borri, A., editors, *Reliability and Optimization of Structural Systems: Proceedings of the sixth IFIP WG7.5 working conference on reliability and optimization of structural systems 1994*, pages 297–304, Boston, MA. Springer US. (page 9)

Appendix A

Snow characteristics for the Carpathian Region

A.1 Interactive snow map

An online, interactive snow map is developed, which can be used to obtain characteristic ground snow load and other structural engineering related snow information for the Carpathian region (Figure A.1). The database presented in Section 3.2.1 is used for the map.

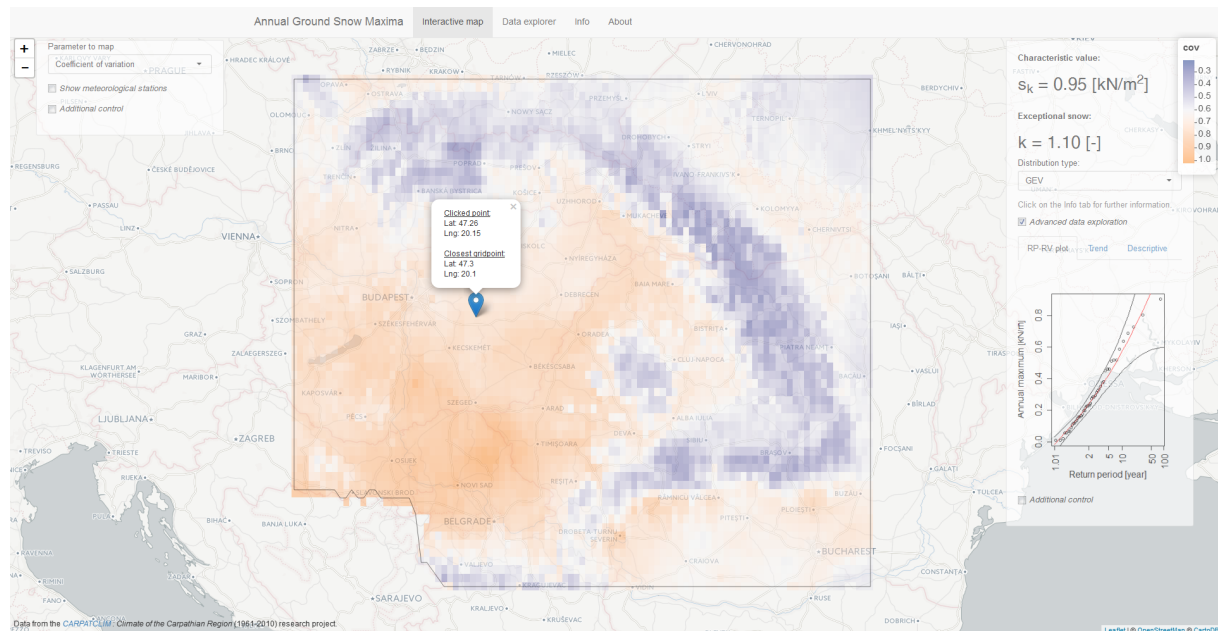


Figure A.1 Screenshot of the interactive snow map.

The source code and an online running instance is available on this page:
<https://github.com/rozsasarpi/Interactive-snow-map-R>

The interactive map is motivated by the:

- often appreciable change in snow maps, ground snow load, and other snow related measures by crossing national borders;
- largely inaccessible previous snow related research even within the seeker's own country, this is the case for Hungary;
- principles of open and reproducible research;
- the need for later update of snow maps, which is hoped to be eased by the published code;
- need for site specific loading conditions;
- difficulty of analyzing, exploring large datasets.

These motivations are valid for other actions as well, e.g. seismic actions, and the presented approach of publicly shared codes, databases, and interactivity may help in those cases as well. The application is developed in R ([R Core Team, 2015](#)) using shiny ([Chang et al., 2015](#)), for details see the source code.

A.2 Posterior distribution of GEV parameters

The posterior distributions of annual ground snow maxima parameters are given here to provide prior information to region with similar climatic conditions (Figure A.2). The posterior distributions are constructed with the following assumptions and considerations:

- Generalized extreme value distribution is used to formulate the likelihood function.
- The posterior distribution of shape, scale, and location parameters are provided.
- Distributions are given for lowlands and for highlands as well due to their distinct characteristics.
- Uniform priors are used for all parameters with practically infinite range.
- The observations for each locations are standardized: centering and scaling (Eq.A.1).
- Three locations are used for each groups, these are far apart from each other to ensure independence (Figure A.3).

The standardization of observations makes it possible to aggregate data from different locations. It is done the following way:

$$x_{s,i} = \frac{x_i - m}{s} \quad (\text{A.1})$$

where:

- $x_{s,i}$ i th standardized observation;
 x_i i th observation;
 m sample mean;
 s corrected sample standard deviation, Eq.A.2.

$$s = \sqrt{\frac{1}{1-n} \cdot \sum_{i=1}^n (x_i - m)^2} \quad (\text{A.2})$$

where n is the sample size.

From these parameters the non-standardized parameters or other snow characteristics can be readily obtained with their posterior distributions as well. It requires further analysis to decide which locations can be considered independent in respect of ground snow maxima. The three-three locations are assumed to be independent due to their distance. If more independent locations can be added then the posterior distributions could be greatly improved.

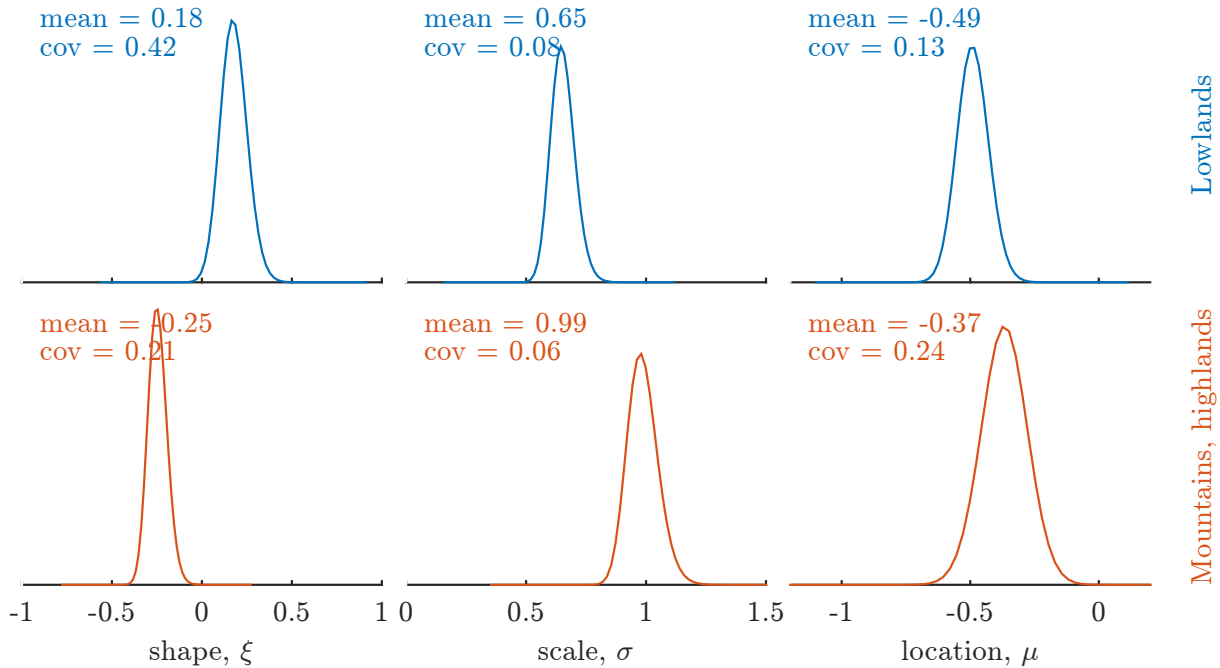


Figure A.2 Posterior distributions of GEV parameters for the lowlands, and mountains and highlands. Corresponding to standardized observations.

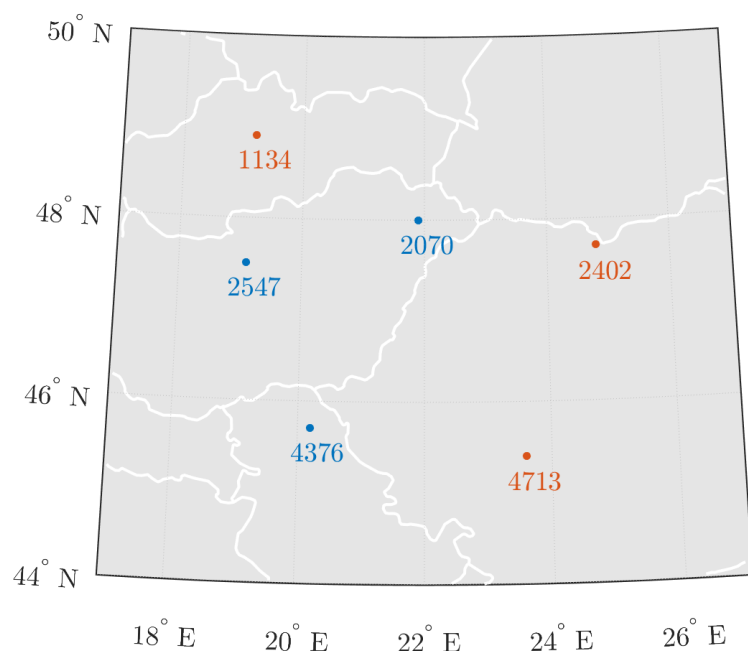


Figure A.3 Position of the selected locations for lowlands (blue), and for mountains and highlands (orange). The numbers are related to the CarpatClim database.

Appendix B

Description of application examples

B.1 Nuclear power plant in Paks, turbine hall

B.1.1 Overview

The Paks Nuclear Power Plant is the only nuclear power plant in Hungary and it covers about 50% of the Hungarian electricity demand. The plant was commissioned in 1982 and its operational time was recently extended by 20 years up to the thirties. Due to its importance and severe consequences of potential failures, regular probabilistic risk assessment is required and performed on the facility. The candidate participated in a comprehensive probabilistic assessment of the facility's load bearing structures and in the development of an improved methodology for fragility curve based probabilistic assessment. From this project the turbine hall is selected to demonstrate the findings of this study. It is a regular steel hall housing the turbines that convert thermal energy into kinetic one. The reliability of the hall is crucial for the reliable performance of the whole facility.

B.1.2 Fragility curves

The reliability of the hall is governed by the system like failure of multiple frames. Furthermore, multiple truss members and failure modes contribute to the failure probability of each frame. For simplicity only a single frame with its governing failure mode is considered. This characterizes well the whole hall system and deemed sufficient for illustration. The location of the selected frame is shown in Figure B.1. The main dimensions with the governing limit states are illustrated in Figure B.2. The corresponding component and system (series) level fragility curves¹ are also presented. In this thesis the g_2 limit state function is used in all analyses of the turbine hall.

For our current purpose it is sufficient to know the fragility curves; further details on how these were obtained can be found in Dunai et al. (2014); Vigh et al. (2014).

¹Fragility curve is a cumulative distribution function with each ordinate is expressing a conditional probability.

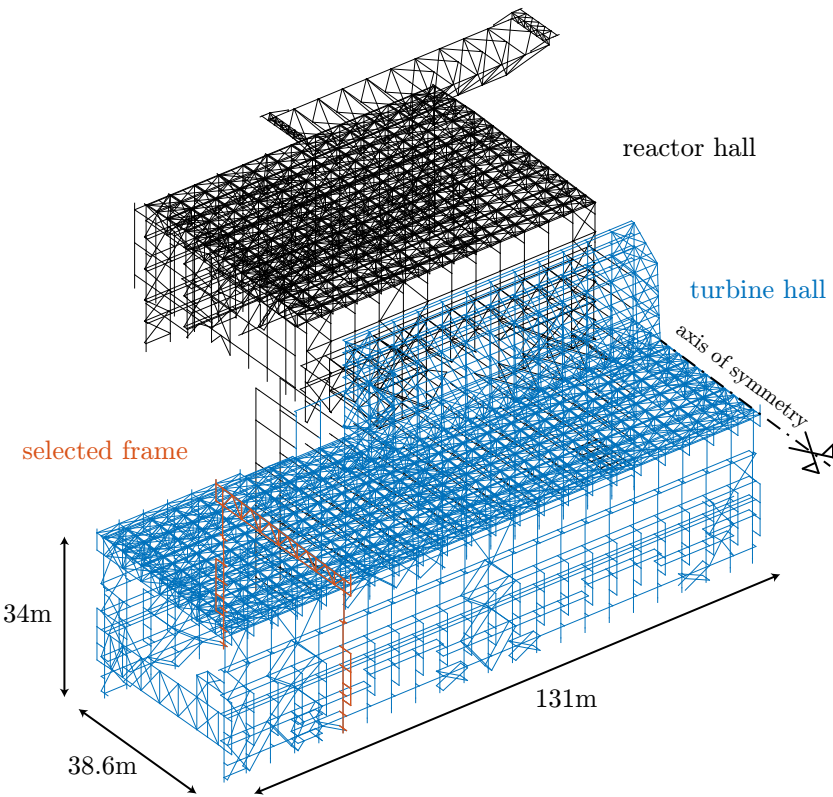


Figure B.1 Main building of Paks Nuclear Power Plant with the selected frame (orange).

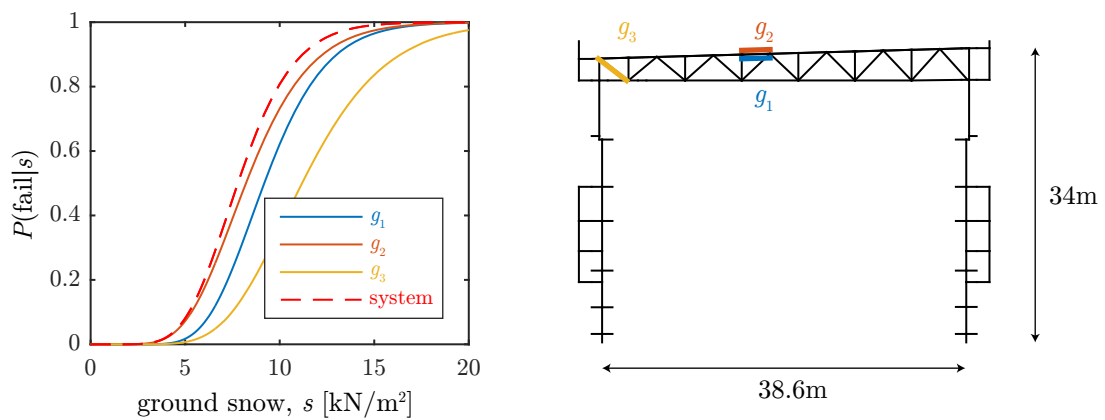


Figure B.2 Selected frame of turbine hall (right) and its fragility curves (left) for governing failure modes. In this thesis the g_2 limit state function (orange) is used in all analysis of the turbine hall.

Table B.1 Main statistics of annual ground snow maxima for Paks Nuclear Power Plant site.

Statistics	Value
Sample size	49
Mean	0.35 kN/m ²
Coefficient of variation (bias corrected)	0.83
Skewness (bias corrected)	1.34
Characteristic value*	1.10 kN/m ²
GEV shape coefficient (ξ)†	0.40

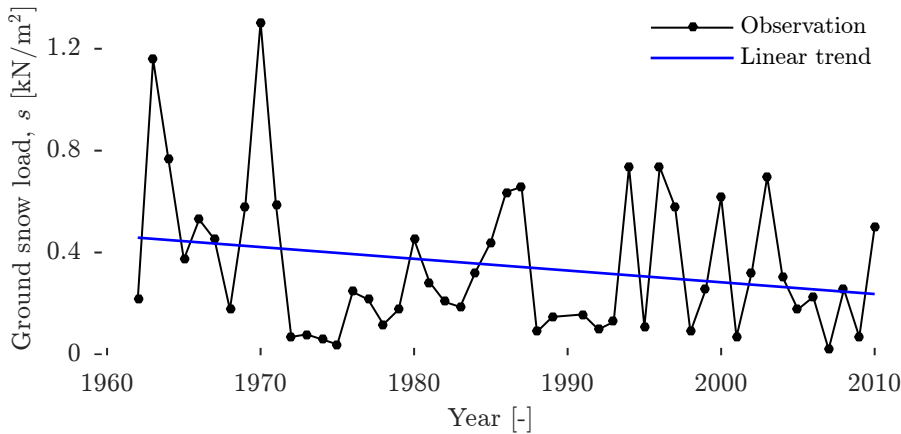
* 0.98 fractile of Gumbel distribution fitted with method of moments in line with [Sanpaolesi et al. \(1998\)](#).

† Obtained using maximum likelihood method and belongs to Fréchet family.

B.1.3 Snow action

The probabilistic model of ground snow load is inferred from the snow water equivalent data of CarpatClim database ([Szalai et al., 2013](#)). The gridpoint with latitude 46.6°N and longitude 18.9°E geographical coordinates is used to obtain the ground snow load for the power plant. The observations are available for 49 full winter seasons (Figure B.3). The main statistics of the annual (winter season) maxima are given in Table B.1.

Reference period of one year is used in all calculations related to the turbine hall. This follows the common practice in probabilistic risk assessment of nuclear power plants.

**Figure B.3** Annual ground snow maxima and linear trend for Paks Nuclear Power Plant site.

B.2 Locomotive workshop in Budapest, Eiffel-hall

B.2.1 Overview

The Eiffel-hall of Budapest is a more than 130 years old wrought iron structure that is up to recently served as one of the largest locomotive workshop in Hungary. The workshop has closed its doors in 2009 and afterwards the structure was classified as a historical

monument. Soon it was designated to a government flagship project with the intention to serve the Hungarian State Opera House and the Erkel Theatre as a workshop and rehearsal center, while preserving the original structures and architectural style.

It is a $95\text{ m} \times 235\text{ m} \approx 22000\text{ m}^2$ floor area hall that is presumably erected between 1883 and 1885. The riveted truss structure has five adjacent halls and made of wrought iron. Semi-probabilistic calculations revealed that snow is the governing action for many structural elements and substantial portion of the roof should be heated to avoid hazardous snow accumulation. Probabilistic analysis of the structure was to be undertaken due to (*i*) the importance and value of the structure; (*ii*) the inadequacy of current standardized methods to handle existing structures, e.g. to account for survived years.

B.2.2 Selected truss member and failure mode

Strength ultimate limit state of a purlin is selected as representative failure mode. The purlin is located in a side hall (Figure B.4) and its failure mode corresponds to the plastic rupture of a truss member under tension (Figure B.5). For simplicity solely this failure mode is considered albeit the failure probability of structure is governed by system like behavior. The reliability of the purlin is analyzed considering the conditions expected to be present after the refurbishment and neglecting the earlier survived years. The details of the involved random variables and formulation of the limit state function can be found in [Dunai et al. \(2016\)](#).

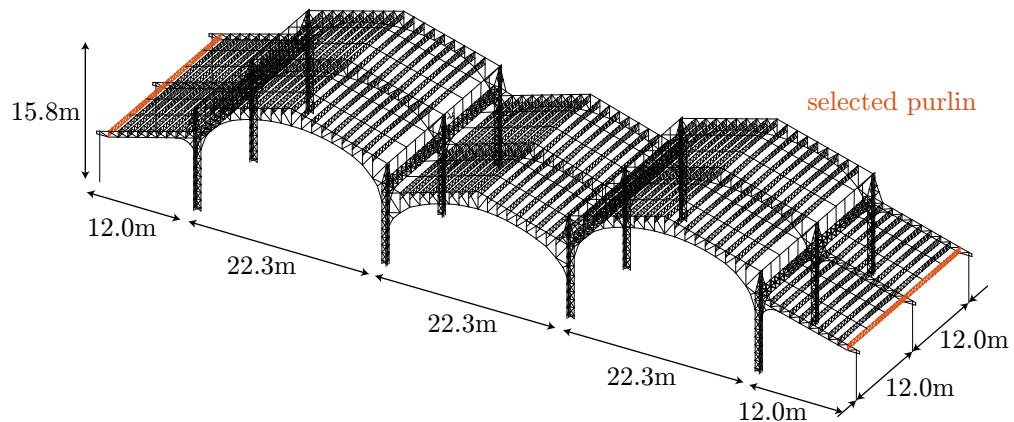


Figure B.4 Overview of the Eiffel-hall with the selected truss purlin (orange).

B.2.3 Snow action

The snow water equivalents are obtained from the CarpatClim database ([Szalai et al., 2013](#)). The gridpoint with latitude 47.5°N and longitude 19.1°E geographical coordinates is used to obtain the ground snow load for the site. The observations are available for 49

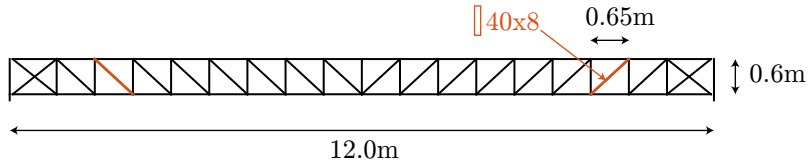


Figure B.5 Selected truss purlin with governing truss member (orange). In this thesis this highlighted member is used in all analysis of the Eiffel-hall.

Table B.2 Main statistics of annual ground snow maxima for Eiffel-hall site.

Statistics	Value
Sample size	49
Mean	0.36 kN/m ²
Coefficient of variation (bias corrected)	0.67
Skewness (bias corrected)	1.06
Characteristic value*	0.97 kN/m ²
GEV shape coefficient (ξ)†	0.05

* 0.98 fractile of Gumbel distribution fitted with method of moments in line with Sanpaolesi et al. (1998).

† Obtained using maximum likelihood method and belongs to Fréchet family.

full winter seasons (Figure B.6). The main statistics of the annual (winter season) maxima are given in Table B.2.

Reference period of 50 years is used in all calculations related to the Eiffel-hall. This is in line with the practice of reliability assessment of common engineering structures.

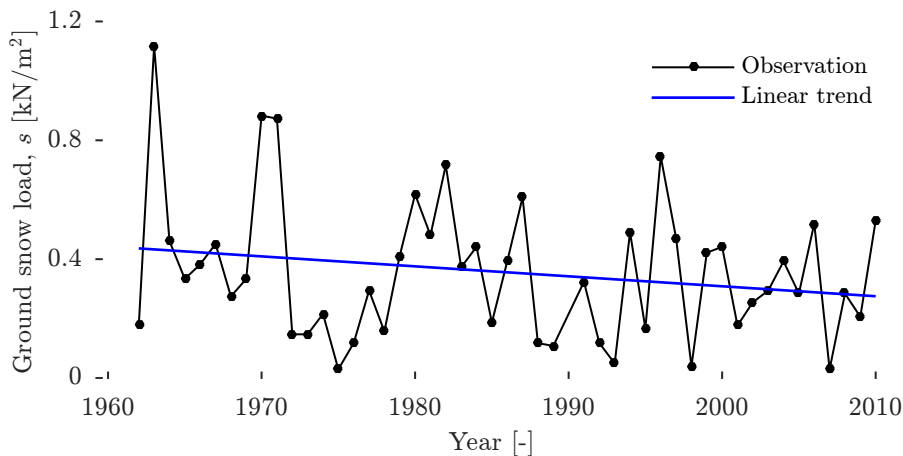


Figure B.6 Annual ground snow maxima and linear trend for Eiffel-hall site.

Appendix C

Statistical tools, models and plots

C.1 Statistical tools

This section introduces the common concepts, terms, notations, and methods that are used in multiple chapters. Those that appear in only a single chapter, for example interval analysis (see Section 4.2.2), are introduced there.

C.1.1 Point estimates

Point estimates are single value “guesses” of population parameters from a sample. There are many methods to make point estimates, these can be compared by their properties such as bias, consistency, efficiency, and sufficiency (Ramachandran and Tsokos, 2009). Here the method of moments, frequentist, and Bayesian methods are considered; all depends on the choice of the distribution function.

Method of moments

The method of moments (MM) is based on equating the sample and distribution moments: for a distribution with n parameters the first n moments are used. It is a widespread technique in civil engineering, which is applied in the Eurocode snow background document for fitting distributions and constructing characteristic ground snow maps (Sanpaolesi et al., 1998). It is a typically asymptotically unbiased though not in general efficient estimator (Ramachandran and Tsokos, 2009). For stationary distributions moments are sufficient statistics; however, they are insufficient for non-stationary ones as they lack information about chronological order. This method is treated separately from statistical paradigms, since due to its simplicity it does not require commitment to any probability interpretation.

Generalized method of moments (GMM) extends the notion of moments and can take into account more conditions than unknown parameters. Parameters are selected by minimizing the distance of sample and model moments while these conditions are weighted according to their relative importance to get an asymptotically efficient estimator

(Hall, 2005). In this study the GMM parameter estimation is formulated as a just-identified problem, this means that the number of constraints is equal to the number of distribution parameters, and unbiased central moment constraints are adopted. Thus, only the asymptotic normality property is utilized to obtain the uncertainty intervals. The real strength of GMM lies in problems where the constraints are naturally set by the underlying theory and the distribution dependence can be avoided, for instance in some economics problems. GMM can be considered to be part of the frequentist approach; however, its separate treatment is explained by its connection to classical method of moments.

Frequentist method

The maximum likelihood (ML) method is used, which is typically an asymptotically efficient and consistent estimation technique that selects the model which is most likely generated the data (Casella and Berger, 2001). Inference of the unknown parameters, $\boldsymbol{\theta}$, is completed by maximizing the likelihood function, $L(\boldsymbol{\theta})$:

$$L(\boldsymbol{\theta}) = \prod_{i=1}^n p(x_i, \boldsymbol{\theta}) \quad (\text{C.1})$$

where x_i denotes the observations, and $p(x)$ is the probability density function. In related methods and in numeric algorithms often the natural logarithm of the likelihood is applied, which is termed the log-likelihood function.

Bayesian method

The Bayesian approach is based on Bayes' theorem, which compared with the frequentist approach additionally requires prior information on the unknown parameters:

$$\begin{aligned} p(\boldsymbol{\theta} | \mathbf{x}) &= \frac{\text{prior} \cdot \text{likelihood}}{\text{evidence}} \\ &= \frac{p(\boldsymbol{\theta}) \cdot p(\mathbf{x} | \boldsymbol{\theta})}{p(\mathbf{x})} \\ &= \frac{p(\boldsymbol{\theta}) \cdot p(\mathbf{x} | \boldsymbol{\theta})}{\int_{\Theta} p(\boldsymbol{\theta}) \cdot p(\mathbf{x} | \boldsymbol{\theta}) \cdot d\boldsymbol{\theta}}. \end{aligned} \quad (\text{C.2})$$

where \mathbf{x} contains observations (data) and $p(\boldsymbol{\theta} | \mathbf{x})$ is the posterior distribution of parameters. The typically used Bayesian point estimate is the mean of the posterior distribution, it corresponds to minimum quadratic loss. It is a typically consistent, asymptotically efficient, and asymptotically unbiased estimator (Gelman et al., 2003). For practical cases with small sample size special care should be taken to the priors as those may have important effect on the inference.

C.1.2 Interval estimates

Point estimates are often accompanied by intervals to express parameter estimation uncertainty due to sampling variability.

Method of moments

We are not aware of any methods to quantify parameter estimation uncertainty using classical method of moments. However, for GMM the asymptotic normality of its estimator makes it possible to construct uncertainty intervals, these are approximate confidence intervals. A p -level confidence interval has the following meaning: if the population sampling is repeated infinitely many times and each time a specific interval is constructed around the point estimate, then p proportion of these intervals would cover the true parameter of the generating distribution. Due to this repeated hypothetical sampling and focus on data variability this approach belongs to the frequentist paradigm. If confidence intervals for other than typical distribution parameters are needed then the model is formulated by the parameter in question, e.g. a specific fractile. The confidence intervals are constructed with a method similar to delta method – detailed in the next section –, although here the weighting matrix plays the role of the observed Fisher information matrix (Eq.C.5); for additional details see [Chaussé \(2010\)](#). The weighting matrix is continuously updated in all GMM inferences in this study.

Frequentist method

The frequentist uncertainty interval is termed confidence interval, its definition is given in preceding section. The following three methods are used in this study to construct it:

- Delta method: it is based on the observed Fisher information matrix and utilizes the asymptotic normality of the ML estimator ([Coles, 2001](#); [Dorfman, 1938](#)).
- Profile likelihood method: it is based on maximizing the log-likelihood function considering all but one parameter to obtain a section/profile of the log-likelihood function, then utilizing some asymptotic property the confidence interval of the free parameter can be estimated. It is more accurate than the delta method but computationally more demanding ([Box and Cox, 1964](#); [Coles, 2001](#)).
- Bootstrapping: it is the resampling of the empirical distribution function ([Efron, 1979](#); [Efron and Tibshirani, 1994](#)). The uncertainty intervals are obtained by taking the fractiles of the bootstrap sample. The resampled empirical distribution function is constructed with plotting position recommended by [Cunnane \(1978\)](#), and with linear interpolation among the points with no extrapolation from the data range. From the three methods this is the most accurate and computationally most expensive as well.

The presentation of these methods can be found in the referred literature, only the delta method is outlined here in more details since that is frequently used in later chapters. The delta method can be used to approximate the confidence interval of parameters, ϕ , that are scalar function, $h(\cdot)$, of inferred parameters, $\boldsymbol{\theta}$:

$$\phi = h(\boldsymbol{\theta}) \quad \mathbb{R}^n \mapsto \mathbb{R}. \quad (\text{C.3})$$

The maximum likelihood estimate of the derived parameter is obtained by substituting the maximum likelihood estimates of the inferred parameters into the scalar function:

$$\hat{\phi} = h(\hat{\boldsymbol{\theta}}) \quad (\text{C.4})$$

where the maximum likelihood estimates are denoted by a hat, for example $\hat{\phi}$. The variance of $\hat{\phi}$ can be approximated as:

$$\text{Var}(\hat{\phi}) \approx \nabla h^T(\hat{\boldsymbol{\theta}}) \cdot \mathbf{I}_o^{-1}(\hat{\boldsymbol{\theta}}) \cdot \nabla h(\hat{\boldsymbol{\theta}}) \quad (\text{C.5})$$

where \mathbf{I}_o is the observed Fisher information matrix, which is the approximate curvature matrix (Hesse matrix) of the negative log-likelihood function. The asymptotic sampling distribution of $\hat{\phi}$ is normal with mean and variance given in Eq.C.4 and Eq.C.5 respectively:

$$\hat{\Phi} \stackrel{\sim}{\sim} \mathcal{N}(\hat{\phi}, \text{Var}(\hat{\phi})). \quad (\text{C.6})$$

The fractiles of this sampling distribution can be used as confidence interval endpoints.

Bayesian method

The Bayesian uncertainty interval is named p -level credible or posterior interval, p denotes the probability that the inferred parameter is within the interval (Gelman et al., 2003). Two out of the infinitely many credible intervals are used in this study (Figure C.1):

- the equal tailed interval (eqi) with the same probability to be below or exceed bounds and
- the highest density interval (hdi) with the largest minimum density value.

C.1.3 Prediction

Structural reliability is inherently predictive, for instance the design of a new structure is in large extent the prediction of future extreme actions and it should be based on a prediction appreciating the uncertainties stemming from scarcity of data, not just on a model that fits best to the observations.

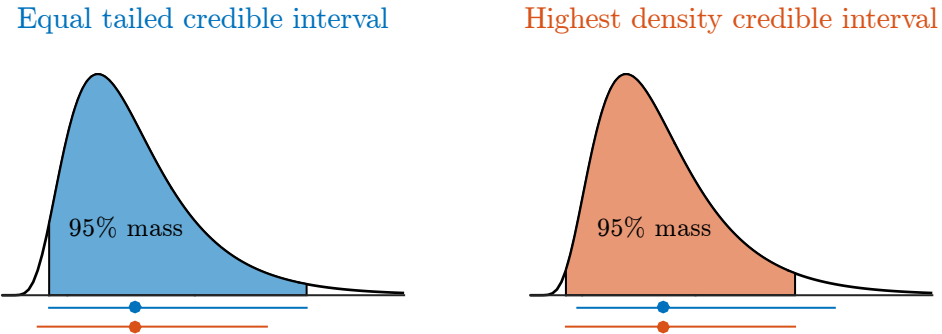


Figure C.1 Illustration of equal tailed and highest density credible intervals.

Frequentist method

Many predictive likelihood based approaches are available in the literature (Bjørnstad, 1990); however, there is no general agreement which one to use and they are rarely applied. Many of these approaches are similar to the Bayesian posterior predictive distribution (see next section) but they try to avoid the prior assumption. As Bayesian statistics is advocated in this study, predictive likelihood based approaches are not used in further chapters.

Bayesian method

An important advantage of the Bayesian approach is that it treats unknown parameters as random variables, hence the incorporation of parameter estimation uncertainty into the model is straightforward. This is done by averaging the conditional models, $p(x|\theta)$, over the posterior distribution of the parameters, $p(\theta|data)$ (Gelman et al., 2003):

$$p(x) = \int_{\Theta} p(x|\theta) \cdot p(\theta|data) \cdot d\theta. \quad (\text{C.7})$$

The resulting function is referred to as posterior predictive, one of its interesting properties is that it automatically penalizes small sample size based predictions.

C.1.4 Goodness-of-fit measures

Once a model is fitted goodness-of-fit checks can be used to compare the data and model, and also to compare models. The former contains for instance P-P, Q-Q, return value-return period, and posterior predictive plots, these are detailed in Annex C.3, while the latter typically based on statistical tests or information theory measures. It is important that model-to-model comparisons do not guarantee good fit since it is a relative comparison and even the best model can perform poorly. Below only the information theory related measures are presented as those will be used in model averaging.

Frequentist method

The Akaike information criterion (AIC) is an asymptotic information criterion that is based on the premise that the model with smallest information loss (Kullback-Leibler divergence) should be preferred (Akaike, 1973; Wit et al., 2012). In the absence of the true model the information loss cannot be calculated in absolute terms; however, the models can be compared and their relative “strength” can be expressed by the difference in *AIC*s or by using Akaike weights (Eq.C.10). In this study the corrected form of Akaike information criterion (AICc) is applied that takes into account the effect of finite sample size (Burnham and Anderson, 2002):

$$AIC = 2 \cdot k - 2 \cdot \ln(L) \quad \text{and} \quad (\text{C.8})$$

$$AICc = AIC + \frac{2k \cdot (k+1)}{n - k - 1} \quad (\text{C.9})$$

where L is the likelihood; k is the number of model parameters; and n is the sample size. Akaike weight can be interpreted as the probability that a particular model is best in Kullback-Leibler divergence sense among the group of all considered models:

$$w_i = \frac{\exp(-1/2 \cdot AICc_i)}{\sum_{j=1}^K \exp(-1/2 \cdot AICc_j)} \quad (\text{C.10})$$

where w_i is Akaike weight of the i^{th} model; and K is the number of models under consideration.

Bayesian method

In the Bayesian paradigm goodness of a model is typically expressed as the probability of the model given the data. This probability for the i^{th} model (M_i) is conveniently denoted as b_i and has a similar role as the Akaike weight (Hoeting et al., 1999):

$$b_i = p(M_i | data) = \frac{p(data | M_i) \cdot p(M_i)}{\sum_{j=1}^K p(data | M_j) \cdot p(M_j)} \quad (\text{C.11})$$

where $p(\cdot | M_i)$ is the posterior predictive distribution for the i^{th} model. Since the integrals in Eq.C.11 can be difficult to compute often the Bayesian information criterion (BIC) is used for model selection:

$$BIC = \ln(n) \cdot k - 2 \cdot \ln(L). \quad (\text{C.12})$$

It is an asymptotic information criterion that neglects prior distributions, the model with smallest *BIC* should be preferred; for use of *BIC* in model selection see Burnham and Anderson (2004). Both presented information criteria (AIC, BIC) penalize model complexity although with different weights. The penalization can be interpreted as Occam’s razor to avoid over-fitting.

C.1.5 Model averaging

Since “all models are wrong” the goodness-of-fit measures typically do not clearly favor one model over the others. An approach to improve the fit and prediction is to average models based on their “goodness”. Both frequentist and Bayesian paradigms offer averaging techniques, these of course yield to “wrong” models but by principle these are better than any of the individual models. Notice that the averaged model is conditioned on the pool of candidate models, thus its performance is dependent on them and does not guarantee good fit.

Frequentist method

In the frequentist paradigm the model averaged (FMA) point estimate is calculated as the weighted sum of the model parameters per different models (Burnham and Anderson, 2002):

$$\hat{\theta} = \sum_{i=1}^K w_i \cdot \hat{\theta}_i \quad (\text{C.13})$$

where the weight w_i is the Akaike weight. Consensus on how to calculate the variance of the model-averaged parameters is missing. The following formula is used in this study (Burnham and Anderson, 2002):

$$\text{Var}(\hat{\theta}) = \sum_{i=1}^K w_i \cdot [\text{Var}(\hat{\theta}_i) + (\hat{\theta}_i - \hat{\theta})^2]. \quad (\text{C.14})$$

As the above equations (Eq.C.13-C.14) show the only requirement is that the averaged parameter is available in each model.

Bayesian method

In the Bayesian paradigm the model averaging (BMA) can be done with less ambiguity with any quantity of interest available in all models or directly on the level of distribution functions as well, weighting with model probabilities (Eq.C.11):

$$p(x) = \sum_{i=1}^K b_i \cdot p(x|M_i). \quad (\text{C.15})$$

Using the model averaged distribution $p(x)$ the desired parameters, e.g. mean value, can be readily calculated.

Numerical considerations

In general, the evaluation of the high-dimensional integrals needed in Eq.C.2 and thus in Eq.C.15 is intractable. However, for small models up to 3-4 parameters – as mostly considered here – it can be readily calculated by numerical integration. It is worth mentioning that most probabilistic models in structural reliability are falling into this category, hence no significant computational limitation is expected. Moreover, as the tail

of the distributions is of crucial importance, numerical integration is more efficient than standard Markov Chain Monte Carlo (MCMC) simulation techniques, which require a large number of simulations to adequately capture the tail.

Numerical comparisons using up to three-parameter distributions show that the numerical integration is computationally more efficient than the Metropolis-Hastings MCMC. The integration is implemented as a simple rectangular rule with parallelization, while the MCMC simulation is serial. The comparison is focused on estimating fractiles required in structural reliability, improvement is achieved by using affine invariant MCMC with ensemble sampler (Goodman and Weare, 2010), which takes advantage of parallel computing. Formulating of the distribution with the fractile in interest might yield to further improvement. Personal desktop computer is used for the comparison.

C.2 Distribution functions

Uniform distribution, $\mathcal{U}(a, b)$

$$F(x) = \begin{cases} 0 & \text{for } x < a \\ \frac{x-a}{b-a} & \text{for } a \leq x < b \\ 1 & \text{for } x \geq b \end{cases} \quad (\text{C.16})$$

Where:

a left end of the interval, $[-\infty, \infty]$;

b right end of the interval, $> a$.

Normal distribution, $\mathcal{N}(\mu, \sigma^2)$

$$F(x, \mu, \sigma) = \frac{1}{2} \cdot \left(1 + \operatorname{erf} \left(\frac{x - \mu}{\sigma \cdot \sqrt{2}} \right) \right) = \Phi \left(\frac{x - \mu}{\sigma} \right) \quad (\text{C.17})$$

Where:

μ location parameter/mean, $[-\infty, \infty]$;

σ scale parameter/standard deviation, $]0, \infty]$;

$\operatorname{erf}(.)$ error function.

Two-parameter lognormal distribution, $\ln\mathcal{N}(\mu, \sigma^2)$

$$F(x, \mu, \sigma) = \frac{1}{2} \cdot \left(1 + \operatorname{erf} \left(\frac{\ln(x) - \mu}{\sigma \cdot \sqrt{2}} \right) \right) = \Phi \left(\frac{\ln(x) - \mu}{\sigma} \right) \quad (\text{C.18})$$

Where:

μ location parameter, $[-\infty, \infty]$;

σ scale parameter, $]0, \infty]$.

Three-parameter lognormal distribution, $\ln\mathcal{N}(\mu, \sigma^2, \tau)$

$$\begin{aligned} F(x, \mu, \sigma, \tau) &= \int_{\tau}^x \frac{1}{(x - \tau) \cdot \sigma \cdot \sqrt{2 \cdot \pi}} \exp \left[\left(-\frac{1}{2} \cdot \left(\frac{\ln(x - \tau) - \mu}{\sigma} \right)^2 \right) \right] \cdot dx \\ &= \Phi \left(\frac{\ln(x - \tau) - \mu}{\sigma} \right) \quad (\text{C.19}) \end{aligned}$$

Where:

- μ location parameter, $[-\infty, \infty]$;
- σ scale parameter, $]0, \infty]$;
- τ shift parameter, $[-\infty, \infty]$.

Generalized extreme value distribution, GEV(μ, σ, ξ)

$$F(x, \mu, \sigma, \xi) = \exp \left(- \left(1 + \xi \cdot \left(\frac{x - \mu}{\sigma} \right) \right)^{-1/\xi} \right) \quad (\text{C.20})$$

Where:

- μ location parameter, $[-\infty, \infty]$;
- σ scale parameter, $]0, \infty]$;
- ξ shape parameter, $[-\infty, \infty]$.

Gumbel distribution, GUM(μ, σ)

Special case of GEV, can be obtained from Eq.C.20 by $\xi \rightarrow 0$.

C.3 Probability plots

P-P plot

A probability plot where theoretical and empirical cumulative distribution functions (probabilities) are plotted against each other. Closer the points to a 45° line closer the empirical distribution to the theoretical. Both distributions can be theoretical but only the former is used in this study.

Q-Q plot

A probability plot where theoretical and empirical fractiles (quantiles) are plotted against each other. Closer the points to a 45° line closer the empirical distribution to the theoretical. Both distributions can be theoretical but only the former is used in this study.

Return period–return value plot

Return period–return value plots are depicting cumulative distribution functions in specially transformed space where specific distribution types are forming a straight line. The plots are named after the related distribution type, for example Normal plot, Gumbel plot. This presentation has the advantage that:

- it is easier to visually compare the models;
- deviation from the particular distribution type is clear;
- the crucial tail regions are enlarged by the logarithmic like scale of the horizontal axis.

The general form of the transformation:

$$F(RV) = P = 1 - \frac{1}{RP} \xrightarrow{\text{transf.}} RV = a_1 \cdot \psi(RP) + a_0$$

Illustrating with Gumbel distribution:

$$\exp\left(-\exp\left(-\left(\frac{RV - \mu}{\sigma}\right)\right)\right) = 1 - \frac{1}{RP} \rightarrow RV = -\sigma \cdot \ln\left(-\ln\left(1 - \frac{1}{RP}\right)\right) + \mu$$

$$\psi(RP) = -\ln\left(-\ln\left(1 - \frac{1}{RP}\right)\right)$$

$$a_1 = \sigma$$

$$a_0 = \mu.$$

Although $P = 1 - 1/RP$ is a typical transformation between probabilities and return periods, it is not the only one. A theoretically more sound approach would be to assume that the extremes follow a Poisson process, which implies exponentially distributed time between occurrences. Using this Poisson assumption the transformation:

$$P = \exp\left(-\frac{1}{RP}\right).$$

The comparison of these two transformations are presented in Figure C.2. With the exception of the 1-10 year range, their difference is negligible; furthermore, the transformation only affect the visual appearance of plots.

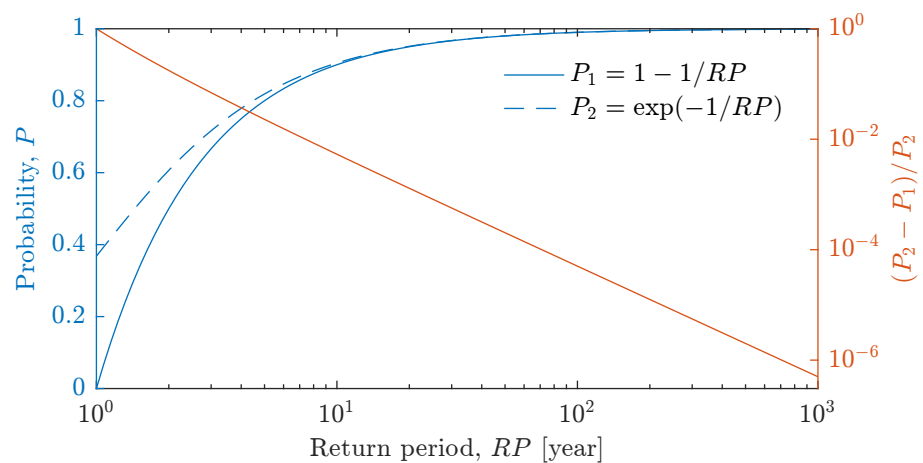


Figure C.2 Comparison of return period–probability transformations.

Appendix D

Summary of contributions in Hungarian

I. Tézis

Statisztikailag elemeztem a Kárpátok régió több, mint 6000 rácspontjának felszíni hő-víz egyenérték adatsorát, melyek az 1961-2010 időszakot fedik le és 49 telet foglalnak magukba. Számos eloszlástípust illesztettem a napi észlelésekkel nyert hómaximumokra és kiterjedt statisztikai vizsgálatok felhasználásával:

- I./a** Megmutattam, hogy szemben a jelenleg szabványosított – Eurocode által is javasolt és Magyarországon alkalmazott – Gumbel-eloszlással, a hegységek és dombságok éves hómaximumait a Weibull-, míg alföldekét a Fréchet-eloszlás írja le jobban. A Gumbel-eloszlás gyakran érdemben alábecsüli az alföldek hómaximumait, így túlbecsüli a szerkezetek megbízhatóságát. A lognormális eloszlás általában még gyengébben teljesít, mint a Gumbel-eloszlás. Megbízhatósági, empirikus (adat vezérelt) és elméleti megfontolások alapján – a vizsgált eloszlástípusok közül – a Weibull-eloszlást javaslom hegységek és dombságok esetén, míg a Fréchet-eloszlást alföldekre.
- I./b** Előállítottam a régió reprezentatív területeihez tartozó hómaximumok jellemző értékeinek posterior eloszlását. Ezek prior információként használhatók hasonló klimatikus adottságú régiók vizsgálatakor. Továbbá, készítettem egy nyílt forráskódú, online, interaktív, 10 km felbontású hótérképet, mely karakterisztikus hóterhek, valamint rendkívüli hóterhek meghatározására használható.

(Rózsás and Sýkora, 2015b,c; Rózsás et al., 2016b; Vigh et al., 2016)

II. Tézis

Elemeztem a statisztikai bizonytalanságok (paraméterbecslési és modellválasztási bizonytalanság), hatását éves felszíni hómaximumok jellemző fraktiliseire és szerkezeti megvízhatóságra. A jelenlegi építőmérnöki gyakorlat többségében elhanyagolja ezeket a bizonytalanságokat, habár elkerülhetetlenül jelen vannak az adatok szűkössége miatt.

- II./a** Megmutattam, hogy a paraméterbecslési bizonytalanság elhanyagolása a jellemző fraktilisek jelentős (20%) alulbecsléséhez vezethet. Továbbá, rámutattam, hogy az alkalmazott eloszlás típusának (modellválasztási bizonytalanság) nagyobb hatása van a jellemző fraktilisekre, mint a paraméterbecslési bizonytalanságnak. Kétparaméteres lognormális, háromparaméteres lognormális, Gumbel- és általánosított extrém eloszlásokat alkalmaztam.
- II./b** Megbízhatósági analízisek felhasználásával megmutattam, hogy a statisztikai bizonytalanságok elhanyagolása akár több nagyságrenddel is alulbecsülheti a tönkremeneti valószínűséget. Illusztráltam, hogy a „legjobb” pontbecslések, mint a maximum likelihood becslés vagy a momentumok módszer alkalmazása megbízhatósági szempontból nem konzervatív. Ezek a jellemző fraktilisek és tönkremeneti valószínűségek gyakorlati szempontból szignifikáns alulbecsléséhez vezethetnek. Az eredmények alapján javaslatot tettem a statisztikai bizonytalanságok kezelésére és figyelembe-vételére biztonsági szempontból kritikus és normál szerkezetek esetére. A bayesi posterior előrejelző eloszlás alkalmazását javaslom megbízhatósági analízisekben, továbbá modell átlagolást a modellválasztási bizonytalanság figyelemben-vételére.

(Rózsás et al., 2016a; Rózsás and Sýkora, 2015a,b,c,d; Rózsás and Vigh, 2014)

III. Tézis

Megvizsgáltam a felszíni hóterhek éves maximumai mérési bizonytalanságának hatásását szerkezetek megbízhatóságára. Ezt a bizonytalanságot a jelenlegi építőmérnöki gyakorlat tipikusan elhanyagolja. Statisztikai és intervallum alapú vizsgálatokra tettem javaslatot és megmutattam, hogy:

- III./a** A mérési bizonytalanság elhanyagolása jelentősen (nagyságrend) alulbecsülheti a tönkremeneti valószínűséget. Meghatároztam a legfontosabb paraméterek azon tartományát, amelyekben a mérési bizonytalanságot figyelembe kellene venni. Ezeket normális, lognormális és Gumbel-eloszlások, többféle relatív szórás (0.2-0.6) és többféle nagyságú mérési bizonytalanság figyelemben-vételével állítottam elő (0-10% az éves maximumok átlagának).

- III./b** Amennyiben a mérési bizonytalanságot generáló mechanizmus ismert, úgy a statisztikai, míg ellenkező esetben az intervallum alapú megközelítést javaslom a bizonytalanság figyelemben-vételére. Alföldek hómaximumai esetén a mérési bizonytalanságok

elhanyagolása elfogadható. Egyéb esetekben fejlettebb módszerek (statisztikai, intervallum) alkalmazása ajánlott.

Gyakorlati alkalmazásokban rendre a megbízhatósági intervallum alsó határa és az előrejelző megbízhatósági index alkalmazását javasolom intervallum és statisztikai alapú megközelítések esetén. A pontbecslések bizonytalansági intervallumokkal való kiegészítését javasolom.

(Rózsás and Sýkora, 2016b)

IV. Tézis

Nemstacionárus extrém érték analízis alkalmazásával megvizsgáltam a Kárpátok Régió elmúlt 49 év felszíni hómaximumaiban mutatkozó hosszú idejű időbeli trendeket. Statisztikai és információelméleti vizsgálatokkal kimutattam, hogy:

IV./a A vizsgált Kárpátok régió területének 97%-án időben csökkenő tendencia mutatkozik a hómaximumokban. Statisztikaillag szignifikáns ($p < 0.05$) csökkenő trendet találtam a régió területének 65%-án. A hipotézisvizsgálatot a hatás mértékének és a teszt erejének vizsgálatával is kiegészítettem. Továbbá, kimutattam, hogy néhány helyszín karakterisztikus hóterhének csökkenése gyakorlati szempontból is szignifikáns. Az időbeli trendeket információelméleti módszerekkel is igazoltam.

IV./b A régió Fréchet-eloszlással jellemzhető helyszíneinek többsége esetén a csökkenő hómaximumnak csekély hatása van a szerkezetek megbízhatóságára. A paraméterbecslés bizonytalansága domináns. Erős csökkenő tendenciával és Weibull-eloszlással jellemzhető helyszínek esetén a csökkenés hatása gyakorlati szempontból is szignifikáns a szerkezeti megbízhatóság vonatkozásában. Ugyanakkor a változás biztonsági szempontból kedvező, mivel növeli a megbízhatóságot.

(Rózsás et al., 2016a,b; Sýkora et al., 2016)

V. Tézis

Megvizsgáltam a széles körben alkalmazott Gauss-kopula feltételezés hatását időben folytonos sztochasztikus folyamatokra és megmutattam, hogy:

V./a Az alkalmazott függőségi szerkezetnek (kopula függvény) jelentős hatása van az időfüggő megbízhatóságra. A túlnyomóan alkalmazott Gauss-kopula feltételezés akár negyed- vagy tízszer akkora tönkremeneti valószínűséget is eredményezhet, mint a többi vizsgált kopula függvény (t , Gumbel-, elforgatott Gumbel-, elforgatott Clayton-kopula). Egy egyszerű esetre megmutattam, hogy a kopula függvény megfelelő megválasztásával tetszőleges nagyságú eltérést hozhatunk létre az átlépési sebességen a Gauss-kopulához viszonyítva.

V./b Az autokorrelációs függvény típusának számottevő hatása van az időfüggő tönkrementeli valószínűségre. A Cauchy- illetve Gauss-autokorrelációs függvényekkel kapott normalizált tönkremeneti valószínűségek aránya 1.41. Az arányszámot kizárolag az autokorrelációs függvény típusa befolyásolja.

V./c Nemfüggetlen felszíni hóteher maximumok esetén az extrém típusú kopulák, mint a Gumbel-kopula, jelentősen jobban illeszkednek az adatokra, mint a Gauss-kopula. A Gumbel-kopula akár négyeszer kisebb átlépési sebességet is eredményezhet, mint a Gauss-kopula.

Amennyiben elegendő észlelés áll rendelkezésre, úgy a kopula függvényt azokból célszerű meghatározni statisztikai módszerekkel. Kevés észlelés esetén több kopula függvény alkalmazása javasolt a modellválasztási bizonytalanság mértékének felméréssére. Utóbbi esetben a Gauss-kopula kizárolagos alkalmazása nem indokolt, az a biztonság kárára is tévedhet. A modell átlagolást javasol a kopula modellválasztási bizonytalanság figyelembevételére.

(Rózsás and Mogyorósi, 2016)